Transcriptional regulation of *Atp2b2* determines the severity of AHL in C57BL/6J Mice

Rebecca R. Minich

A dissertation

submitted in partial fulfillment of the

requirements for the degree of

Doctor of Philosophy

University of Washington

2015

Reading Committee:

Bruce L Tempel, Chair

Edith Wang

G. Stanley McKnight

Program Authorized to Offer Degree:

Pharmacology

University of Washington

Abstract

Transcriptional regulation of *Atp2b2* determines the severity of AHL in C57BL/6J Mice

Rebecca R. Minich

Chair of the Supervisory Committee:
Professor Bruce L Tempel
Otolaryngology-Head and Neck Surgery, Pharmacology

Along with Na+/Ca^{2+} exchangers, plasma membrane Ca^{2+} ATPases (ATP2Bs) are main regulators of intracellular Ca^{2+} levels. Mouse mutations in *Atp2b2* indicate that tight regulation of this gene is imperative for normal cell physiology, specifically in the auditory system. Additionally, mutations in *Atp2b2* worsen hearing loss associated with mutations in the tip-link protein Cadherin 23 (CDH23) (Noben-Trauth et al. 2003; Schultz et al. 2005). This interaction is likely due to the necessity of Ca^{2+} in maintaining the structural integrity of the tip-links (Sotomayor et al. 2010). C57BL/6J (B6) mice have a severe age-related hearing loss (AHL) phenotype partially due to mutations in CDH23 (Noben-Trauth et al. 2003; Kane et al. 2012) . In this dissertation, we investigate whether *Atp2b2* is another contributor to AHL of B6 mice in

three parts: (I) The *αAtp2b2* minimal promoter was identified to better understand transcriptional regulation of *Atp2b2*. Further characterization determined that ATOH1 and EGR1 are modulators of *αAtp2b2* transcription in OC-1 and N2A cells. Shift assays identify a binding site for EGR1 in the minimal promoter of *αAtp2b2* 71 bases upstream of the transcriptional start site (TSS). (II) Two discreet measures of gene expression show misregulation of *Atp2b2* transcript in B6 mice. We found that the proximal promoter of *αAtp2b2* does not play a role in the misregulation of *Atp2b2* transcript. However, two lncRNAs were identified in this region. Gene expression analysis and overexpression studies suggest that these lncRNAs inhibit expression of *Atp2b2* transcript. This implicates misregulation of *Atp2b2* by lnc83 in AHL of B6 mice. (III) To further investigate the contribution of *Atp2b2* to B6 AHL, two congenic mice were generated: (1) B6 haplotype at *Atp2b2* in a CB background (CB.B6^{Atp2b2}) and (2) CB haplotype at *Atp2b2* in a B6 background (B6.CB^{Atp2b2}). We found that B6.CB^{Atp2b2} mice have an intermediate auditory phenotype at high frequencies and normal hearing at low frequencies. CB.B6^{Atp2b2} mice have a slight elevation of threshold at 5.6 kHz at 6 months of age. At 12 weeks of age, *Atp2b2* expression is normal in brainstem tissue of B6.CB^{Atp2b2} and CB.B6^{Atp2b2} mice while lnc83 transcript levels are elevated in CB.B6^{Atp2b2}mice. From this data we conclude that mutations in the *Atp2b2* gene are necessary but not sufficient to cause the B6 AHL phenotype.

TABLE OF CONTENTS

List of Figures v

List of Tables vii

List of Abbreviations viii

Chapter 1. Introduction 1

1.1 The burden of disabling hearing impairment 1

1.2 The mammalian auditory system 2

1.3 The genetic basis of AHL 4

1.3.1 Age-related hearing loss locus (ahl) 5 and Gipc3 5

1.3.2 Pcdh15 and AHL 5

1.3.3 Pou3F4 in AHL 5

1.3.4 Atp2b2 and noise-induced hearing loss (NIHL) 6

1.3.5 Cdh23 and ahl 6

1.4 The digenic interaction of *Cdh23* and *Atp2b2* 6

1.5 The importance of calcium and calcium regulators 7

1.6 Animal and disease models associated with ATP2Bs 9

1.7 Studies of *dfw* mice identify the need for tight regulation of *Atp2b2* 10

1.8 Conclusion 11

Chapter 2. Characterization of the *αAtp2b2* Promoter 14

2.1 Introduction 15

2.1.1 Function and regulatory mechanisms of ATP2Bs 15

2.1.2 ATP2B2 splicing and alternate start site variations 16

2.1.3 Importance of studying transcriptional regulation of ATP2Bs 17

2.1.4 Goals of the study 17

2.2 Methods 18

2.2.1 Cloning 18

2.2.2 Luciferase assay 18

2.2.3 Overexpression assay 19
2.2.4 Electrophoretic Mobility Shift Assay (EMSA) 20
2.3 Results 22
2.3.1 Genomic modifications at Atp2bs indicate transcriptional hot-spots 22
2.3.2 Identifying the promoter of the αAtp2b2 transcript 23
2.3.3 ATOH1, EGR1, GATA3, POU4F3, and USF1 may bind the αAtp2b2 promoter ... 24
2.3.4 EGR1 and ATOH1 modulate the isolated αAtp2b2 promoter in OC-1 Cells 25
2.3.5 Identifying the region of EGR1 binding in the αAtp2b2 promoter 26
2.3.6 EGR1 effects endogenous levels of Atp2b2 transcript 26
2.3.7 Shift assays indicate that EGR1 binds to the αAtp2b2 promoter at [-71 to -98] 27
2.4 Discussion 29
2.4.1 The αAtp2b2 promoter and upstream repressor elements 29
2.4.2 Developmental expression patterns of Atoh1 and Atp2b4 30
2.4.3 EGR1 plays a crucial role in auditory pathways 30
2.4.4 Gene interplay of ATP2Bs in response to transcription factors 31
2.4.5 Characterization of the αAtp2b2 promoter enables gene modulation 31

Chapter 3. *Atp2b2* Misregulation in B6 Mice with AHL 47

3.1 Introduction 48
3.1.1 Cdh23 and AHL in B6 mice 48
3.1.2 dfw mutants reveal Atp2b2 misregulation in B6 mice 48
3.1.3 The known digenic interaction of Cdh23 and Atp2b2 49
3.2 Methods 51
3.2.1 Animals 51
3.2.2 Auditory testing 51
3.2.3 Gene expression analysis with quantitative PCR (qPCR) 52
3.2.4 Western analysis 54
3.2.5 Cloning 54
3.2.6 Luciferase assays 55
3.2.7 LncRNA overexpression assay 57
3.3 Results 58

3.3.1 Recapitulating the allelic discrimination in CB/B6 hybrid mice 58
3.3.2 Hearing is normal in CB/B6 hybrid mice 58
3.3.3 Atp2b2 transcripts are partially downregulated in young B6 mice 59
3.3.4 Atp2b2 transcripts are downregulated in B6 mice at 12 weeks of age 60
3.3.5 Investigation of potential modulators of Atp2b2 transcript in B6 mice 60
3.3.6 The promoter in downregulation of Atp2b2 transcript in B6 mice 62
3.3.7 LncRNAs in B6 mice 64
3.3.8 Lnc83 may play a role in the downregulation of Atp2b2 transcript in B6 mice 65
3.4 Discussion 67
3.4.1 Misregulation of Atp2b2 transcript in B6 mice 67
3.4.2 Identification of Atp2b2 transcriptional regulators 68
3.4.3 Promoter Studies 68
3.4.4 LncRNA Studies 69
3.4.5 Lnc83 may function as a transcriptional inhibitor of Atp2b2 69
3.4.6 Characterization of subtle gene-expression changes and human disease 70
Chapter 4. Characterization of *Atp2b2* in Congenic Mice 85
4.1 Introduction 86
4.1.1 Investigations of ahl in B6 mice and the involvement of Cdh23 86
4.1.2 Cdh23 congenic mice 87
4.2 Methods 89
4.2.1 Animals 89
4.2.2 Auditory testing 89
4.2.3 qPCR 90
4.3 Results 92
4.3.1 Development of Atp2b2 congenic lines 92
4.3.2 Hearing in young mice 92
4.3.3 ABRs at the onset of hearing loss 93
4.3.4 Middle aged ABRs 93
4.3.5 Atp2b2 and lncRNA expression in congenic mice 94
4.4 Discussion 96

4.4.1 The Atp2b2 gene from CB mice rescues hearing loss in B6 mice 96
4.4.2 Lnc83 overexpression and downregulation of the Atp2b2 transcript 97
4.4.3 Intronic regions play a role in disease 98

Chapter 5. Conclusions and Future Studies 107

5.1 The *Atp2b2* promoter and the vast transcriptional landscape 107
5.2 *Atp2b2* regulation in CB and B6 inbred strains 108
5.3 Development of a new *Atp2b2* model in auditory neuroscience 109

Bibliography 110

LIST OF FIGURES

Figure 1.1. Anatomy of the ear. 12
Figure 1.2. Cross section of the OC 13
Figure 2.1. Mouse *Atp2b2* genomic region adapted from the UCSC genome browser.... 35
Figure 2.2. Human *Atp2b2* genomic region adapted from the UCSC genome browser... 36
Figure 2.3. Promoter construct cartoon with genomic location 37
Figure 2.4. The *αAtp2b2* minimal promoter is contained in the 5'UTR and CpG island. 38
Figure 2.5. OC-1 baseline expression of transcription factors 39
Figure 2.6. Transcription factors of interest and their *αAtp2b2* promoter binding sites... 40
Figure 2.7. Transcription factors affect *αAtp2b2* promoter activity 41
Figure 2.8. EGR1 likely binds in the CpG Island 42
Figure 2.9. ATOH1 and EGR1 effect expression of *Atp2b2* and *Atp2b4* 43
Figure 2.10. Mobility shift assay of probe [-71 to -98] 44
Figure 2.11. Supershift assay: EGR1 binds to probe [-71 to -98] 45
Figure 2.12. Genomic comparison of the *Atp2b* genes 46
Figure 3.1. Ca^{2+} in the endolymph binds to *Cdh23* and maintains structural integrity 73
Figure 3.2. Transcript in hybrid mice is predominately from the CB allele 74
Figure 3.3. CB/B6 mice have hearing similar to CB mice 75
Figure 3.4. *Atp2b2* transcripts are downregulated in brainstem of 5 week-old B6 mice.. 76
Figure 3.5. *Atp2b2* transcripts are downregulated in 12 week-old B6 mice 77
Figure 3.6. ATP2B2 is not significantly different in CB and B6 78
Figure 3.7. SNP3 may decrease activity of the *αAtp2b2* promoter 79
Figure 3.8. CB and B6 *αAtp2b2* promoter activity is the same in OC-1 cells 80
Figure 3.9. Predicted lncRNAs in mouse and human 81
Figure 3.10. Lnc83 is upregulated in B6 brainstem and cochlea 82
Figure 3.11. Lnc82 and lnc83 do not affect *αAtp2b2* promoter activity 83
Figure 3.12. Lnc83 inhibits *Atp2b2* transcript expression in N2A cells 84
Figure 4.1. Karyotype for inbred and congenic strains 99

Figure 4.2. Congenic intervals at Chr 6 100
Figure 4.3. 5 week-old congenic and inbred mouse ABRs..... 101
Figure 4.4. 12 week-old congenic and inbred mouse ABRs..... 102
Figure 4.5. 6 month-old congenic and inbred mouse ABRs..... 103
Figure 4.6. 6 month-old congenic and inbred mouse ABRs at 5.6 kHz 104
Figure 4.7. *Atp2b2* transcript expression in 12 week-old mouse brainstem 105
Figure 4.8. LncRNA expression in 12 week-old mouse brainstem 106

LIST OF TABLES

Table 2.1. qPCR primers for transcription factors. 33
Table 2.2. Probe sequences for shift assays. 34
Table 3.3. qPCR Primers used in *Atp2b2* and lncRNA gene expression experiments 71
Table 3.4. SNPs in the proximal promoter of *Atp2b2* 72

LIST OF ABBREVIATIONS

5’ UTR	5’ untranslated region
ABR	Auditory brainstem response
Actg	Gamma (γ) actin
Actb	Beta (β) actin
AHL	Age-related hearing loss
ahl	Age related hearing loss locus (chromosome 10)
ANOVA	Analysis of Variance
ATP	Adenosine triphosphate
Atp2b	Plasma membrane calcium ATPase
B6	C57BL/6J
B6.CB^{Atp2b2}	B6.CBACa-*Atp2b2*$^{CBA/CaJ}$
BCA	Bicinchoninic Acid
bp	Base pairs
Ca^{2+}	Calcium
Can	Canonical
CB	CBA/CaJ
CB.B6^{Atp2b2}	CBACa.B6-*Atp2b2*$^{C57BL/6J}$
Cdh23	Cadherin 23
cDNA	Complimentary DNA
Chr	Chromosome
dB	Decibels
DFN	Non-syndromic deafness
DFNB	Non-syndromic deafness, autosomal recessive
dfw	Deafwaddler
DHS	DNase I hypersensitivity
EMSA	Electrophoretic mobility shift assay
ENCODE	Encyclopedia of DNA elements
H3K4me	Histone 3 lysine 4 methylation
H3K27a	Histone 3 lysine 27 acetylation
IRES-EGFP	Internal ribosome entry site and enhanced green fluorescent protein
JAX	The Jackson laboratory
kb	Kilobase (1 thousand bases)
kHz	Kilohertz
lnc82	Long non-coding RNA Gm15082
lnc83	Long non-coding RNA Gm15083
lncRNA	Long non-coding RNA
luc^{+}	Luciferase gene
Mb	Megabase (1 million bases)
MET	Mechanoelectrical transduction
miRNA	Micro RNA

N2A	Neuro-2A (cell line)
NCX	Sodium/calcium exchanger
NIDCD	National institute on deafness and other communication disorders
NIHL	Noise induced hearing loss
OC	Organ of Corti
OC-1/2	Immortomouse organ of Corti (cell line)
Pcdh15	Protocadherin 15
pcDNA	Plasmid construct driven by the Cytomegalovirus (CMV) promoter
PCR	Polymerase chain reaction
pGL3	Firefly luciferase gene plasmid
PIE	Empty pcDNA vector +IRES-EGFP
pRL-TK	Thymidine kinase promoter driven renilla luciferase plasmid
qPCR	Quantitative PCR
RISC	RNA-induced silencing complex
RNA Pol	RNA polymerase
SC	Santa Cruz
SEM	Standard error of the mean
SERCA	Sarcoplasmic/endoplasmic reticulum Ca^{2+} ATPase pump
SHIELD	Shared Harvard inner ear laboratory database
siRNA	Silencing RNA
SNP	Single nucleotide polymorphism
std. dev.	Standard deviation
TK	Thymidine kinase
TSS	Transcriptional start site
UCSC	University of Santa Cruz
USH	Usher syndrome

ACKNOWLEDGEMENTS

I would like to start by thanking two of the finest educators I have ever known, Dr. Hot and Dr. Cold (better known as Mr. Michael Sinclair and Dr. John Goudie). These two, along with the amazing staff at Parkwood Upjohn Elementary and the Kalamazoo Area Mathematics and Science Center cultivated my insatiable wonder of the natural world leading me to seek a career in science.

Pete and Janet Minich, with every chemistry set and mini microscope, you fueled my wonder while making me feel clever, brilliant and deserving of knowledge. Barb Minich and Erica Riegle, you have been my partners in crime from day one. Thank you for tolerating my nerdiness and, more importantly, encouraging me to enjoy life. David Tindle, Allison Pellerito, and Lindsay Hatter, without you I would have given up on science a long time ago. Maria Brym and Tara Goldman, you are hard-working, intelligent and beautiful, you are my inspiration. Carly Schiffer, you have more muchness than I will ever know, faking courage like yours got me through this. Scott Shawcroft, thank you for being my ally and my unwavering support system through all the ups and downs of lab and life.

Thank you to UW Pharmacology and the Auditory Neuroscience Training Grant for financing my academic career. Special thanks to Bill Catterall and Diane Schulstad for going beyond the call of duty. Jin Li, Claire Watson, Jessica Weatherstone, Ayaka Iwata, Braulio Peguero, Linda Robinson, Jenny Thornton, Val Street and Carol Robbins, every experiment in these pages was possible because of you, this degree is as much yours as it is mine. Thank you friends of Pharmacology, especially, Wendy Yang, Darragh Kerr, Jamie Rose Kuhar, Josh Cohen, Jake Hyer and Jennifer Deem for being a sounding board, a resource and a life raft through this entire trip.

To my thesis committee: Edith Wang, Stan McKnight, Sandy Bajjalieh, and Dave Raible, your patience and guidance over the last 5 years was invaluable - any brilliance in these pages was cultivated by your genius. Thank you to Ed Rubel and Jenny Stone for your guidance and help. Finally, to my thesis advisor Bruce Tempel, thank you for your support and guidance.

DEDICATION

To the wonderful people in my life that keep telling me,
"you've got this".

Chapter 1. INTRODUCTION

1.1 THE BURDEN OF DISABLING HEARING IMPAIRMENT

Sensory systems are a unifying part of life in the animal kingdom. In a world where it is 'eat or be eaten' properly functioning sensory systems are fundamental to survival. The auditory system is no exception. For animals to hunt properly or detect predators they must be able to hear acutely throughout their life. For our ancestors, it was no different. On the African savannah we would have answered the question, "is that rustling in the grass a lion or the wind?"

Although our societal structure protects us from the necessity of flawlessly functioning sensory systems, impairment is still a burden. According to a 2011 World Health Organization estimate there are 360 million people in the world with disabling hearing loss which equates to approximately 5.3% of the world's population. Of these, 328 million are adults and 32 million are children (Olusanya et al. 2014). The prevalence is greatest in developing regions such as South Asia, Asia Pacific and Sub-Saharan Africa. In some cases, the prevalence in low-income regions is nearly double that in high-income regions such as the US.

In children, hearing impairment can lead to delays in language acquisition and reading proficiency. In addition to developmental delays, children face educational disadvantage, social isolation and stigmatization. In adults, hearing impairment can lead to the inability to interpret speech, reducing the ability to communicate with others. This causes social isolation and depression and an overall decrease in the quality of life of the individual. Although the social and educational burdens alone make this an important public health issue, there is also a steep economic cost in the form of disability, loss of days worked and the cost of devices to improve hearing (Olusanya et al. 2014). Given these challenges, it is imperative that scientists and clinicians

research this disorder. Clinical focus should be on the development of affordable and accurate devices for the hearing impaired. Basic research studies, such as this one, should focus on developing ways to quell or reverse the development of hearing loss. The following dissertation investigates the genetic and molecular mechanisms of AHL in a mouse model.

The introductory chapter will discuss the anatomy of the auditory system, the prevalence of AHL and outline the genetic basis of this disease. Focus will be on the molecular basis of AHL in the B6 mouse. Specifically, we will discuss the importance of Ca^{2+} and its extrusion pump ATP2B2 in the stereocilia of the auditory hair cells. This thesis identifies transcriptional regulatory elements of this pump which could be used in future research to modulate pump expression and potentially auditory sensitivity. To better understand hearing impairment the following section investigates the function of select molecular players in the detection of auditory stimuli.

1.2 THE MAMMALIAN AUDITORY SYSTEM

The structure and function of the ear may seem fairly straightforward when compared to internal organs like the adrenal gland or the pancreas however the internal structure of the ear has a delicate complexity with new frontiers still being explored. The peripheral auditory system is divided into three parts: the outer, middle and inner ear.

The outer ear is primarily composed of the ear cartilage, or pinna, and the ear canal. This anatomical structure funnels sound into the ear amplifying and localizing sound. The middle ear is composed of the ear drum and the malleus, incus, and stapes. The eardrum, or tympanic membrane, vibrates in response to sound waves in the ear canal. This vibration moves the bones of the middle ear. These are the smallest bones in the body and function to convert sound waves in the air into mechanical stimulus. This mechanical stimulus is carried through the middle ear to the inner ear. The cochlea is a highly complex organ made up of a number of cell types that must

work in concert to convert the mechanical stimulus from the middle ear into electrochemical impulses that are understood by the brain.

Anatomically, the cochlea is a shell shaped fluid filled bony labyrinth that houses the organ of Corti (OC), the main sensory organ of the inner ear. As the stapes vibrates through the oval window, it pushes fluid into the cochlea of the inner ear displacing the basilar membrane. The cochlea is organized tonotopically which means that different parts of the cochlea are stimulated by different frequencies of sound. The base of the cochlea is stimulated by high frequency sound waves while the apex responds best to low frequency stimulation (Fig. 1.1).

Hair cells rest on top of the basilar membrane surrounded by an ion rich fluid called the endolymph. The hair cells of the OC are highly specialized cells responsible for converting mechanical stimuli produced by sound waves into electrochemical impulses in a process termed mechanotransduction. The apically positioned stereocilia of the outer hair cells are linked together by tip-links composed of Cadherin23 (CDH23) and Protocadherin 15 (PCDH15) (Fig. 1.2) (Kazmierczak et al. 2007). As the basilar membrane is displaced, a shearing force against the tectorial membrane causes deflection of the stereocilia. This puts tension on the tip-links leading to opening of the mechanoelectrical transduction channels (MET channels). MET channel opening causes hair cell depolarization and influx of Ca^{2+} and K^{+} leading to membrane depolarization and neurotransmitter release. ATP2B2 is highly expressed in the stereocilia of the outer hair cells and is largely responsible for pumping Ca^{2+} out of the cell into the endolymph (Wood et al. 2004; Carafoli 2011).

The dendrites of spiral ganglion neurons are the first to receive inputs from the auditory hair cells. The cell bodies of the spiral ganglion are housed in the modiolus of the cochlea and axons extend into the central nervous system making connections with the cochlear nerve. Afferent nerve

fibers are predominately found connected to the inner hair cells. Efferent nerve fibers are connected to the three rows of outer hair cells. These hair cells contain a specialized motor protein called prestin. The outer hair cells shorten in response to depolarization and lengthen in response to hyperpolarization. This contraction and expansion creates movement in the OC that amplifies auditory stimulus (Review: Fettiplace and Hackney 2006). In this section we discussed the normal function of the auditory system. The next section will outline some known gene mutations that lead to aberrant processing in the auditory system causing AHL.

1.3 THE GENETIC BASIS OF AHL

Hearing loss increases drastically with age, the NIDCD has reported that 30% of US adults age 65 to 74 are affected with hearing loss compared to only 18% of adults age 34 to 45 (NIDCD). Additionally, studies of families and twins have found that there is high heritability of AHL (Gates et al. 1999; Wingfield et al. 2007). Unfortunately the genetic basis of AHL does not simplify treatment or prevention. The progression of hearing loss is complex with numerous environmental and genetic components. Numerous genome wide association studies have fallen short of identifying human genes underlying AHL (Bowl and Dawson 2015).

Given the difficulty of identifying likely candidate genes for AHL in humans, scientists have resorted to studying models of hearing impairment in other organisms. Similar to strategies used to identify genes involved in congenital hearing loss, the mouse is one of the most widely used models for studying AHL. Anatomically, the mouse ear is highly comparable to the human ear. Genetically, the majority of human genes are conserved in mice and can be easily manipulated and studied. Lastly, mouse strains are well characterized with a vast amount of genotypic and phenotypic information catalogued in internet databases. All of this makes the mouse a highly useful and sought after model for auditory research. The rest of this section outlines the most recent

knowledge of AHL loci in mice. we will focus on mammalian genes that are known to cause hearing loss in mice and humans (Bowl and Dawson 2015).

1.3.1 *Age-related hearing loss locus (ahl) 5 and Gipc3*

Gipc stands for "GAIP interacting protein" where "GAIP" is "G-Alpha interacting protein". This gene was recently identified as the causal gene for hearing loss associated with the *ahl5* locus located on mouse Chromosome (Chr) 10. The function of this protein in the auditory system is not well understood. There is some evidence that suggests this protein may be involved in hair cell transduction. Human orthologues found on Chr 19 are thought to cause deafness associated with DFNB15 and DFNB95 (Charizopoulou et al. 2011).

1.3.2 *Pcdh15* and AHL

Mutations in *Pcdh15*, which is located on mouse and human Chr 10, illuminate a digenic interaction with *Cdh23*. This is not surprising because these two proteins compose the tip-links of the stereocilia. Research has shown that mutations in these two genes interact to produce a worsened phenotype in mice. Similar mutations in human *Pcdh15* and *Cdh23* genes are found in patients with Usher syndrome (USH1F) (Zheng et al. 2005).

1.3.3 *Pou3F4* in AHL

The *Pou3F4* gene encodes a transcription factor found on the X-Chr of both mice and humans. Pou3F4 knockouts exhibit profound deafness. In young mice, heterozygous females do not exhibit hearing loss. However, as females age, a population of these mice exhibit heightened thresholds. This gene is associated with the human hearing loss locus DFN3 (Minowa et al. 1999; Xia et al. 2002)

1.3.4 *Atp2b2* and noise-induced hearing loss (NIHL)

The *Atp2b2* gene is located on mouse Chr 6 and human Chr 3. This gene is implicated in a number of mouse and human models of congenital hearing loss. Here, researchers investigated the effect of *Atp2b2* mutations on susceptibility to NIHL. They found that mutations in *Atp2b2* confer increased susceptibility to NIHL (Kozel et al. 2002; Bowl and Dawson 2015). This is just one of the many examples of hearing loss associated with the *Atp2b2* gene.

1.3.5 *Cdh23* and *ahl*

The first *ahl* locus was mapped to Chr 10 and further investigation identified $Cdh23^{ahl}$ as the causal gene. CDH23 is an important protein that, along with PCDH15, composes the tip-links of the stereocilia (Noben-Trauth et al. 2003). These structures are extremely important for concerted depolarization of the hair cells. If structural integrity of the tip-links is jeopardized, they do not function and the link between adjacent stereocilia is compromised. In *ahl*, a mutation in the intronic region of *Cdh23* causes skipping of exon 7 affecting the function of the protein, This gene is implicated in human deafness locus DFNB12 and Usher's syndrome (USH1D) (Bowl and Dawson 2015). Both *Cdh23* and *Atp2b2* are involved in AHL or NIHL.

1.4 THE DIGENIC INTERACTION OF *CDH23* AND *ATP2B2*

In the last section we discussed that both *Cdh23* and *Atp2b2* are involved in AHL or NIHL. In this section, we will illustrate that the *Cdh23* and *Atp2b2* genes interact and propose the molecular basis of this digenic interaction. Mutations in *Cdh23* were originally identified as modifiers of the *deafwaddler* (*dfw*) mutant (Noben-Trauth et al. 1997). The *dfw* mutant was identified by P.W. Lane in 1987 in the Mouse Newsletter. Although the mutated gene was unknown, the researchers

noted that the mice had a recessive mutation causing hearing and vestibular system impairment with a wobbly gait. These *dfw* mice were bred with *Cdh23*^{ahl} and wildtype *Cdh23* mice. It was found that hearing impairment was exacerbated in *dfw* mice containing the *Cdh23*^{ahl} variant. The *dfw* gene was identified in the Tempel lab as *Atp2b2* (Street et al. 1998) . This protein is found at high levels in the brain and is located in the stereocilia of hair cells. As stated earlier, ATP2B2 functions to pump Ca^{2+} out of the cell against its electrochemical gradient. In the cochlea, ATP2B2 moves Ca^{2+} from the hair cell stereocilia into the endolymph.

Although it is not immediately apparent how mutations in *Cdh23*, a tip-link protein, might exacerbate hearing impairment associated with the Ca^{2+} pump gene, *Atp2b2*, several studies have helped formulate a hypothesis. First, mutation of *Atp2b2* leads to decreased Ca^{2+} concentration in the endolymph (Wood et al. 2004). Second, the structural integrity of the tip-links is dependent on Ca^{2+} concentration (Sotomayor et al. 2010). The endolymph is the fluid that surrounds the tip-links. If the concentration of Ca^{2+} in this fluid is decreased because of mutations in *Atp2b2*, it is likely that phenotypes associated with mutations in *Cdh23* will be exacerbated. We therefore hypothesize that Ca^{2+} regulation and trafficking is the basis for the digenic interaction between *Cdh23* and *Atp2b2*. To better understand this interaction, it is important to investigate mechanisms of Ca^{2+} regulation. The next section discusses the role of Ca^{2+} in the cell and the ways it is regulated and controlled.

1.5 THE IMPORTANCE OF CALCIUM AND CALCIUM REGULATORS

Cells fight a constant battle between homeostasis and adaptation. Survival depends on the ability to respond to a stimulus and quickly return to a resting state. Failure to do so will, sooner or later, result in cell death. Multicellular organisms face an additional homeostatic challenge, communication. To cope with the constant sending and receiving of messages, cells have evolved

ways to maintain intracellular homeostasis while being responsive to stimulus. The class of molecules that perpetuate signals within the cell are termed second messengers and they interpret and carry out a wide array of instructions. Calcium (Ca^{2+}) is the universal second messenger and is highly regulated in the body.

Although the vast majority of Ca^{2+} is contained in our bones and teeth (1400 grams) there is a small amount in circulation and inside cells. This circulating Ca^{2+} amounts to only 10 grams but facilitates numerous processes from muscle contraction to vesicular release in neurons (Carafoli 2003). In a resting cell, typical intracellular Ca^{2+} concentrations are between 0.1 to 1.0μM, while extracellular levels are as much as 20,000 times greater (2mM) (Carafoli 1991; Clapham 2007; Strehler 2015). The concentration of Ca^{2+} within the cell must be maintained at very low levels so the cell is able to detect increases in Ca^{2+} ions and signal appropriately. If the gradient across the plasma membrane is disrupted and intracellular Ca^{2+} levels remain high this can mean death for the cell. The necessity for tight regulation over intracellular Ca^{2+} levels has led to the evolution of numerous Ca^{2+} containment and extrusion mechanisms.

Unlike proteins, Ca^{2+} ions cannot be controlled by chemical modification. Therefore, the cell employs ion adaptors or Ca^{2+} binding proteins. The most ubiquitously expressed binding protein is calmodulin (For Review: Clapham 2007). In addition to acting as a sink for Ca^{2+} in the cytoplasm, these proteins serve as downstream players in Ca^{2+} signaling cascades. Additionally, they are highly conserved across species and maintain certain structural elements that allow them to bind to Ca^{2+}. "EF hand" helix-turn-helix motifs act like the thumb and forefinger of the hand binding to the Ca^{2+} ion and are found in calmodulin and parvalbumin, two well characterized Ca^{2+} binding proteins (Clapham 2007). Another indicator of the importance of Ca^{2+} ions as second messengers is the compartmentalization of Ca^{2+} signals and the existence of Ca^{2+} adaptors that

function to decode the relatively non-specific influx of Ca^{2+} ions based on localization (Clapham 2007; Mojumder et al. 2008).

In addition to buffering Ca^{2+}, the cell utilizes pumps to maintain low intracellular Ca^{2+} levels. The Na^{+}/Ca^{2+} exchanger (NCX) is ubiquitously expressed in cells. NCX is an electrogenic exchanger that swaps three extracellular Na^{+} ions for two intracellular Ca^{2+} ions pushing Ca^{2+} ions out of the cell. However, the NCX transporter must be supplemented. Maintaining the large electrochemical Ca^{2+} gradient is critical for normal cell physiology and necessitates an energy dependent mechanism of Ca^{2+} ion expulsion. The first ATPase, Sarcoplasmic/Endoplasmic Reticulum Ca^{2+} ATPase pump (SERCA), is found in the sarcoplasmic reticulum and is used to sequester Ca^{2+} in the cell. The second class of cellular ATPases are the ATP2Bs, and they function to pump Ca^{2+} against its electrochemical gradient out of the cell. In the next section will investigate the entire class of ATPases and their role in disease.

1.6 Animal and disease models associated with ATP2Bs

ATP2Bs are ubiquitously expressed in the plasma membrane. Four paralogs are found in mammalian cells: ATP2B1, ATP2B2, ATP2B3 and ATP2B4. These proteins are highly similar but differ in their tissue expression and speed of activation. The importance of ATP2Bs for normal cellular function is indicated in several ways: Their widespread tissue expression, their role in disease, and the lack of viability of *Atp2b* null mutant mice (Tempel and Shilling 2007). In Mice: ATP2B1 and ATP2B4 are the housekeeping ATP2Bs expressed in all tissues (Strehler 2015). Null mutations of *Atp2b1* are embryonic lethal and null mutations of the *Atp2b4* gene cause problems with sperm motility (Prasad et al. 2004). ATP2B2 is expressed predominately in mouse brain and mammary glands; null mutations cause profound deafness and ataxia (Lane 1987;Street et al. 1998). In humans: genome wide association studies have linked Single Nucleotide Polymorphisms

(SNPs) in the *ATP2B1* gene to increased cardiovascular risk (Hirawa et al. 2013) and a missense mutation in the *ATP2B4* gene was recently associated with spastic paraplegia (Ho et al. 2015) . Similar to mice, a missense mutation in *ATP2B2* is associated with heightened severity of hearing loss in humans (Schultz et al. 2005; Ficarella et al. 2007). Additionally, misregulation of human *ATP2B1*, *ATP2B2*, and *ATP2B4* genes are associated with a number of cancers (For review: Roberts-Thomson 2010).

1.7 STUDIES OF *DFW* MICE IDENTIFY THE NEED FOR TIGHT REGULATION OF *ATP2B2*

The ATP2B2 protein is highly expressed in the auditory system and, due to the inherent sensitivity of sensory systems; it is an ideal model for studying the fine tuning of Ca^{2+} regulation. The *dfw* mutant mice, dfw^{2J} and dfw^{i5}, have null mutations in *Atp2b2* resulting in negligible expression of *Atp2b2* transcript and protein (Street et al. 1998; Watson and Tempel 2013) . Heterozygous mutant mice express about 50% of the normal protein levels and have significantly impaired hearing sensitivity (Watson and Tempel 2013). This suggests that one normal copy of *Atp2b2* is insufficient to produce a normal hearing phenotype and defines *Atp2b2* as haploinsufficient.

The necessity for fine tuning of the ATP2B2 protein is further revealed in studies with the original *dfw* mutant mouse. This mouse has a hypomorphic mutation in the *Atp2b2* gene which decreases, but does not completely abolish, activity of the ATP2B2 protein. Studies of pump kinetics in homozygous mutants estimate that total function of ATP2B2 is ~30% of normal animals (Penheiter et al. 2001). In heterozygous mice, total pump function is estimated to be ~65% (15% from the mutant allele) and the mice do NOT have detectable hearing loss (McCullough and Tempel 2004). This is surprising considering the small 15% increase in function over null

heterozygotes *dfw*^{2J} and *dfw*^{i5}. This narrow window for tolerable protein dysfunction exhibits the necessity for precise regulation of ATP2Bs.

1.8 CONCLUSION

In the introductory chapter we have introduced AHL and genes that are associated with this disorder. From there we introduced the digenic interaction of *Atp2b2* and *Cdh23* and discussed the importance for tight control of Ca^{2+} in all cells. The unique role of ATP2Bs was discussed in their capacity as energy dependent extrusion pumps. The second chapter of this thesis will summarize known regulatory mechanisms of ATP2Bs and investigate transcriptional regulation of these genes. The proximal promoter of *αAtp2b2* is identified and several transcription factors are implicated in the modulation of this promoter.

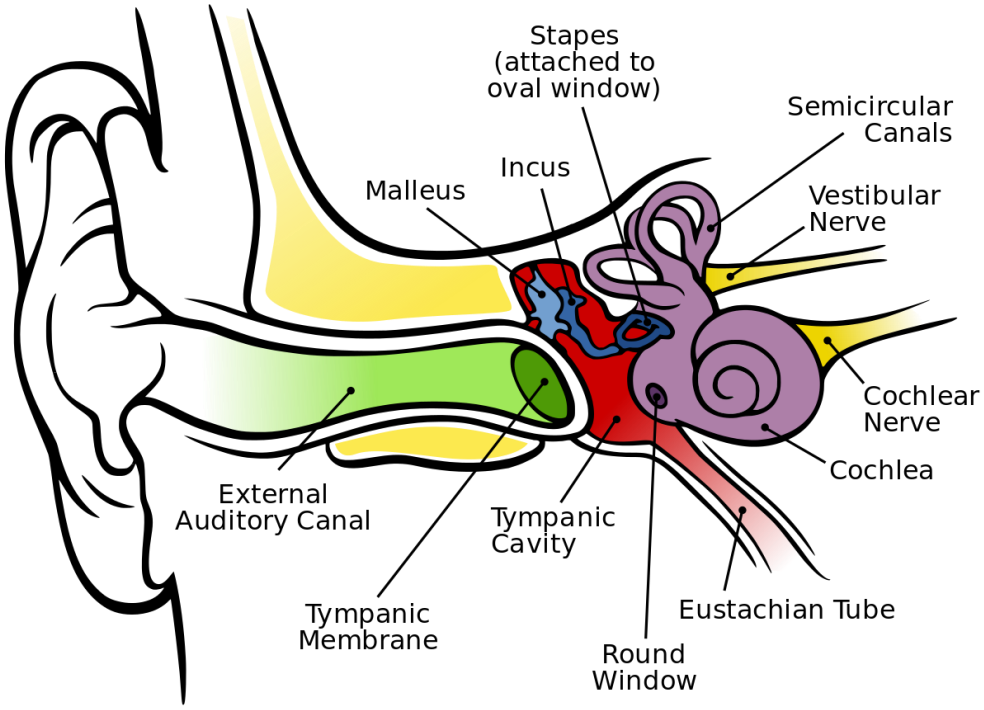

Figure 1.1. Anatomy of the ear.

Shown is a cross section of the ear (by Chittka and Brockmann 2005, used under CC BY 2.5). Sound is collected by the outer ear and travels down the ear canal. The tympanic membrane vibrates in response to sound waves. The bones of the middle ear: the malleus, the incus and the stapes move in response to the vibrations of the tympanic membrane converting the air waves into mechanical stimulus. The stapes inserts into the oval window of the cochlea, a shell shaped organ that is organized tonotopically. In humans, the base responds to high frequency sounds around 20 kHz and the apex responds to low frequency sounds around 0.1 kHz. The cochlea is a highly complex structure that converts mechanical stimulus into electrochemical impulses that are sent to the brain.

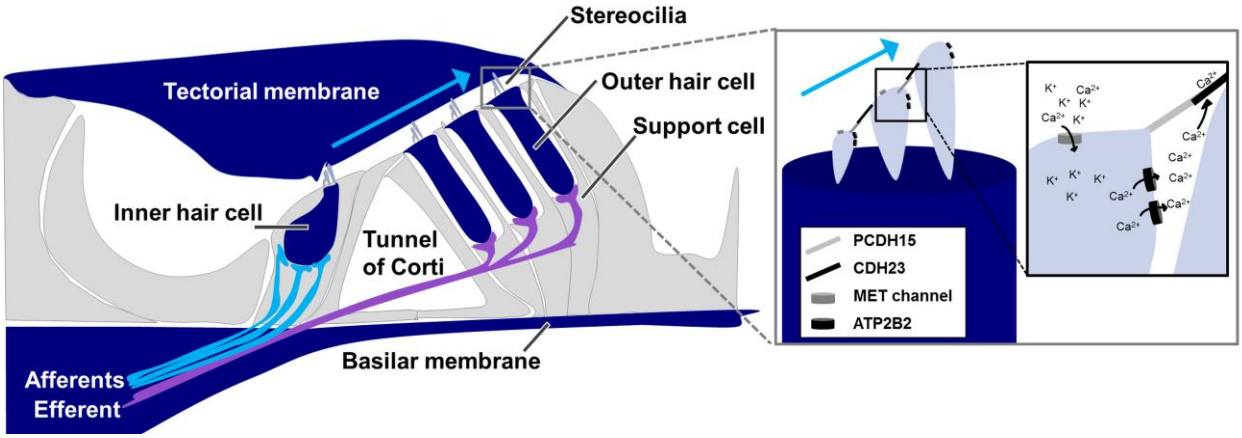

Figure 1.2. Cross section of the OC

Shown above is a cross section of the OC in the cochlea. As the stapes moves it pushes fluid in the cochlea producing pressure waves. These waves displace the basilar 'basement' membrane of the cochlea. The displacement of the basilar membrane causes movement of the hair cells. Note single row of inner hair cells and the three rows of outer hair cells. Movement of the basilar membrane causes deflection of the stereocilia which are inserted into the tectorial membrane. This deflection causes tip-links to pull in a concerted way on adjacent stereocilia (see inset) activating MET channels leading to depolarization of the hair cell. ATP2B2 pumps Ca^{2+} out of the cell maintaining endolymph Ca^{2+} levels and decreasing intracellular Ca^{2+} back to baseline. CDH23 is part of the tip-link and requires Ca^{2+} ions to maintain its structural integrity.

Chapter 2. CHARACTERIZATION OF THE *αATP2B2* PROMOTER

Summary

ATP2Bs are main regulators of intracellular Ca^{2+} levels. There are four paralogs of *Atp2bs* found in different locations of the mouse genome; the isoform encoding the protein with the fastest activation is *Atp2b2*. In mice, the *Atp2b2* transcript has several alternate TSS variants: α, β, μ and δ. These variants are expressed in a tissue and developmentally specific manner. The α and β *Atp2b2* transcripts are equally expressed in the brain; *αAtp2b2* is the only transcript found in the outer hair cells of young mice (Silverstein and Tempel 2006). A series of mouse mutations in the ATP2B2 protein indicate that tight regulation of this protein is imperative for normal cell physiology, specifically in auditory hair cells. Although ATP2Bs are important regulators of Ca^{2+} in many cell types, little is known about their transcriptional regulation. This study defines the proximal promoter elements including the 5' untranslated region (5'UTR) and a CpG island of the *αAtp2b2* transcript. Further investigations indicate that ATOH1 and EGR1 modulate promoter activity. Specifically, EGR1 increases expression of *Atp2b2* transcripts in two cell lines, one neuronal and one hair cell progenitor cell line, and binds to the CpG island of the *αAtp2b2* promoter. This study has important implications for physiology and auditory neuroscience because it (1) elucidates transcriptional regulatory mechanisms for *Atp2b2*, (2) identifies transcription factors that modulate expression of *Atp2b2* in the brain and peripheral auditory system and (3) allows for future studies of *Atp2b2* expression modulation that can exhibit the need for tight regulation of *Atp2b2* in the auditory system.

2.1 INTRODUCTION

Carefully controlling Ca^{2+} concentrations is a fundamental activity for cells. In the previous chapter we investigated a number of mechanisms that drive intracellular Ca^{2+} levels down to tolerable levels. Here we further investigate the ATP2B family of proteins. These pumps use energy to extrude Ca^{2+} fine tuning the concentration of Ca^{2+} inside and outside the cell (Carafoli 1994).

2.1.1 *Function and regulatory mechanisms of ATP2Bs*

ATP2Bs are part of a large family of P-type ATPases that utilize ATP to pump cations across cellular membranes. The "P-type" designation is given to these pumps because they auto-phosphorylate a key aspartate residue necessary for pump function. Additionally, P-type ATPases are characterized by two intermediate binding states known as E1 and E2 (Axelsen and Palmgren 1998). The ATP2Bs are the branch of this family that specifically pump the cation Ca^{2+}. These pumps exist in the apical and basal compartments of cells and may or may not have sensitivity to calmodulin (Chicka and Strehler 2003) .

The function of the pump in the cell is highly regulated by alternative splicing and the four paralogs of ATP2B undergo similar alternative splicing at two sites. The first is A-site near the N-terminus and the second is the C-site near the COOH terminus. The A-site is implicated in membrane trafficking and the C-site contains the calmodulin binding domain. Splicing at the A-site creates 3 different transcripts: w, x, and z and splicing at the C-site creates 2 alternate transcripts: a and b.

2.1.2 *ATP2B2 splicing and alternate start site variations*

Unlike the other ATP2B isoforms, ATP2B2 has an extra insert at the A-site termed the 'y' variant and, at the C-site, two exons are inserted in the 'a' variant. The A-site is implicated in membrane trafficking of ATP2B2. The 'w' spliceoform traffics to the apical membrane while the x and z spliceoforms traffic to the basolateral membrane. The mechanism for trafficking the w, x and z variants is unknown but may involve the phospholipid sensitive domain of ATP2B2 which is close to the A-splice site (Chicka and Strehler 2003).

The C-site creates the full length 'b' variant which has normal sensitivity to calmodulin and the 'a' variant which creates a truncated protein with decreased sensitivity to calmodulin (Carafoli 2011). However, in the full length protein ('b' variant) it was found that ATP2B2 is significantly less sensitive to calmodulin stimulation than ATP2B4. In fact, in auditory hair cells, the ATP2B2 variant present is the 'w/a' variant. This truncated version has lower Ca^{2+} exporting ability and little dependence on calmodulin stimulation (Carafoli 2011).

In addition to the complex splice variants found in the coding regions of the transcript, ATP2B2 has a highly regulated 5'UTR with four known alternate TSSs creating the α, β, δ, and μ transcripts. These variants are expressed in a tissue and developmentally specific manner. For instance, the α and β *Atp2b2* transcripts are equally expressed in the brain and only the *αAtp2b2* transcript is found in the outer hair cells (Silverstein and Tempel 2006) . Although there are no studies determining the role of the alternate TSS in splicing of *Atp2b2* there are other models indicating that alternate start sites can dictate splicing (Wong et al. 2010; Banday et al. 2011). Given the tissue specific expression of the TSS variants it seems likely that start site selection influences *Atp2b2* splicing.

2.1.3 *Importance of studying transcriptional regulation of ATP2Bs*

Disease models and null mutations detailed in the introduction outline the necessity for tight regulation of ATP2Bs for normal physiology. In previous sections we summarized the wealth of information that exists for post-transcriptional mechanisms regulating ATP2Bs. Although useful, this highlights the gross lack of research into the mechanisms of transcriptional initiation of ATP2Bs. To date, ATP2B1 is the only isoform with a characterized promoter (Du et al. 1995) with no studies looking at the promoter of the *Atp2b2* gene. It is clear that understanding the intricacies of ATP2B gene transcription will be important for combating the pathophysiology of disorders associated with this family of Ca^{2+} regulators. With over 30 different splice variants and 4 different genes, the ATP2B-"ome" is vast. Studying the transcriptional regulation of these genes will give researchers the necessary tools to better understand and modulate gene expression in disease states.

2.1.4 *Goals of the study*

In this section we have outlined what is known about function and regulation of ATP2Bs, specifically ATP2B2. In the next section we will investigate the promoter elements of the ATP2B family using the encyclopedia of DNA elements (ENCODE) data from the UCSC genome browser. We will further investigate the mouse *α* and *βAtp2b2* promoter elements and compare these to the human *Atp2b2* gene. Finally, we identify transcription factors that bind to and modulate expression of the *αAtp2b2* promoter, the transcript found in the auditory outer hair cells and neurons.

2.2 METHODS

2.2.1 *Cloning*

2.2.1.1 Promoter constructs:

PCR was used to amplify 5.5 kb proximal promoter in 3 pieces off of genomic DNA from the DBA/2J inbred mouse strain. Exons of the 5'UTR were amplified from cDNA of dfw^{2J} brainstem. A synthetic NcoI cut site was added to the 5'UTR at the translational start site. These four pieces were cloned into topo vectors and sequenced. They were then restriction digested into 4 pieces (Topo1: HindIII and AVRII, Topo2: AVRII and BssSI, Topo3: BssSI and Hpy99I, Topo4: Hpy99I and NCOI) and ligated into the firefly luciferase vector (PGL3) from Promega.

2.2.1.2 Transcription factor constructs:

cDNA of the transcription factors was subcloned from Addgene plasmids (ATOH1: Catalog # 33333- pMSCV-ATOH1wt-IRES-GFP, EGR1: Catalog# 11729 – pcDNA3-EGR1 and GATA3: Catalog # 1332 pcDNA-GATA3) or isolated from cDNA of mouse CB cochlear or brainstem tissue (USF1 and POU4F3). All cDNAs were ligated into the pcDNA3.1a vector with an IRES EGFP element at the 3' end. EGFP expression was noted in cells transiently transfected with the constructs. Transcription factor transfection efficiency was measured for all constructs by normalization of EGFP and transcription factor transcript to *γ-actin* (*Actg*) and *Hmbs.* We found similar transfection efficiency for each of the transcription factor constructs.

2.2.2 *Luciferase assay*

Cells were plated twenty four hours before transfection. OC-1 and OC-2 cells were plated at a density of $4x10^4$ cells per well in a 24 well plate. Cells were harvested 48 hours after transfection

with passive lysis buffer and assayed using the dual luciferase Reporter Assay System (Promega: E1910) with a manual luminometer (Promega).

2.2.2.1 Promoter expression assay

The *αAtp2b2* promoter constructs driving firefly luciferase expression (400 ng/well) were transfected into OC-1 or OC-2 mammalian cells along with an internal renilla luciferase reporter (5ng/well) using a 1:4 ratio of DNA:transfection reagent (Fugene HD, Promega: E2311) .

2.2.2.2 Transcription factor overexpression with promoter

The *Atp2b2-luciferase* promoter constructs (200 ng/ well) were co-transfected into OC-1 mammalian cells along with an internal renilla luciferase standard (2.5 ng/well) and a transcription factor expression vector (200ng/well) using a 1:4 ratio of DNA:transfection reagent (see above).

2.2.3 *Overexpression assay*

OC-1 cells (Holley Lab) were grown at 33 °C and 5% CO2 in MEM with Glutamax (41090-036, Gibco) supplemented with 10 % FBS and 50U/ml of γ-Interferon. Neuro2A cells were grown at 37 °C and 5% CO2 in DMEM (Invitrogen) supplemented with 10% FBS and 1% Streptomycin and ampicillin. All cells were plated twenty four hours before transfection in 12 well plates. OC-1 cells were plated at a density of $8x10^4$ cells per well and Neuro2A cells were plated at a density of $1x10^5$ cells per well. Transcription factor constructs were transfected at 800ng/well using a 1:3 ratio of DNA:transfection reagent. Cells were incubated with constructs for 48 hours and then harvested in 400 µl of Qiazol. mRNA was extracted using Qiagen RNeasy Universal Plus mini kit and subsequently converted into cDNA using (random hexamer: Invitrogen and SMARTscribe RT:Clontech). Baseline expression experiments utilized primers designed to recognize cDNA of specific proteins (Table 2.1) and IQ Sybr green supermix (BioRad: 170-8886) on a Bio-rad Q5

icycler or CFX96. Quantification of *Atp2b2* and *Atp2b4* expression was done using premade TaqMan gene expression assays from applied biosciences (*Hmbs* Assay ID: Mm01143545_m1, *Atp2b2* Assay ID: Mm00437640_m1, *Actg* Assay ID: Mm01963702_s1, *Atp2b4* Assay ID: Mm01285597_m1) utilizing SSO Advanced universal probes supermix (BioRad: 172-5281). Expression levels were normalized to housekeeping genes (*Hmbs* and *Actg*) for analysis (For full methods see: Silverstein and Tempel 2006).

2.2.4 *Electrophoretic Mobility Shift Assay (EMSA)*

HeLa cells (CCL-2; ATCC) were grown at 37 °C and 5% CO_2 in DMEM (11995; Invitrogen) supplemented with 10% FBS and 1% ampicillin/streptomycin. HeLa cells were grown to confluency in two T-75 flasks and extracted using trypsin. Cells were thoroughly washed and nuclear extracts were isolated using cell extraction buffer (Thermofisher scientific: FNN0011). Protein concentration was determined using a bicinchoninic acid (BCA) Protein Assay Reagent kit (Thermofisher scientific: 23227). The EMSA was performed using the LightShift Chemiluminescent EMSA protocol (catalog number 21048; Thermoscientific) with 18 µg of HeLa nuclear extract per 20µl reaction. The reactions were incubated at room temperature for 30 minutes without the addition of the biotin labeled probe. Upon addition of the biotin labeled probes, the reactions were incubated for another 30 minutes. For the supershift assays, 2ug of antibody was added to the reaction prior to the addition of biotin labeled probes and incubated for 30 minutes. The EGR1 antibody was purchased from Abcam (catalog # ab174509, Rabbit polyclonal IgG to N-terminus). The ATP2B2 negative control antibody was purchased from ThermoFisher (Catalog#: PA1-915; Rabbit polyclonal IgG). The reactions were electrophoresed in 0.5% TBE on 5% polyacrylamide gels. The gels were run at 4 °C for 2.5-3 hours at 60 volts. Gels were transferred at 350 milliamps for 1 hour at 4 °C to Biodyne B nylon membranes (catalog # 77016;

Pierce), cross-linked for 15 minutes with 312nm bulbs. Gels were visualized using the Chemiluminescent Nucleic Acid Detection Module (catalog # 89880; Thermoscientific). Double-stranded DNA probes were made by boiling complimentary single-stranded probes at a concentration of 25um in annealing buffer for 5 min in 1 liter of boiling water. The boiling water was removed from the heat and the tubes were allowed to slow cool to room temperature. The EGR1 positive control was designed based on the canonical binding site for EGR1, the other positive control was purchased from Santa Cruz (catalog # SC-2529). All other probes were developed using binding site predictions and consensus information from Motifmap, MatInspector and tfbind. Biotin labeled probes were purchased from IDT (Table 2.2).

2.3 RESULTS

2.3.1 *Genomic modifications at Atp2bs indicate transcriptional hot-spots*

The genomic region surrounding *Atp2b2* is vast and complex. With 22 exons and 4 alternative TSSs there are a number of opportunities for regulatory modulation. Of the four distinct *Atp2b2* transcripts α and β are the neuronal transcripts and α is the primary transcript of the outer hair cells (Silverstein and Tempel 2006). The genomic region surrounding *αAtp2b2* and *βAtp2b2* transcripts in mice and humans can be seen in figures 2.1 and 2.2 respectively. These transcripts share the same coding exons but differ in their 5'UTR. The *αAtp2b2* transcript has 3 exons (Iα, IIα, IIIα) and the *βAtp2b2* transcript has one exon downstream of the *αAtp2b2* exons (Iβ) (Fig. 2.1). The human *Atp2b2* gene has a similar architecture with three exons for α*Atp2b2*and a unique coding exon for *βAtp2b2* (Fig. 2.2).

Utilizing the UCSC genome browser and ENCODE data, we compared regulatory elements of the *Atp2b2* gene in mouse and human. The region directly surrounding the Iα and Iβ exons of mouse both contain predicted CpG islands; known transcriptional initiation sites for ubiquitously expressed genes (Fig. 2.1) (Lenhard et al. 2012). The human *Atp2b2* promoters also contains CpG islands suggesting a similar mechanism of transcriptional initiation (Fig. 2.2).

Next we looked at two mouse tissues, heart and cerebellum, to identify transcriptionally active domains in the *Atp2b2* gene. Chromatin features of interest included DNase I hypersensitivity (DHS), an indication of uncoiled, accessible DNA; RNA polymerase II (RNA Pol II) occupancy, the enzyme that transcribes DNA into RNA; and histone 3 lysine 4 trimethylation (H3K4me3), a hallmark of transcriptionally active promoters. The heat map for the region surrounding the 5' end of *Atp2b2* reveals several distinct signals in 8 week-old mouse cerebellum indicative of active transcription that are not detected in 8 week-old mouse heart (Thurman et al. 2012) (Fig. 2.1). In

particular, the regions directly surrounding the noncoding Iα and Iβ exons contain significant levels of H3K4me3 and RNAP II binding and coincide with predicted CpG islands. Together these data suggest that α*Atp2b2* and *βAtp2b2* transcripts are both transcribed in the cerebellum and have unique promoters and start sites allowing for differential regulation and tissue specific expression. We have elected to focus on *αAtp2b2* transcript because of its unique expression profile in the brain and sensory epithelium.

2.3.2 *Identifying the promoter of the αAtp2b2 transcript*

The location of the CpG islands and pattern of histone methylation in the cerebellum suggests that promoter elements are likely located directly upstream of the *αAtp2b2* TSS. To test this empirically, the 5'UTR and 5kb region containing the CpG island were cloned into a luciferase reporter vector (Fig. 2.3). All constructs are numbered relative to the TSS, which maps to the negative strand of Chr 6 at base 114,042,026 (verified NCBI and Ensembl). The "full-length" α*Atp2b2* promoter construct contains 5,399 bases located directly upstream of the TSS from 114,042,027 [closest to TSS] to 114,047,365 [farthest from TSS]. Only the exons of the 5'UTR were included in the construct, the 5'UTR spans approximately 200kb of the genome (Fig. 2.3).

A panel of 10 sensory epithelium and neuronal derived mouse cell lines were screened for expression of *Atp2b2* transcripts to identify the best cell line for luciferase promoter assays. Only the Immortomouse OC derived cell line (OC-1) and the neuroblastoma cell line Neuro-2A (N2A), expressed detectable levels of *Atp2b2*. We decided to use OC-1 cells and the related OC-2 cells for our promoter characterization studies (Rivolta and Holley 2002) . A series of α*Atp2b2* luciferase reporter constructs were transiently transfected into OC-1 and OC-2 cell lines. The fold change in promoter activity over empty pGL3 vector was determined (Fig. 2.4). The greatest amount of luciferase activity above background was observed with the shortest promoter construct

containing sequences from –287 to +572 relative to the TSS. The inclusion of an additional 500 base pairs of 5' sequence (+572/-855) had no detectable effect on promoter activity. When the length of the promoter fragment was extended further in the 5' direction, the amount of luciferase activity began to decrease until it reached baseline levels. Reversing the orientation of the promoter or removal of the 5'UTR and CpG islands completely abolished any detectable activity (Fig. 2.4). These data demonstrate that the 5'UTR and CpG islands are necessary and sufficient for promoter activity. This maps the core promoter between +572 to -287 bases upstream of the TSS. The remaining proximal promoter region most likely contains important tissue specific enhancer and repressor elements.

2.3.3 *ATOH1, EGR1, GATA3, POU4F3, and USF1 may bind the αAtp2b2 promoter*

Binding prediction software, MatInspector and tfbind (Tsunoda and Takagi 1999; Cartharius et al. 2005) were used to predict transcription factor binding sites in the proximal promoter of the *αAtp2b2* transcript. The entire region (-5399 to +572bps) was analyzed and is predicted to bind thousands of transcription factors. To narrow down likely candidates, OC-1 cell line cDNA was analyzed for expression of factors that were present in the luciferase assay (Fig. 2.5). Data was cross referenced with published microarray data (From: Rivolta 2002) . Then, their expression profiles in sensory epithelium were investigated using the Shared Harvard Inner Ear Laboratory Database, SHIELD (Shen et al. 2015). Figure 2.6 summarizes this data for the transcription factors tested. *Atoh1*, *Gata3* and *Pou4f3* are necessary for hair cell development and maintenance (van der Wees et al. 2004; Hertzano 2004; Alvarado et al. 2009; Pan et al. 2012). Usf1 plays roles in metabolism, tissue repair and cancer (Horbach et al. 2015). Early Growth Response Element 1 (EGR1) is an immediate-early gene that is involved in synaptic plasticity, retinal formation and is involved in acoustic trauma pathways and potentially plays a role in hair cell regeneration (Wei et

al. 2000; Lomax et al. 2001; Hawkins et al. 2007; Schippert et al. 2009; Smith and Rajadinakaran 2013; Hu et al. 2014).

Although MatInspector and tfbind software did not predict the binding of POU4F3 or ATOH1 to the α*Atp2b2* transcript promoter, manual investigation of the region identified potential binding sites for each of these transcription factors (Fig.2.6 A). In the α*Atp2b2* transcript promoter at site -1509 to -1516 there is a predicted binding site for POU4F3: ATTAATCA based on its core consensus sequence: ATTAATKA (Daily et al. 2011). This sequence is only found once in the α*Atp2b2* promoter and is not found at all in the 5kb proximal promoter of the *βAtp2b2* transcript. There is also a predicted ATOH1 binding site at -175 to -182: CTCATGGC based on the core consensus sequence: CASCTGKY (Daily et al. 2011). Although there were numerous binding site predictions for EGR1, the site selected is located in the CpG island, it was predicted with high probability by both tfbind and MatInspector software and is a clustering of several predicted sites (Fig. 2.6 A). Gata3 and Usf1 had only one high probability predicted binding site within the CpG island.

2.3.4 *EGR1 and ATOH1 modulate the isolated αAtp2b2 promoter in OC-1 Cells*

To determine which of these transcription factors binds to and modulates the α*Atp2b2* transcript promoter, cDNA of the candidate transcription factors was cloned into a pcDNA3.1a vector upstream of IRES+EGFP. These vectors were co-transfected into OC-1 cells along with the α*Atp2b2* luciferase reporter containing bases +572 to -2133. The [+572/-2133] construct was used because it contains all of the potential binding sites for the transcription factors and is the longest promoter construct that shows activity over baseline in the OC-1 cell line. Figure 2.6 shows the region in detail with the location of transcription factor binding sites and the CpG island. The transfection assays revealed that GATA3, POU4F3 and USF1 had no effect on promoter activity.

(Fig. 2.7). ATOH1 moderately decreased α*Atp2b2* promoter activity while EGR1 produced a significant 2-fold increase (Fig. 2.7).

2.3.5 *Identifying the region of EGR1 binding in the αAtp2b2 promoter*

EGR1 is capable of activating the [+572/-2133] construct in a neuronal and a sensory epithelium cell line, indicating functional significance in a mammalian cell model. To map the location of potential EGR1 binding sites within the promoter, three different luciferase reporter constructs with activity over baseline: [+572/-287], [572/-855], and [+572/-2133] were co-transfected with EGR1 or empty vector into OC-1 cells. All three constructs showed a significant increase in luciferase activity with co-expression of EGR1 (Fig. 2.8). These data suggest that the EGR1 may bind in the region between +572 to -287 bases of the TSS. Due to limitations of restriction sites in this region, putative binding sites for EGR1 were not narrowed further, especially given that removal of the CpG island abolishes promoter activity. Additionally, mutagenesis was not performed because putative EGR1 binding sites are contained in the 80% GC rich CpG island making amplification, manipulation and sequence verification unreliable.

2.3.6 *EGR1 effects endogenous levels of Atp2b2 transcript*

The luciferase results indicate that EGR1 and ATOH1 have a functional effect on the isolated *αAtp2b2* transcript promoter. This observation does not necessarily reflect how these transcription factors behave in the endogenous cell system. To test their effects on native *Atp2b2* transcript expression, EGR1 and ATOH1 were overexpressed in N2A and OC-1 cells that transcribe *Atp2b2* endogenously. Due to the low basal levels of *Atp2b2* expression, TaqMan assays with high target specificity and accuracy were utilized. However, this approach does not discriminate between the different *Atp2b2* transcripts so only changes in total *Atp2b2* transcript levels were quantified. It is

known that ATP2B2 proteins are able to compensate for one another and both N2A and OC-1 cells express large amounts of *Atp2b4*. *Atp2b4* is found in the cochlea, at low levels in murine hair cells at P-12 (Furuta et al. 1998; Watson et al. 2014; Shen et al. 2015) and ubiquitously in the rest of the body. Thus, we also monitored the expression levels of both *Atp2b2* and *Atp2b4*.

In OC-1 and N2A cells, EGR1 increased the transcript levels of *Atp2b2* compared to the empty vector, recapitulating our luciferase results (Fig. 2.9A, B). ATOH1 expression did not recapitulate the slight inhibition of *Atp2b2* transcription detected in the luciferase assay (Fig. 2.9A, B). In OC-1 and N2A cells, EGR1 did not affect *Atp2b4* transcript expression (Fig. 2.9C, D). However, ATOH1 significantly increased *Atp2b4* transcript in OC-1 cells (Fig. 2.9C). This increase appears to be cell type specific given that ATOH1 overexpression does not affect *Atp2b4* transcript expression in N2A cells (Fig. 2.9D).

2.3.7 *Shift assays indicate that EGR1 binds to the αAtp2b2 promoter at [-71 to -98]*

To identify potential EGR1 binding sites, data from MatInspector was cross-referenced with the tfbind software predictions with matrix similarity of 0.75 or higher (highest predicted binding being 1.0). The result was 26 predicted sites with 17 located near the CpG Island in clusters. (Fig. 2.6). Three overlapping sites in the CpG Island (found [-71 to -98] base pairs upstream of the TSS) were of particular interest (Fig. 2.6). EMSAs were performed to experimentally test the protein binding potential of these sites. Two positive control DNA probes were designed. The Canonical probe (Can) was designed using the EGR1 consensus sequence, the second was purchased from Santa Cruz (SC) (Cao et al. 1993; Daily et al. 2011) (Table 2.2). EGR1 protein levels were measured in OC-1, HeLa and NIH/3T3 cells by immunoblotting. Protein expression of EGR1 was not detectable in OC-1 cells (data not shown) or in NIH/3T3 cells (Fig. 2.10A). EGR1 was found in the nucleus and cytoplasm of HeLa cells (Fig. 2.10A).

All EMSAs were performed using HeLa cell nuclear extracts (Fig. 2.10B, C). No protein binding activity was detected with two tests probes for sequences either downstream or at the TSS (data not shown). A mobility shift is observed only with the DNA probe that included the CpG island located upstream of the TSS [-71 to -98] (Fig. 2.10B). Formation of this shifted DNA-protein complex is inhibited when increasing concentrations of the unlabeled [-71 to -98] DNA probe was added as competitor. Four nucleotides in EGR1 binding cluster of the [-71 to -98] probe were modified to investigate sequence specificity of binding (Table 2.2). Introduction of these mutations into the [-71 to -98] probe completely abolished protein binding when compared to the wild-type probe (Fig. 2.10C). To determine if EGR1 is the protein responsible for the mobility shift, antibody targeting EGR1 was added to the binding reactions. For these assays, the shifted complexes were resolved into 3 distinct populations. The formation of complex II was dramatically inhibited upon addition of the EGR1 specific antibody but not the negative control antibody targeting ATP2B2 (Fig. 2.11). These results suggest that EGR1is binding to the [-71 to -98] probe in a sequence specific manner to stimulate *αAtp2b2* promoter activity.

Although there are different populations (I and III) that remain bound to the probe in the presence of EGR1 antibody it is likely that this is non-specific binding or it is binding of the probe to a protein besides EGR1 and there are a number of predicted SP1 binding sites in the CpG island. Previously published experiments have exhibited the similarities between binding sites for SP1 and EGR1 and it therefore seems plausible that this is the identity of the protein found in the mobility shift assay (Deckmann et al. 2012; Consortium 2012). Given the ubiquity of SP1 it is likely that it plays a role in regulation of the *αAtp2b2* promoter and other CpG island promoters such as *βAtp2b2*.

2.4 DISCUSSION

The Ca^{2+} ATPases play an important role in maintaining homeostasis of the cell but little is known about initiation of transcription of these genes. *Atp2b2* has the fastest activation and is one of the primary ATP pumps found in the brain and sensory epithelium. Investigations of this gene have highlighted it's pivotal role in normal function of the auditory system as well as the vestibular system (Street et al. 1998; Konrad-Martin et al. 2001; Wood et al. 2004; Silverstein and Tempel 2006; Bortolozzi et al. 2010; Watson and Tempel 2013). Of the two transcripts found in the brain, only the *αAtp2b2* transcript is found in the outer hair cells of young mice. This study focused on the α transcript because of its unique and pivotal role on the normal function of the auditory system.

2.4.1 *The αAtp2b2 promoter and upstream repressor elements*

Studies of the genomic region surrounding the *Atp2b2* gene indicate that the minimal promoter of the α transcript is likely located directly adjacent to the TSS. Luciferase assay data has narrowed this down to the region 855-2133 base pairs upstream of the TSS. This, taken together with the abolishment of activity upon removal of the CpG island and the 5'UTR, leads to the conjecture that the minimal promoter elements are contained in the region +572 to -287 base pairs around the TSS. Interestingly, OC-1 Cells, which have a low basal expression of *Atp2b2*, show activation of the promoter out to 2133 base pairs upstream of the TSS whereas OC-2 cells show activity over baseline only out to 855 base pairs upstream of the promoter. It is possible that this decrease in activity is due to repressor elements upstream of 855 base pairs. This is supported by the predicted binding of MAF1 at numerous sites in the promoter, this transcription factor is a known transcriptional inhibitor (Cieśla and Boguta 2008).

2.4.2 *Developmental expression patterns of Atoh1 and Atp2b4*

αAtp2b2 proximal promoter activity decreases moderately when ATOH1 is expressed in OC-1 cells and endogenous expression data indicates that it causes increased expression of *Atp2b4* transcript. Upon further investigation, it is noted that expression of *Atoh1* transcript peaks in outer hair cells around postnatal day 0 while *Atp2b4* is only detected at E16 and P0. Although it appears that ATOH1 plays a role in modulation of *Atp2bs* in OC-1 cells, it does not have an effect in the N2A cell line. This suggests that the effects of *Atho1* are cell type specific. This is expected given that ATOH1 is specifically expressed in hair cell progenitors and is necessary for hair cell development (Bermingham et al. 1999; Pan et al. 2012).

2.4.3 *EGR1 plays a crucial role in auditory pathways*

EGR1 increases expression of *Atp2b2* in both OC-1 and N2A cells. The low level of *Atp2b2* expression in both of these cell lines speaks to other forms of transcriptional initiation given that they both endogenously express EGR1. Interestingly, the effect of EGR1 on expression seems specific to *Atp2b2* as overexpression had little to no effect on the expression of *Atp2b4* in either OC-1 or N2A cells. EGR1 is an immediate-early gene that is involved in synaptic plasticity, retinal formation and the acoustic trauma pathways. Interestingly, it has been implicated in auditory hair cell regeneration pathways (Wei et al. 2000; Lomax et al. 2001; Hawkins et al. 2007; Schippert et al. 2009; Smith and Rajadinakaran 2013; Hu et al. 2014). This verifies the importance of the ATP2B2 pump in signaling and developing cells, which have a high metabolic load and require efficient methods of Ca^{2+} expulsion.

2.4.4 *Gene interplay of ATP2Bs in response to transcription factors*

Study of the expression profiles of *Atp2b2* and *Atp2b4* transcript in response to EGR1 and ATOH1 overexpression elucidate an interesting interplay between these two genes. It is known that ATPases compensate for each other in knockout animals (Prasad et al. 2004) and notably, when the *Atp2b2* gene is knocked out in mouse, ATP2B4 can be found in the stereocilia of the hair cells (Wood et al. 2004). Additionally, we compared the proximal promoters of the four *Atp2b* paralogs and found that the *Atp2b4* gene is the only *Atp2b* that does not have a predicted CpG island upstream of the TSS. This unique promoter composition may explain why ATP2B4 is able to compensate for ATP2B2 in the stereocilia of the hair cells when the other CpG ATP2Bs do not (Fig. 2.12). Given this data, there is likely a developmental or compensatory interplay between these two transcripts.

2.4.5 *Characterization of the αAtp2b2 promoter enables gene modulation*

In this chapter of the thesis, we identify the proximal promoter elements of *αAtp2b2*. This is the first investigation of the promoter of the *Atp2b2* gene and is the second investigation of a promoter of the *Atp2b* family. Further investigations indicate that ATOH1 and EGR1 modulate promoter activity. Specifically, EGR1 increased expression of *Atp2b2* transcripts in two cell lines, one neuronal and one hair cell progenitor cell line. EGR1 was also found to bind to a specific sequence 71 bases upstream of the TSS in the CpG island of the *αAtp2b2* promoter. Interestingly, there appears to be interplay between *Atp2b2* and *Atp2b4* transcript expression in OC-1 cells. This reinforces previous studies showing that ATP2B4 is upregulated to compensate for *Atp2b2* null mutants (Wood et al. 2004). This study has important implications for physiology, neuroscience and auditory neuroscience because it (1) elucidates transcriptional regulatory mechanisms for

αAtp2b2 (2) identifies transcription factors that modulate expression of *αAtp2b2* in the brain and peripheral auditory system and (3) allows for future physiology studies involving modulated expression of the *αAtp2b2* promoter. In the next chapter we will investigate other transcriptional mechanisms that regulate the *Atp2b2* gene and compare them in two inbred mouse strains, CB and B6.

Table 2.1. qPCR primers for transcription factors.

Primer Name	Primer Sequence
Actg F	5’ - GAA GGA GAT CAC AGC CCT AGCA - 3’
Actg R	5’ - GAC AGT GAG GCC AGA ATG - 3’
Hmbs F	5’ - CAG GCC ACC ATC CAG GTC - 3'
Hmbs R	5’ - GAA TGT TCC GGG CAG TGA TT - 3'
Atoh1 F	5’ - GAG TGG GCT GAG GTA AAA GAG T - 3'
Atoh1 R	5’ - GGT CGG TGC TAT CCA GGA G - 3'
Egr1 F	5’ - CCT ATG AGC ACC TGA CCA CA - 3'
Egr1 R	5’ - AGC GGC CAG TAT AGG TGA TG - 3'
Gata3 F1	5’ - AAC CAC GTC CCG TCC TAC TA - 3'
Gata3 F2	5’ - GGC TAC GGT GCA GAG GTA TC - 3'
Gata3 R	5’ - GAT GGA CGT CTT GGA GAA GG - 3'
Pou4f3 F	5’ - ATG CGC CGA GTT TGT CTC - 3’
Pou4f3 R	5’ - GGC TTG AAC GGA TGA TTC TT - 3'
Usf1 F	5’ - CTG AAA CCG AAG AGG GAA CAG - 3'
Usf1 R	5’ - GTT GGG GTC AGG AAA AGT GG - 3'
Usf1 F2	5’ - CAG GGC TCA GAG GCA CTA CT - 3'
Usf1 R2	5’ - GGG AAT AAG GGT GGG TCC T - 3'

The following primers were used to quantify gene expression in OC-1 and N2A cells.

Table 2.2. Probe sequences for shift assays.

EGR1 Probes	**Sequence**
[-71 to -98]	GCC CGA GGG GAG CGG GGG AGG AGA GAG C
Mutant [-71 to -98] (Mutant)	GCC CGA *A*GG *T*AG C*A*G GG*T* AGG AGA GAG C
Santa Cruz Positive Control (SC)	CGA CGC TGC GTG GGC GGA GCG GGG GCG A
Canonical Positive Control (Can)	GGA TCC AGC GGG GGC GAGCGG GGG CGA

The SC positive control probe was purchased from Santa Cruz. The Canonical Positive control probe was designed utilizing the canonical consensus sequence found on motif map (Daily et al. 2011).

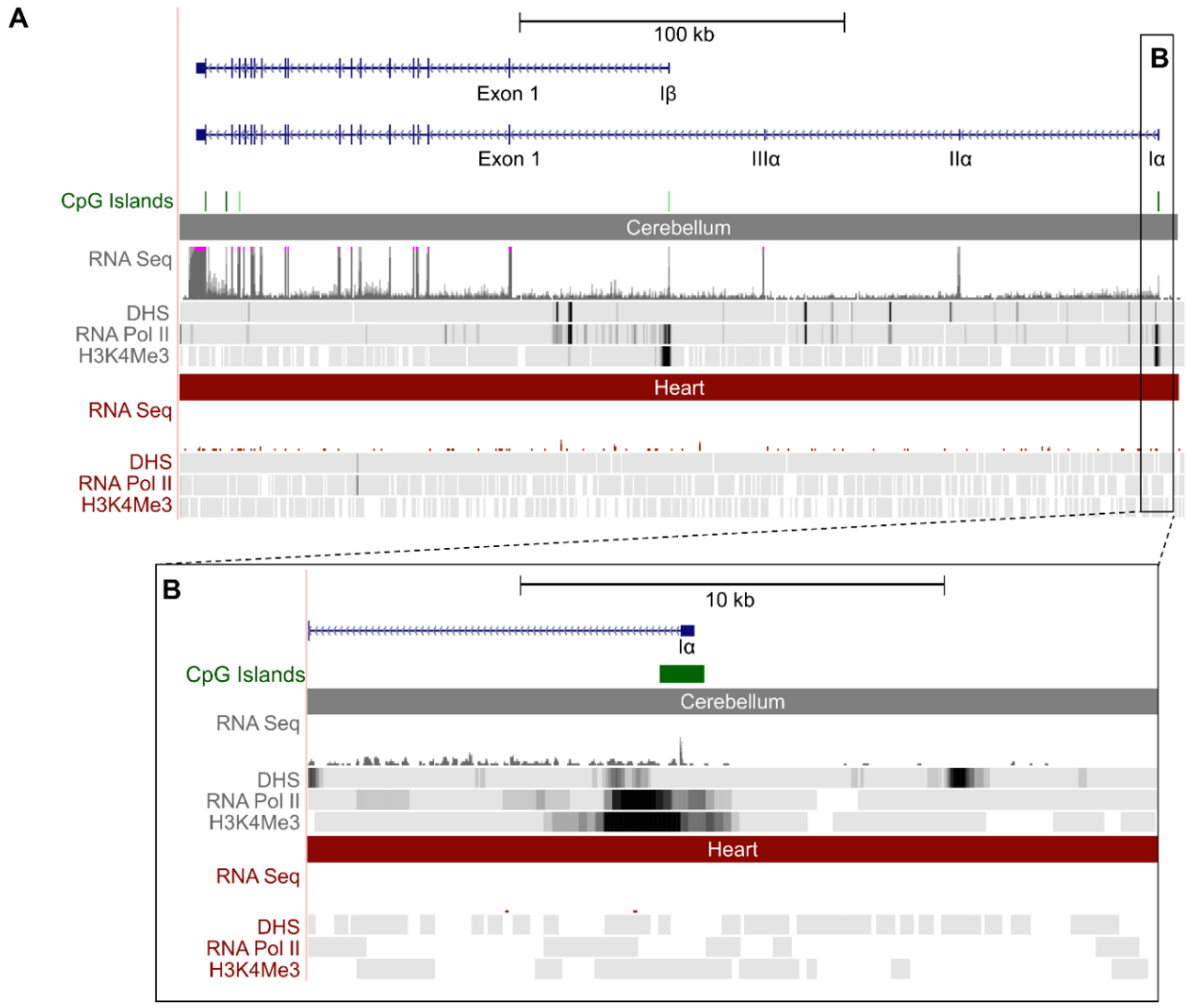

Figure 2.1. Mouse *Atp2b2* genomic region adapted from the UCSC genome browser

Atp2b2 transcripts are shown in blue. A. The whole genomic region surrounding *Atp2b2* is shown. Marks for transcriptional modulation are shown in 8 week-old mouse cerebellum vs 8 week-old mouse heart tissue. RNA-seq data shown suggests that both the α and β transcripts of *Atp2b2* are expressed in the Cerebellum. Neither transcript appears to be expressed in the heart. These two tissues give a good contrast for the activation and inhibition marks. DHS, RNA polymerase II binding (RNA Pol II) and H3K4Me3 are markers of transcriptional activation. B. The region surrounding the *αAtp2b2* transcript is expanded to show more detail (Consortium 2012).

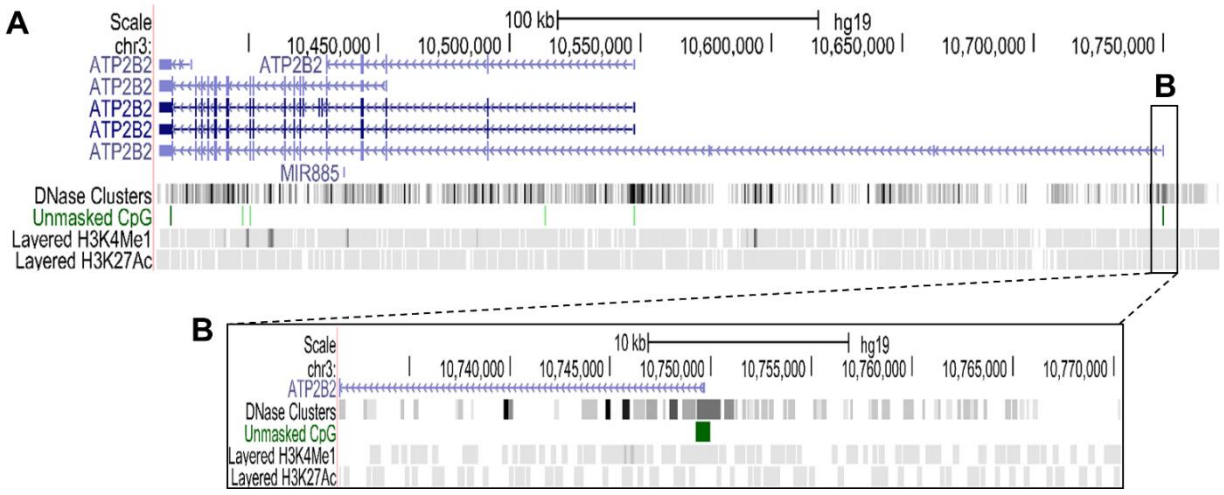

Figure 2.2. Human *Atp2b2* genomic region adapted from the UCSC genome browser

Atp2b2 transcripts are shown in blue. A. The whole genomic region surrounding *Atp2b2* is shown. Marks for transcriptional modulation are shown in human cell lines. Histone modifications shown are markers of transcriptional activity. B. The region surrounding the *αAtp2b2* transcript is expanded to show detail including a prominent CpG island (Consortium 2012).

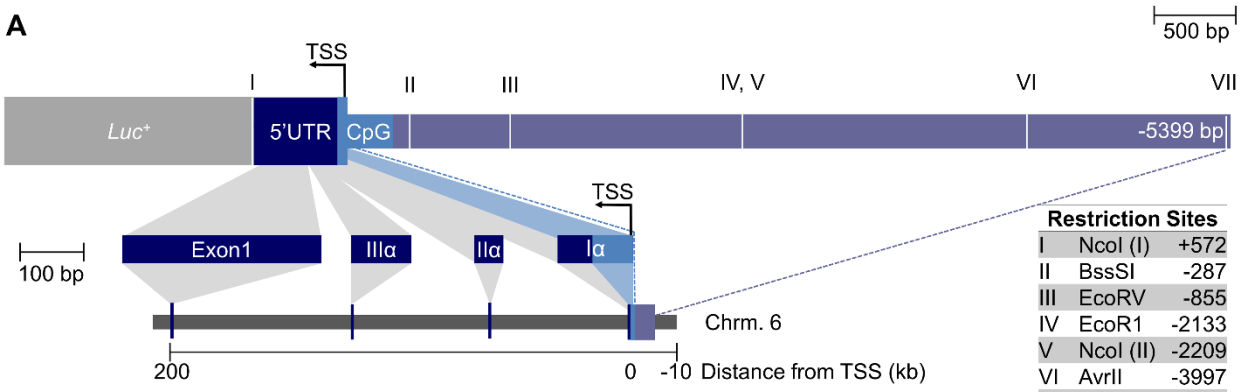

B

Construct elements		Genomic location	Construct location	Size (bp)
5'UTR	Exon 1	113,842,332 - 113,842,645	+572 to +260	313
	IIIα	113,920,509 - 113,920,603	+259 to +165	95
	IIα	113,980,542 - 113,980,587	+164 to +119	46
	Iα	114,041,909 - 114,042,026	+118 to +1	118
Proximal Promoter		114,042,027-114,047,365	-1 to - 5399	5399

Figure 2.3. Promoter construct cartoon with genomic location

A: Map of gene location for the α*Atp2b2* promoter elements and restriction sites. The gene for *Atp2b2* is located on the reverse strand. This schematic represents the full promoter construct cloned into the luciferase reporter vector. The full proximal promoter construct contains the 3 exons of the 5'UTR (Iα, IIα, IIIα) and the 1st translated exon (Exon 1) up to the translational start. Together these exons account for about 572 bases in the total construct. The rest of the ~5 kb construct contains the DNA directly upstream of the Iα exon (purple bar). The CpG island is contained between +62 and - 219 bases around the TSS (blue bar). The restriction sites used to create promoter construct truncations are indicated by roman numerals on the cartoon, their exact locations can be found in the table at the right. B: The genomic location, construct location and size of each element of the promoter construct are outlined in the table.

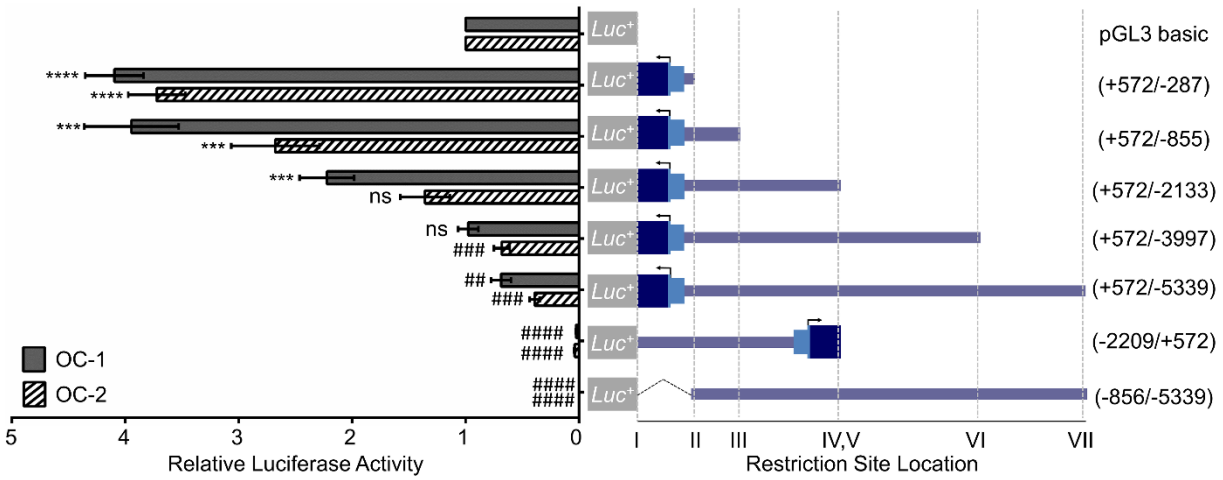

Figure 2.4. The *αAtp2b2* minimal promoter is contained in the 5'UTR and CpG island

The promoter is directional. Transcription is not initiated without the CPG island and the 5'UTR. Activator elements are contained within the first 1.5-2.5 kb of the promoter. Based on evidence from this figure, elements upstream of 2.5kb seem to be inhibitory. Comparisons to the pGL3 empty luciferase vector were done using students two-tailed t test (* indicates greater than baseline, # indicates less than baseline: $P \leq 0.05$*$P \leq 0.01$**, $P \leq 0.001$***, $P \leq 0.0001$****). Error bars indicate average of data and SEM.

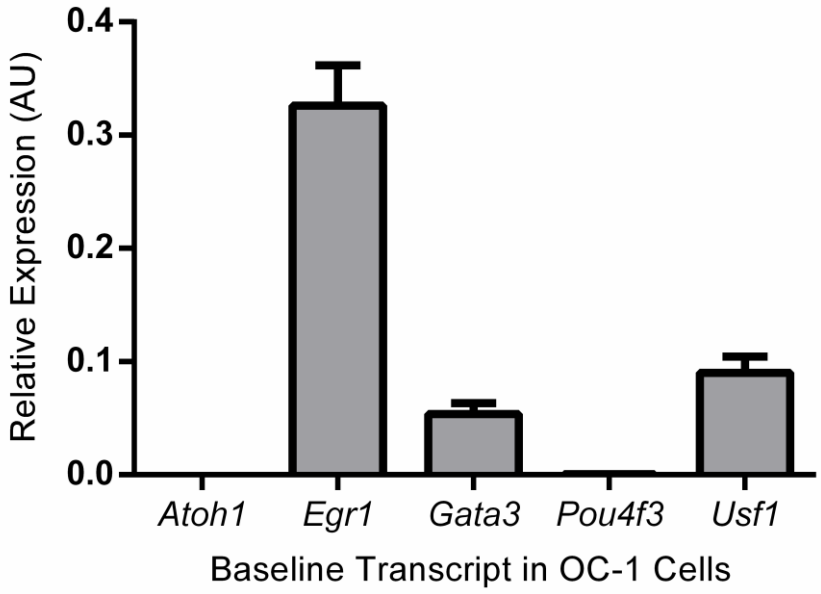

Figure 2.5. OC-1 baseline expression of transcription factors

Shown here is the gene expression of transcription factors of interest in the OC-1 cell line. This indicates that *Egr1, Gata3* and *Usf1* transcripts are expressed in OC-1 cells and suggests that the associated proteins were probably found in the cells during the luciferase assays. This indicates a potential role for these transcription factors in activation of the *αAtp2b2* promoter. Error bars indicate average of data and SEM.

A

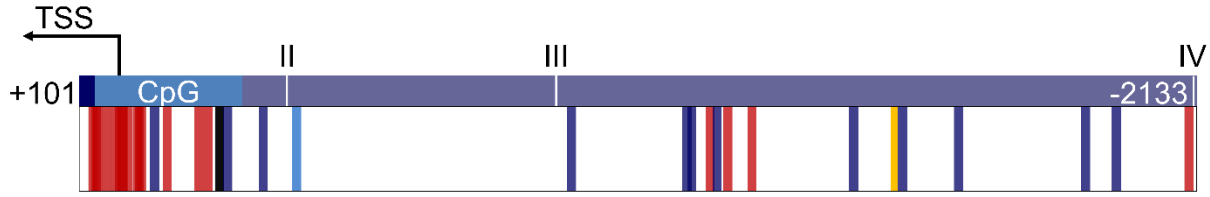

B

TF	Symbol	OC-1 Expression	HC Expression
Atoh1		NO	YES
Egr1		YES	YES
Gata3		YES	YES
Pou4f3		YES/NO	YES
Usf1		YES	YES

Figure 2.6. Transcription factors of interest and their *αAtp2b2* promoter binding sites

Transcription factors were selected based on a multi-faceted in silico search. Predicted binding sites were identified manually for POU4F3 and ATOH1. Binding sites for GATA3, USF1 and EGR1 were identified using tfbind and MatInspector software. Hair cell expression and enrichment was determined utilizing the SHIELD database. Expression in OC-1 was determined utilizing qPCR and cross-referenced with published microarray data (Tsunoda and Takagi 1999; Rivolta 2002; Cartharius et al. 2005; Shen et al. 2015).

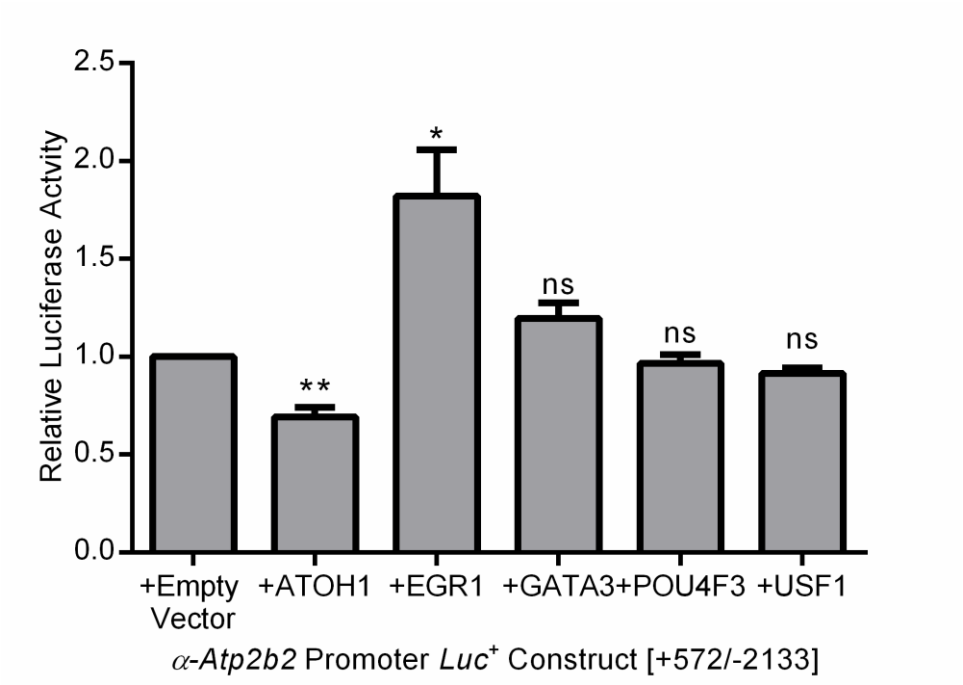

Figure 2.7. Transcription factors affect *αAtp2b2* promoter activity

Luciferase activity was normalized to promoter construct co-transfected with empty vector. Values were compared to a theoretical value of 1 utilizing a one-sample t test (*P $\leq$ 0.05, **P $\leq$ 0.01) Note: Gata3 is ns but has a P=0.0874. Error bars indicate average of data and SEM.

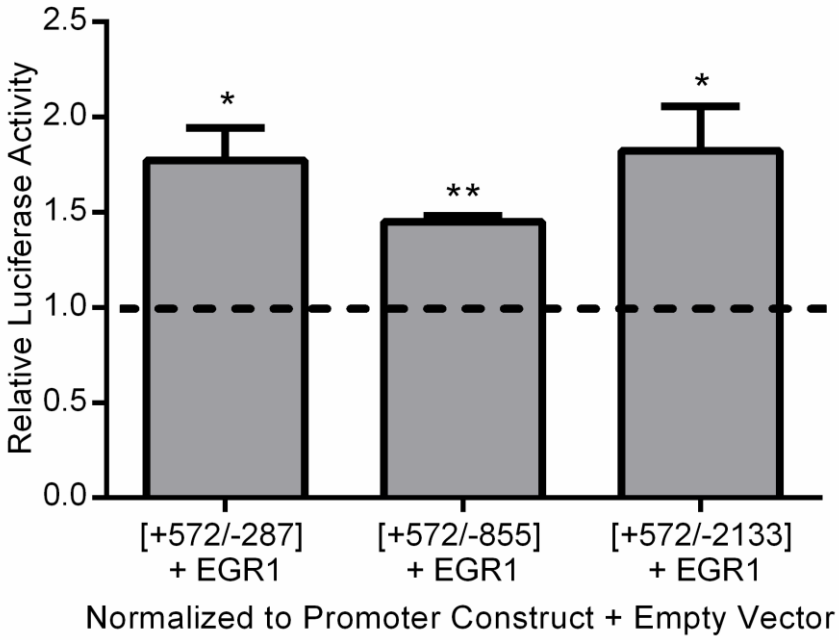

Figure 2.8. EGR1 likely binds in the CpG Island

EGR1 Activation was compared in three promoter truncations to narrow down the region of EGR1 activity. The promoter constructs were co-transfected with EGR1 or Empty vector. The ratio shown is comparing the luciferase activity of the promoter co-transfected with EGR1 over the luciferase activity of the promoter construct co-transfected with empty vector. Normalized values were compared to a theoretical value of 1 using a one sample t-test. Activation occurs over baseline promoter activity in all three constructs suggesting that the binding site is contained in the region of the CpG island (*$P \leq 0.05$ and **$P \leq 0.01$). Error bars indicate average of data and SEM.

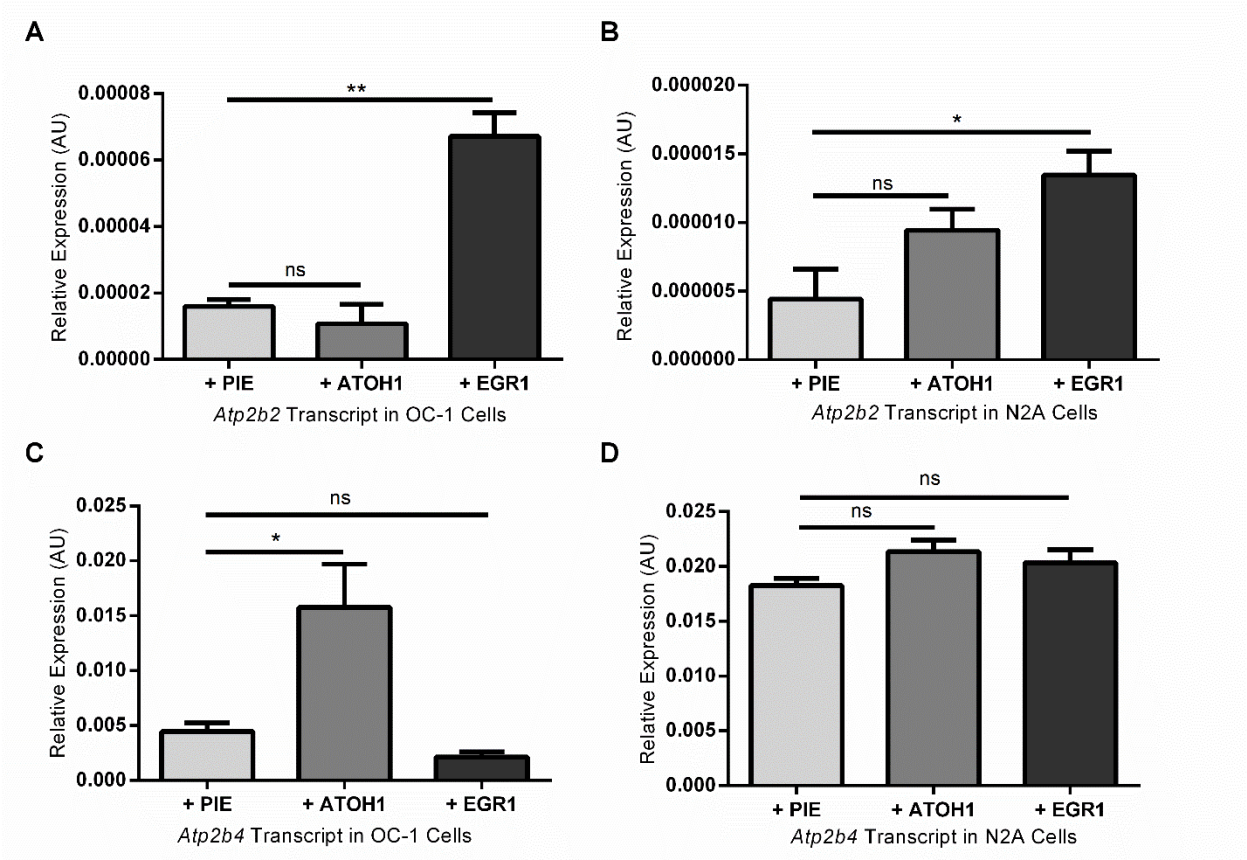

Figure 2.9. ATOH1 and EGR1 effect expression of *Atp2b2* and *Atp2b4*

A, B: EGR1 increases expression of *Atp2b2* transcript in both OC-1 and N2A cells compared to pcDNA empty vector + IRES-EGFP (PIE). ATOH1 has no significant effect on *Atp2b2* transcript expression in either cell line compared to PIE. C, D: EGR1 has no statistical effect on *Atp2b4* transcript expression in OC-1 or N2A cells compared to PIE. ATOH1 increases expression of *Atp2b4* transcript in OC-1 cells but has no significant effect in N2A cells. Comparisons to PIE were made using a two tailed students t-test (*P $\leq$ 0.05, **P $\leq$ 0.01). Error bars indicate average of data and SEM.

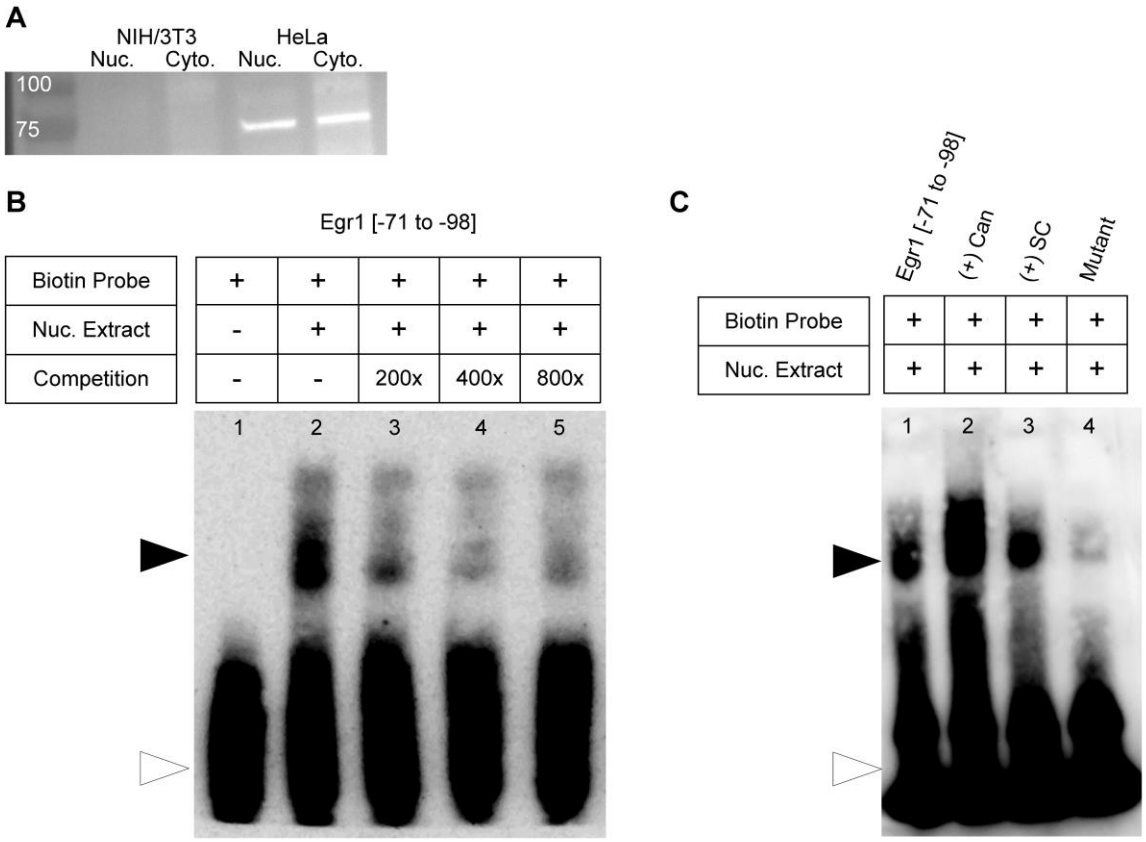

Figure 2.10. Mobility shift assay of probe [-71 to -98]

A. Western blot of EGR1 protein expression in NIH/3T3 or HeLa cells. Nuclear and Cytoplasmic fractions were compared. HeLa nuclear extract was used for shift assays due to its detectable expression of EGR1. B. Lane 1 - Free unbound biotin labeled probe is shown and is indicated by an open arrow head. Lane 2 - Contains HeLa nuclear lysate, a shift is indicated by closed arrowhead. Lanes 3-5 – Self competition with unlabeled probe at increasing concentrations indicates specificity of the shift in Lane 2. C. Lane 1 - 3 Positive shifts for the [-71 to -98] probe as well as two positive control probes designed to bind EGR1 (see Table 2.2) Lane 4 – [-71 to -98] mutant probe, 4 nucleotides in the EGR1 cluster region were modified and the shift is abolished. All blots shown are 10 minute exposures.

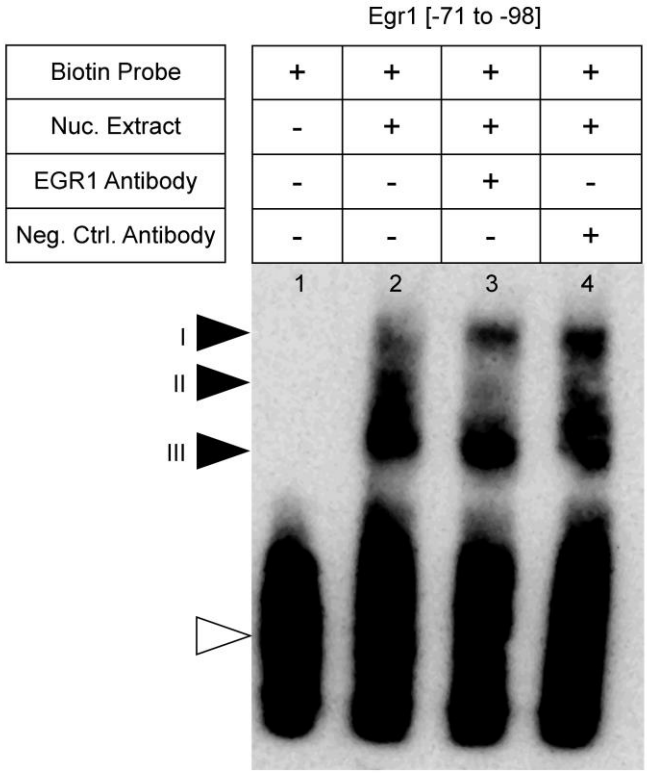

Figure 2.11. Supershift assay: EGR1 binds to probe [-71 to -98]

Lane 1 - shows free unbound biotin labeled probe which is indicated by the open arrow head. Lane 2 – contains HeLa nuclear lysate and recapitulates the shift from Figure 2.10. There are 3 binding populations in the shift indicated by closed arrow heads (I, II, III). Lane 3 – Reaction contains polyclonal IgG antibody targeting EGR1 along with HeLa nuclear lysate. Addition of the anti-EGR1 appears to abolish the binding of the second population to the probe (II). Lane 4 – Reaction contains HeLa nuclear lysate and polyclonal IgG antibody targeting ATP2B2. This antibody does not abolish the II shift and acts as a negative control for the supershift observed in Lane 3. Blot was exposed for 10 minutes.

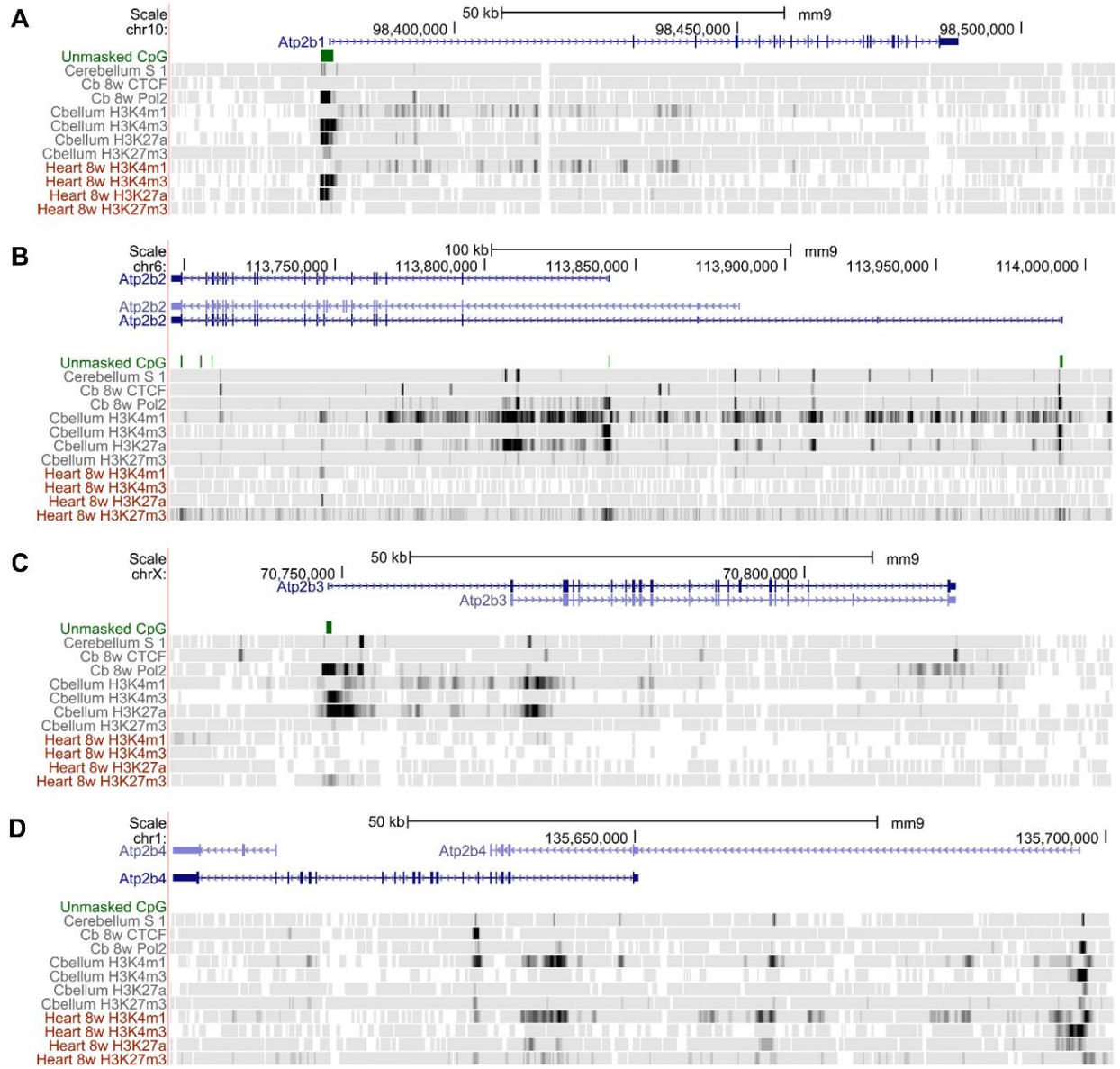

Figure 2.12. Genomic comparison of the *Atp2b* genes

Atp2b transcripts are shown in blue. Marks for transcriptional modulation are shown in 8 week-old mouse cerebellum and 8 week-old mouse heart tissue. Marks Included: CTCF transcription factor binding (CTCF), RNA polymerase II binding (Pol2), H3K4me3, H3K4me1, H3K27a, and H3K27me3 (indicates repression). A, B, C, D - *Atp2b1*, *Atp2b2*, and *Atp2b3* have predicted CpG islands at TSSs, *Atp2b4* does not. *Atp2b1* and *Atp2b4* are transcriptionally active in both tissues. *Atp2b2* and *Atp2b3* appear to be active in the cerebellum only (Consortium 2012).

Chapter 3. *ATP2B2* MISREGULATION IN B6 MICE WITH AHL

Summary

The B6 mouse has a fairly severe AHL phenotype. A recent study has shown that this loss is only partially caused by mutations in the *Cadherin 23* (*Cdh23*) gene which encodes the tip-link protein CDH23 (Kane et al. 2012). Hearing loss due to mutations in *Cdh23* are exacerbated by mutations in the ATP2B2 protein, which regulates intracellular Ca^{2+} levels (Noben-Trauth et al. 1997; Schultz et al. 2005). This interaction is likely due to the necessity of Ca^{2+} in maintaining the structural integrity of tip-links composed of CDH23 (Sotomayor et al. 2010). Although there are no mutations in the B6 *Atp2b2* gene, we show here using two discreet measures of gene expression that there is a decrease of *Atp2b2* transcript in B6 mice starting as early as 5 weeks of age. Given the digenic interaction of *Atp2b2* and *Cdh23* it is likely that misregulation in *Atp2b2* is a contributor to the AHL phenotype of B6. Our investigation of the genomic region surrounding *Atp2b2* implicates transcriptional processes in the misregulation of *Atp2b2* in B6 mice. Studies of these elements have determined that the promoter of the *αAtp2b2* is not likely involved. Further investigations have led to the discovery of long non-coding RNAs (lncRNAs) in this region, Gm15082 (lnc82) and Gm15083 (lnc83). Importantly, lncRNAs are emerging as key players in transcriptional regulation of nearby genes (Wang and Chang 2011). Expression studies indicate that lnc83 is upregulated in the brainstem and cochlea of B6 mice. Overexpression of lnc83 in mammalian cells indicates that this gene may play a functional role in the inhibition of *Atp2b2* transcript. We postulate that overexpression of lnc83 likely downregulates *Atp2b2* transcript in B6 exacerbating CDH23 protein dysfunction and contributing to the B6 AHL phenotype.

3.1 INTRODUCTION

3.1.1 *Cdh23 and AHL in B6 mice*

Mechanotransduction is affected when proteins in the auditory system are mutated or misregulated. In the B6 inbred mouse strain, AHL was attributed to a SNP in the intronic regions of the *Cdh23.* This mutation is shown to cause in-frame skipping of exon 7. This is hypothesized to decrease adhesion and stability of the CDH23 protein, eventually causing AHL (Noben-Trauth et al. 2003). However, recent studies with congenic mice have shown that mutations in CDH23 alone are not sufficient to cause the AHL phenotype in B6 mice (Kane et al. 2012). This has led to the search for an interacting gene.

3.1.2 *dfw mutants reveal Atp2b2 misregulation in B6 mice*

There are several well characterized mouse mutations of the *Atp2b2* gene. These mice, called the *dfw* mutants, exhibit hearing loss and ataxia. Our lab recently characterized a new *dfw* mutant, dfw^{i5}. The dfw^{i5} mutation is caused by the substitution of Lysine-580 into a stop codon and arose on a DBA/2J background. This new mutation was compared to the previously characterized dfw^{2j} mutation which is caused by a frame shift just upstream of the dfw^{i5} mutation. The dfw^{2j} mutation arose on the BALB/cByJ background. Both mice were backcrossed to CB, the standard good hearing mouse, for at least 10 generations. It was predicted that these two mutants would have similar phenotypes but when auditory sensitivity was compared in heterozygotes we found that dfw^{i5} mice have significantly worse hearing than the dfw^{2J} mice (Watson and Tempel 2013). The molecular basis of this phenotype was studied using an allelic discrimination. This technique measures the amount of mutant transcript in the heterozygote *dfw* mice. This assay showed that dfw^{i5} heterozygote mice express double the mutant transcript of the dfw^{2J} heterozygote mice

(unpublished manuscript). Although *dfw*^{i5} and *dfw*^{2J} mice are primarily isogenic the region directly surrounding each mutation is identical to the strain in which the mutations originally arose (DBA/2J - *dfw*^{i5}, BALB/cByJ - *dfw*^{2j}). Our lab has shown that in the area surrounding *Atp2b2*, DBA/2J is like CB and BALB/cByJ is like B6. These findings were verified using the MGI database and 4x sequencing of the 5,000kb region directly upstream of the *Atp2b2* gene. We hypothesize that the downregulation of *Atp2b2* transcript in *dfw*^{2J} mutant heterozygote mice is due to the B6 haplotype surrounding the gene.

To test this empirically, we performed a second allelic discrimination with the CB and B6 ancestral strains. To do this we crossed a CB mouse with a B6 mouse. In the F1 progeny, which have one allele from each of the inbred strains, we measured the amount of *Atp2b2* transcript expressed from either the CB or the B6 allele. We hypothesized that there would be more *Atp2b2* transcript expressed from the CB allele than the B6 allele. The results of the allelic discrimination confirm our hypothesis exhibiting that the F1 progeny of CB and B6 mice have twice as much transcript from the CB allele than they do from the B6 allele (unpublished manuscript). These results show that *Atp2b2* is misregulated in B6 mice when compared to CB.

3.1.3 *The known digenic interaction of Cdh23 and Atp2b2*

As was previously outlined in Chapter 1, studies in mice and humans have found that hearing loss caused by mutations in the *Cdh23* gene are exacerbated by mutations in *Atp2b2* (Noben-Trauth et al. 2003; Schultz et al. 2005; Watson and Tempel 2013). The mechanism of this interaction is not well understood but it is known that tip-links are sensitive to Ca^{2+} concentration in the extracellular endolymph (Fig. 3.1). Given that tip-links require Ca^{2+} to function properly and that ATP2B2 maintains the concentration of Ca^{2+} in the endolymph (Wood et al. 2004; Sotomayor et al. 2010) we hypothesize that downregulation of *Atp2b2* weakens the tip-links

leading to worsened auditory sensitivity in B6. This is a unique example of the pathology of *Cdh23* and *Atp2b2* because this is the first evidence that transcript misregulation of *Atp2b2* could contribute to AHL.

3.2 METHODS

3.2.1 *Animals*

C57BL/6J (B6) (JAX stock No: 000664) and CBA/CaJ (CB) (JAX Stock No: 000654) male inbred mice were used in age ranges from 5 weeks to 20 weeks of age. Tissue was collected from 5 and 12 week-old CB and B6 brainstem and cochlea. Auditory testing was performed at 5 and 20 weeks of age. CB and B6 mice are obtained from JAX and replaced every three generations to retain an isogenic stock. Animals are kept in a 12 hour light/dark cycle with minimal environmental exposure to noise. All procedures in this study are approved by the University of Washington Institutional Animal Care and Use Committee.

3.2.2 *Auditory testing*

Auditory sensitivity was measured using Auditory Brainstem Response (ABR). Frequencies ranged from 5.6 kHz to 40 kHz. Prior to auditory screening, mice were anesthetized using a mix of ketamine (130mg/kg) and xylazine (10mg/kg). Once animals were anesthetized they were placed in a sound proof box with a heat lamp and heating pad; animals were then secured with a bite bar. The system was calibrated at the beginning of each test session to confirm the output of the speaker was in the normal range. Responses were measured by two electrodes placed subcutaneously at the forebrain and brainstem. A reference electrode was placed at the hind limb and electrocardiogram recordings were used to monitor anesthesia.

A series of 300 tones per frequency and intensity were administered. Tones were 5ms long with a 0.5ms rise fall $\cos^2$ function. Brain waves were recorded for 25ms with a 40ms spacing between repetitions. ABRs are amplified 1000x filtered and digitized by a pre-amplifier (P55; Grass Telefactor West Warwick, RI). Post-amp gain ranged from 30-35 (dB) for all animals (Mo.#

3362 K-H Corp). Threshold was determined visually as the lowest intensity that evoked a reproducible and recognizable brain wave in at least two out of three trials.

3.2.3 *Gene expression analysis with quantitative PCR (qPCR)*

3.2.3.1 qPCR CB and B6 mice brainstem and cochlea

Rough dissections of 5 week-old and 12 week-old brainstem from CB and B6 mice were performed on the bench top and immediately transferred to a microtube filled with RNA*later*. 5 week-old and 12 week-old CB and B6 mice Cochleae microdissections were performed using a light microscope (Zeiss) in RNA*later*. The vestibular portion of the cochleae were removed and vasculature, neuronal tissue and bone were trimmed. Once cleaned, the cochleae were perfused with and stored in RNA*later*. Both tissues were stored at 4^{o}C for at least a week to allow the RNA*later* solution to properly perfuse the tissues. Tissues were then moved to storage at -80^{o} C for later use.

RNA was isolated using the RNeasy Plus Universal Mini Kit according to manufacturer's protocol (Qiagen No: 73404). Homogenization for brainstem was accomplished using a Polytron PT 1200 rotor-starter homogenizer. For cochleae, the tissue was homogenized with a sterile mortar and pestle. RNA extraction efficiency was measured using a Nanodrop spectrophotometer (Thermoscientific). 260/280 ratios of 2.00 or higher and 260/230 ratios greater than 1.00 were acceptable; If ratios were significantly lower than these values tissues were excluded. Any tissues exhibiting anomalous expression profiles were submitted to a grub's outlier test.

Total RNA (up to 2µg) was reverse transcribed into complimentary DNA (cDNA) using SMARTscribe reverse transcriptase (Clontech) and random hexamer primers (Applied Biosystems). These samples were used for qPCR analysis using Sybr green master mix (BioRad). Reactions were performed on a Q5 iCycler or a CFX96 (BioRad). Total-*Atp2b2*, *αAtp2b2*,

βAtp2b2, lnc82 and lnc83 cycle thresholds were normalized to two housekeeping genes (*β-Actin* (*Actb*) and *Actg* for brainstem and 5 week-old cochlea, *Hmbs* and *Actg* for 12 week-old cochlea). Genorm software was used to determine stable housekeeping genes for each age and tissue type (Vandesompele et al. 2002). Primer sequences can be found in Table 3.3. For full analysis techniques see: (Silverstein and Tempel 2006). Data is the average of at least three runs where replicates within a run had a relative standard deviation (Std. dev.) of less than 0.03 (Std. dev./CT > 0.03 were excluded).

3.2.3.2 qPCR for lncRNA overexpression in N2A cells

RNA extraction and conversion protocols are the same as above. To quantify *Atp2b2* transcript expression in N2A cells, premade TaqMan gene expression assays from applied biosciences were used: (*Hmbs* Assay ID: Mm01143545_m1, *Atp2b2* Assay ID: Mm00437640_m1, *Actg* Assay ID: Mm01963702_s1). Reactions were run using SSO Advanced universal probes super mix (BioRad 172-5281). Absolute threshold values were normalized to housekeeping genes *Actg* and *Hmbs*. Samples were run in triplicate (n=3), data is the average of at least three runs where replicates within a run had a relative standard deviation (std. dev.) of less than 0.03 (std. dev./CT > 0.03 were excluded).

3.2.3.3 Allelic Discrimination

Allele specific TaqMan probes (Applied Biosystems) were designed to distinguish between the CB and B6 allele in the F1 cross of CB and B6 inbred mice. The TaqMan probe recognizes rs30756873 [B6 (C) →(A) CB], which is amino acid 731 [B6 (E) →(D) CB]. cDNAs for these mice were prepared as above. Data is the average of duplicates of a single run of four hybrid mice (For full methods see: Watson thesis, 2012).

3.2.4 *Western analysis*

12 week-old brainstem tissue was dissected from CB and B6 inbred mice and snap frozen in liquid nitrogen or dry ice. Tissue was homogenized in lysis buffer supplemented with protease inhibitor. Relative concentrations of total protein were measured using a BCA assay. Samples were diluted in a 1:1 ratio with SDS-sample buffer and boiled for 10 min at 50^{o}C. Total protein loaded onto the gel ranged from 5-10ug. Prepped samples were loaded onto 4-20% gradient polyacrylamide gels (BioRad) and transferred onto nitrocellulose membranes. Membranes were incubated with antibodies against ACTB and ATP2B2 (ThermoFisher PA1-915). They were subsequently incubated with secondary antibodies; anti-mouse and anti-rabbit (Invitrogen). Relative levels of ATP2B2 were calculated by normalization of chemiluminescence signal of ATP2B2 antibody to ACTB antibody upon addition of a substrate (Amersham ECL Prime). A Fotodyne imager was used to take images and ImageJ software was used to analyze the blots. ATP2B2 quantification was normalized to an internal Standard to allow comparison across blots. Data is the average of each animal, where each animal was blotted ~2 times.

3.2.5 *Cloning*

3.2.5.1 Promoter constructs:

For full methods see Chapter 2, PCR was used to amplify 5.5 kb proximal promoter in 3 pieces off of genomic DNA from the DBA/2J inbred mouse strain. Exons of the 5'UTR were amplified from cDNA of *dfw^{2J}* brainstem. Promoter truncations were ligated into the pGL3 vector from Promega.

3.2.5.2 Minigene constructs

These constructs contain 250 bases surrounding SNPs of interest (rs30608672 and rs29969841). The thymidine kinase (TK) minimal promoter was cut out of the pRL-TK renilla luciferase vector. The TK minimal promoter and SNPs were then ligated upstream of the *Luc*$^{+}$ gene in the pGL3 vector (Promega) using a synthetic NCO1 cut site (Fig. 3.7).

3.2.5.1 LncRNA constructs

lnc82 and lnc83 were amplified from CB mouse cochlea or brainstem cDNA using the following primers: BamH1 82 F: 5' – GTC AGA GGA TCC AGT TGA GCT GGG GTT - 3', 82 BamH1 R 5' – AGC CGA GGA TCC GCA CAA AGA TTT ATT - 3', 83 BamH1 F: 5' – GTC AGA GGA TCC ACA GTG ACA TCT CCC - 3' and 83 BamH1 R: 5' – AGC CGA GGA TCC CAG CCT GCT TTC TTA - 3'. A number of clones were identified but the lengths that correspond to the exons on the ENSEMBL database were used (lnc82 ~2kb, lnc83 ~1.2kb). These were ligated into TOPO vectors (Invitrogen) amplified, sequenced and subsequently cut out using synthetic BamH1 cut sites. These pieces were ligated into the multicloning site of the pcDNA3.1a vector. Expression is driven by the CMV promoter.

3.2.6 *Luciferase assays*

3.2.6.1 CB vs B6 minigene comparison

Cells were plated twenty four hours before all transfections. OC-1 cells were plated at a density of $4x10^4$ cells per well in a 24 well plate. TK promoter constructs in the pGL3 vector (400 ng/ well) were transfected into OC-1 mammalian cells along with an internal renilla luciferase standard (5ng/well) using a 1:4 ratio of DNA:transfection reagent (Fugene HD, Promega: E2311) . Cells were harvested 48 hours after transfection with passive lysis buffer and assayed using the dual

luciferase reporter assay system (Promega: E1910) with a manual luminometer (Promega). Luciferase activity was normalized to the empty TK promoter vector.

3.2.6.2 CB vs B6 Promoter comparison

Cells were plated twenty four hours before all transfections. OC-1 cells were plated at a density of $4x10^4$ cells per well in a 24 well plate. *αAtp2b2* promoter constructs in the pGL3 vector (400 ng/ well) were transfected into OC-1 mammalian cells along with an internal renilla luciferase standard (5ng/well) using a 1:4 ratio of DNA:transfection reagent (Fugene HD, Promega: E2311) . Cells were harvested 48 hours after transfection with passive lysis buffer and assayed using the dual luciferase reporter assay system (Promega: E1910) with a manual luminometer (Promega). Luciferase activity of the promoter truncation constructs for each strain were normalized to the empty pGL3 vector. Data is the average of at least three plates with three replicates per plate.

3.2.6.3 LncRNA overexpression promoter study

αAtp2b2 promoter constructs in the pGL3 vector (200 ng/ well) were co-transfected into OC-1 mammalian cells along with an internal renilla luciferase standard (2.5ng/well) and a lncRNA vector (200ng/well) using a 1:4 ratio of DNA:transfection reagent (see above). Cells were harvested 48 hours after transfection with passive lysis buffer and assayed using the dual luciferase Reporter Assay System (Promega: E1910) with a manual luminometer (Promega). Chemiluminescence of promoter vector alone + the empty pcDNA3.1a vector was compared to promoter vector+lnc83 expression vector. Both were normalized to empty vector. Data is the average of three plates with three replicates in each plate.

3.2.7 *LncRNA overexpression assay*

N2A cells were grown at 37 °C and 5% CO2 in DMEM (Invitrogen) supplemented with 10% FBS and 1% Streptomycin and ampicillin. All cells were plated twenty four hours before transfection in 12 well plates. N2A cells were plated at a density of $1x10^5$ cells per well. LncRNA constructs were transfected at 800ng/well using a 1:3 ratio of transfection reagent. Cells were incubated with constructs for 48 hours and then harvested in 400 µl of Qiazol. Transfection efficiency was measured as the expression of the lncRNAs normalized to *Actg* and *Hmbs*. Primers used can be found in Table 3.3. It was found that lnc82 has a much lower transfection efficiency than lnc83. Normalized expression values for lnc83 were typically 100x greater than lnc82.

3.3 RESULTS

3.3.1 *Recapitulating the allelic discrimination in CB/B6 hybrid mice*

Our lab has shown that in the brainstem of F1 progeny of CB and B6 inbred mice there is twice as much transcript from the CB allele than from the B6 allele at 5 weeks of age. This suggests that there is misregulation of *Atp2b2* in B6 mice. Given that these mice have AHL, we decided to look at a group of older mice to determine if the trend holds after the onset of hearing loss in B6 mice. According to a number of studies, the onset of hearing loss in B6 mice is somewhere between 12 weeks and 24 weeks of age (Henry 2002; Frisina et al. 2011; Kane et al. 2012). In the lab, we are able to detect differences at as young as 12 weeks of age. Given this time point we chose to perform another allelic discrimination on mice at 20 weeks of age. Figure 3.2 shows the percent of *Atp2b2* transcript from each allele in the F1 progeny of CB and B6 mice. These mice have one allele from each of the mice and should hypothetically have 50% of transcript from each of these alleles. However, when quantified it was found that about 2/3 or 66.7% of the *Atp2b2* transcript is coming from the CB allele where only 1/3 or 33.3% of the transcript is coming from the B6 allele. This preliminary data recapitulates the findings from the young mice and suggests that this diversion in transcript regulation exists in young and old mice.

3.3.2 *Hearing is normal in CB/B6 hybrid mice*

AHL in B6 mice is genetic but it is not solely attributable to mutations in the *Cdh23* gene (Kane et al. 2012). In F1 progeny of CB and B6 mice the typical 50%-50% expression of transcript is skewed with ~65% coming from the CB allele and ~35% coming from the B6 allele. In the Kane publication the congenic mice investigated have intermediate phenotypes with or without the *Cdh23 gene*. To determine if CB auditory genes compliment the mutations found in B6, we

investigated the auditory phenotypes of F1 hybrid of CB and B6. These mice were aged until the onset of hearing loss at 20 weeks of age. They were compared to a CB mouse as a control. We were able to show that at both 5 and 20 weeks of age the F1 progeny of CB and B6 (CB/B6) mice have an auditory phenotype similar to the CB control (Fig. 3.3). This supports published studies showing that CB/B6 mice maintain good hearing throughout the life. At much later time points, over 1 year of age, it appears that CB/B6 mice have better hearing than the CB inbred strain. It is expected that this is likely due to hybrid vigor (Frisina et al. 2011).

3.3.3 *Atp2b2 transcripts are partially downregulated in young B6 mice*

Although the molecular basis of the interaction between *Atp2b2* and *Cdh23* is not known we hypothesize that it involves *Atp2b2* in the OC, specifically in the hair cells, which contributes to the concentration of Ca^{2+} in the endolymph. There are two dominant transcripts in the OC of adult mice: the α and the β *Atp2b2* transcripts (Silverstein and Tempel 2006). At Postnatal day 9 only the *αAtp2b2* transcript is found in the outer hair cells. In the rest of the brain and cochlea these transcripts are expressed relatively equally. Given the tissue specific expression of these transcripts and their unique transcriptional regulation it was necessary to determine which transcripts are misregulated in B6 mice. To do this, cDNA from CB and B6 mouse tissue was analyzed using qPCR with primers designed to look at α*Atp2b2,* β*Atp2b2,* and total *Atp2b2* transcript.

At 5 weeks of age, there was no difference in transcript expression in whole cochlea (Fig. 3.4A). However, a two-way Analysis Of Variance (ANOVA) reveals that all transcripts tested have a genotype affect in the brainstem (**p=0.008) (Fig. 3.4B). It is unsurprising that there is normal expression of *Atp2b2* in the B6 cochlea at this time point given that these mice have normal hearing and that this transcript is highly regulated. Given that we were able to see downregulation in the brainstem at this early time point it suggests that there is some compensation occurring in

the cochlea to maintain normal levels of *Atp2b2* transcript. This led us to investigate 12 weeks of age which is near the onset of hearing loss.

3.3.4 *Atp2b2 transcripts are downregulated in B6 mice at 12 weeks of age*

Hearing loss in B6 mice is noted as early as 12 weeks of age, therefore this time point was investigated for expression of *Atp2b2* transcript in CB and B6 mice. At this time point, the cochlea no longer compensates for the downregulation seen in the brainstem and all transcripts of the cochlea are affected (Fig. 3.5A). It was noted that the *Actb* transcript was no longer stable in cochlear dissections at this time point. This suggests that cellular remodeling is already occurring in this organ. Genorm software was used to predict a new housekeeping gene for use in the aging cochlea and out of a panel of 8+ genes, the *Hmbs* gene was selected to replace *Actb* as a normalization gene.

In the brainstem, the phenotype is worsened at 12 weeks of age. Downregulation of *Atp2b2* is now significant in both transcripts and two measures of total transcript, one in the 5'UTR and one between exons 6 and 7 (data not shown) (Fig. 3.5B). Protein levels were also investigated. Although there is a trend towards decreased total ATP2B2 in B6 it was not significant (Fig. 3.6). Power analysis utilizing variability of preliminary data indicated that a very large sample size would be needed to detect a significant change. It was concluded that western assays have insufficient sensitivity to detect the small changes in protein expression found in the preliminary data (Fig. 3.6).

3.3.5 *Investigation of potential modulators of Atp2b2 transcript in B6 mice*

Two distinct measures have indicated that there is misregulation of *Atp2b2* transcript in B6 mice. It is important to note that in the *Atp2b2* gene there are over 300 SNPs in intronic and exonic

regions according to the MGI database. That being said, these SNPs implicate a number of potential causes for misregulation of *Atp2b2* in B6 mice. The following transcriptional and translation modulators have been investigated for their role in the downregulation of *Atp2b2* transcript in the B6 mouse:

1) Splice site variants and untranslated regions - There are no known SNPs that would affect splice sites or untranslated regions between the two strains.

2) SNPs in translated exons and protein stability - There is only one non-synonymous SNP in the coding region of *Atp2b2* and it is found in CB; E → D at amino acid 731. This is not expected to affect protein stability as these are extremely similar amino acids with similar size and charge.

3) MicroRNA and chromatin remodeling – although these cannot be completely ruled out, it is unlikely that the downregulation of *Atp2b2* in B6 is caused by an element outside of the genomic region directly surrounding the *Atp2b2*. This is because the misregulation of *Atp2b2* transcript was first identified in a congenic mouse with the region surrounding *Atp2b2* isolated from the background strain.

4) Intronic regions – These regions are prematurely overlooked in many studies, with the formation of G-quadraplexes and methylation sites, intronic regions are extremely important for transcriptional regulation of genes. *Atp2b2* is an extremely complex gene and given that there are no SNPs in regions surrounding the splice sites of the gene this area was thought of with care but mostly overlooked as the "final frontier" in determining what modulators might be causing misregulation of *Atp2b2* transcript in B6 mice.

5) Proximal promoter – There are a number of SNPs between CB and B6 in the area of the proximal promoter. α*Atp2b2* and β*Atp2b2* have unique promoters and both have a similar number

of SNPs between the strains. Given the hair cell hypothesis of the digenic interaction of *Cdh23* and *Atp2b2*, this study focuses on characterization and comparison of the α*Atp2b2* promoter.

6) LncRNAs – In addition to SNPs in the promoters of the two *Atp2b2* transcripts found in the brain, there are also lncRNAs in this region. The lncRNAs have SNPs between the strains that could affect their behavior. Both are found in the intronic regions of the 5'UTR making them good candidates for further investigation.

Here we have briefly summarized the potential regulators of the *Atp2b2* transcript in mouse. Although there are a number of possible mechanisms for downregulation, we began our search by investigating the SNPs in the proximal promoter region of *αAtp2b2.* We also investigated the mechanism and role of two lncRNAs. The findings from these studies are summarized in the rest of this section.

3.3.6 *The promoter in downregulation of Atp2b2 transcript in B6 mice*

We hypothesize that the molecular basis of the digenic interaction of *Atp2b2* and *Cdh23* involves ATP2B2 protein in the stereocilia of the hair cells. The α*Atp2b2* transcript is the main *Atp2b2* transcript found in the outer hair cells of young mice so we focused on the *αAtp2b2* promoter for our comparison study. To detect sequence nucleotide changes that are polymorphic between CB and B6, we sequenced the 5kb region upstream of the TSS of *αAtp2b2*. From this analysis, we identified 9 SNPs. These SNPs were analyzed using MatInspector, a software engine that predicts transcription factor binding sites (Cartharius et al. 2005). This software predicts that 5 SNPs in the B6 promoter of the *Atp2b2* gene will alter the binding of transcription factors found in the ear. Of these 5 SNPs, 2 are good candidates for altering transcription factors important for normal auditory development (e.g. Pou4F3 and Dlx5) (Ryan 2002). This suggests that B6 may

have a 'weaker' *αAtp2b2* promoter than CB leading to decreased transcriptional expression of the *αAtp2b2* transcript.

To quickly compare two SNPs anticipated to alter transcription factor binding in B6, minigene constructs were developed (Fig. 3.7A). SNP 5 (rs29969841) is located 1957 bases upstream of the TSS and is a G→A conversion. This SNP is predicted to alter the binding of: DLX/Pou3F3, BSX, SOX30, and MAF1 (Table 3.4). However, luciferase activity data for SNP5 suggests that it does not affect transcription factor binding in the B6 mouse (Fig. 3.7B). SNP 3 (rs30608672) is located 3944 bases upstream of the TSS and is a G→C conversion. SNP 3 is predicted to affect the binding of the following transcriptional modulators: TLX, HOXC8, PRDM5, VAX1, HOXC9, OCT1, DX1 (Table 3.4). SNP 3 shows inhibition over baseline for both strains and shows further inhibition in the B6 SNP decreasing luciferase expression ~30% compared to CB (Fig. 3.7C). This suggests that SNP 3 could be involved in transcriptional repression of *αAtp2b2* in B6.

To study SNP 3 and other SNPs found in the native *Atp2b2* promoter the 5,000 base proximal promoter of CB and B6 along with the exons of the 5'UTR were cloned into a luciferase vector. When truncations of the proximal promoter were compared across strains there was no difference in luciferase expression (Fig. 3.8). This suggests that the SNPs do not affect the binding of transcription factors in the native promoter. It is possible that these SNPs affect endogenous promoter architecture by interfering with methylation patterns or other 3D genomic architecture. However, any changes found in the *αAtp2b2* promoter will not necessarily translate to *βAtp2b2*. Given that both transcripts are affected and that the luciferase assay doesn't indicate any robust changes in promoter activity it is unlikely that the promoter alone is contributing to the decreased transcript expression of *Atp2b2* in B6 mice. This contradicts the minigene assay which indicates repression of luciferase activity in the construct containing B6 SNP3. This is likely because the

minigene system is highly artificial suggesting that SNP3 likely does not play a functional role in inhibition of the native promoter.

3.3.7 *LncRNAs in B6 mice*

Investigation of the genomic region surrounding the *Atp2b2* gene on Ensembl revealed the existence of two processed untranslated transcripts in the 5'UTR of *Atp2b2* (Ensembl version 82, GRCm38.p4). These are long noncoding RNAs, lncRNAs. The first, lnc83 has exons that span the first exon of the *αAtp2b2* transcript. The second lncRNA, lnc82 is found near the first exon of the β transcript of *Atp2b2* (Fig. 3.9A). The human *ATP2B2* region contains similar lncRNA transcripts in the region surrounding the TSS (Fig. 3.9B).

Non-coding RNAs were originally overlooked in the genome as they did not code for protein. In recent years, many studies have exhibited the functional abilities of these elements from whole chromosome silencing to transcriptional and post-transcriptional regulation (Wang and Chang 2011). LncRNAs are defined as transcribed RNAs that are greater than 200 nucleotides in length and do not encode a protein greater than 100 amino acids in length. This definition is important because it separates lncRNA from their smaller counterpart, micro RNA (miRNA). This distinction is necessary because, unlike miRNA, which usually reside in the cytoplasm and control gene expression by inhibiting translation, lncRNA are usually involved in transcriptional regulation of genes. The mechanisms of lncRNA are not well understood but it is known that they can negatively or positively regulate genes on their own chromosome (in cis) or on different chromosomes (in trans). Many studies demonstrate that lncRNAs frequently act in cis in an inhibitory manner (examples: Xist, DHFR minor, linc-hoxa1) (Huarte et al. 2010; Wang and Chang 2011; Maamar et al. 2013). The location of lnc82 and 83 upstream of *Atp2b2* make these transcripts good candidates for transcriptional regulation of *Atp2b2* in the mouse.

To determine if lnc82 or lnc83 play a role in the downregulation of *Atp2b2* in the B6 mouse, qPCR was used to compare levels in CB and B6 brainstem and cochlea. These tests indicate that lnc83 is expressed higher in the cochlea than lnc82 suggesting that lnc83 may play a specific role in regulation of *Atp2b2* in the cochlea. Additionally, lnc83 is upregulated in B6 mouse brainstem and cochlea with no change in the expression of lnc82 (Fig. 3.10). This suggests that there is a regulatory change that is specific to lnc83 which is not a universal change in lncRNA expression. In silico studies of the region surrounding lnc83 reveal SNPs in the proximal promoter. Studies in the Tempel lab of lnc83 during normal development indicate that the expression of *Atp2b2* increases as the expression of lnc83 decreases. This indicates an inverse correlation of lnc83 and Atp2b2 expression (Watson et al. 2014). We hypothesize that lnc83 plays a role in *Atp2b2* downregulation in B6 mice.

3.3.8 *Lnc83 may play a role in the downregulation of Atp2b2 transcript in B6 mice*

3.3.8.1 Lnc83 and the *αAtp2b2* proximal promoter

Based on mechanistic studies of lncRNAs, the promoter is a likely target for lnc83 binding and subsequent inhibition of *Atp2b2* gene expression (Wang and Chang 2011). This study focuses on the *αAtp2b2* promoter since it is the primary transcript of the outer hair cells. Lnc83 exons straddle the 5'UTR exons of *αAtp2b2* and are situated well upstream of the other *Atp2b2* transcripts (Fig.3.9). Additionally, lnc83 is the dominate lncRNA in the cochlea suggesting a more influential role in regulation of transcripts found in this tissue (Fig. 3.10). To determine if lnc83 affects expression of the *αAtp2b2* promoter, OC-1 cells were co-transfected with the promoter vector from Chapter 2, [-572/+2133], and either lnc82 or lnc83 expression constructs. Promoter activity was unaffected by the overexpression of lnc82 and lnc83 (Fig. 3.11). It is possible that the lncRNAs act outside of 5kb proximal promoter where they have complementarity in the genome (Fig. 3.9).

It is also possible that the lncRNAs function through other mechanisms besides directly binding to the DNA (Wang and Chang 2011).

3.3.8.2 The effects of LncRNAs on endogenous *Atp2b2* expression

To determine the functional role of the lncRNAs, they were overexpressed in N2A cells. Out of a panel of 10+ neuronal and OC cell lines N2A cells had the most consistent basal expression of *Atp2b2* transcript. It was found that lnc82 had a lower transfection efficiency which was curious. It is possible that the cell has mechanisms in place to downregulate this gene or that the transcript is unstable and quickly degraded. Considering the ~2kb length of the transcript this could be due to the size of the construct. Both lnc82 and lnc83 were compared to empty vector (pcDNA3.1a). Final data shows that both lnc82 and lnc83 appear to inhibit expression of *Atp2b2* transcript in N2A cells but only lnc83 was significantly different from empty vector (Fig. 3.12). This assay has the caveat of extremely low basal expression of *Atp2b2* transcript, but it was sufficient to show significant inhibition in N2A cells. This suggests that lnc83 plays a functional role in the inhibition of *Atp2b2* transcript in N2A cells but further experiments are necessary to determine the significance in mammals.

3.4 DISCUSSION

Previous research has identified *Atp2b2* as an important gene in the auditory system indicating that ATP2B2 protein mutations lead to deafness and ataxia. Through studies of the *dfw* mutants, it is also known that *Atp2b2* is haploinsufficient (McCullough and Tempel 2004) . This indicates a necessity for tight control over *Atp2b2*. Studies of dfw^{i5} and dfw^{2J} indicate that subtle transcriptional differences in *Atp2b2* are dependent on background strain. Studies in these mice, which are 10-20 generations into the same background strain, only maintain differences in the *Atp2b2* gene, identifying Chr 6 and specifically the *Atp2b2* gene as the cause of *Atp2b2* transcriptional misregulation.

3.4.1 *Misregulation of Atp2b2 transcript in B6 mice*

Two distinct measures have shown that the *Atp2b2* transcript is misregulated in B6 mice (allelic discrimination and qPCR). Not only is there an effect on total transcript but at two ages of mice, 5 weeks and 12 weeks, there was a significant effect of genotype for *αAtp2b2* and *βAtp2b2* transcripts. In the cochlea, there was no effect of genotype at 5 weeks of age. As the animal aged, the difference became apparent and a genotype effect was noted in 12 week cochlear tissue. With all *Atp2b2* transcripts affected in the brainstem and cochlea there is a chance that physiological problems in these animals are not limited to hair cell dysfunction and endolymph Ca^{2+} concentration. Additionally, there appears to be an aging component to the downregulation of *Atp2b2* transcript. Although we do not know how transcript inhibition manifests in these mice it is clear that there is misregulation of *Atp2b2* in the brain and peripheral system of B6 mice when compared to CB mice.

A caveat of this study is the inability to measure decreased expression of ATP2B2 protein in brainstem of B6 mice. Given the necessary number of animals to reach sufficient power to determine statistical significance it was determined that western analysis is not sensitive enough to detect the predicted 20% change in protein expression. It is also possible that the downregulation of transcript does not affect total protein amount, but affects isoform expression and localization.

3.4.2 *Identification of Atp2b2 transcriptional regulators*

Although there are a number of ways transcripts can be misregulated, we have narrowed the causal region for *Atp2b2* misregulation to the *Atp2b2* locus on Chr 6. This distinction is important because it implicates elements within the *Atp2b2* gene and excludes elements in the rest of the genome. An obvious exception would be elements in the *Atp2b2* locus that affect protein function or transcript stability, however, our preliminary studies disqualified these factors. Once potential regulators were narrowed to the intronic regions of *Atp2b2*, we focused on the most likely candidates; the proximal promoter and lncRNAs.

3.4.3 *Promoter Studies*

Promoter truncations and minigene constructs were used to identify potential effects of SNPs on activity of the promoter. Minigene constructs indicated that there may be a difference in transcription factor binding/activation but in the full promoter and truncation constructs these differences did not amount to measureable changes in activity. However, we only studied the proximal promoter of the *αAtp2b2* transcript and the isolated promoter system removes any epigenetic modification that may be present in the endogenous mouse promoters. Additionally, the cell lines used for testing are not a perfect model of hair cells or of brainstem neurons and may be insensitive to subtle changes in promoter activity and modulation. This necessitates further studies

to rule out the contribution of *Atp2b2* promoters in downregulation of *Atp2b2* transcript in B6 mice.

3.4.4 *LncRNA Studies*

Lnc83 is upregulated prior to the onset of hearing loss at 5 weeks of age and at the onset of hearing loss at 12 weeks of age in both the brainstem and cochlea. We hypothesize that lnc83 functions to inhibit expression of *Atp2b2* transcript in B6 mice. However, much debate surrounds the functional significance of lncRNAs. In this study, we found that there is usually an inverse relationship between *Atp2b2* expression and lnc83 expression (or lnc83 is high when *Atp2b2* is low). However, in the mouse cochlea at 5 weeks of age, lnc83 is upregulated in B6 mice but there is no difference in the *Atp2b2* transcript expression. It is postulated that there are compensatory mechanisms in the 5 week-old B6 mouse cochlea to prevent downregulation of the *Atp2b2* transcript by lnc83. As the cochlea ages, cell remodeling occurs and this could leave the cochlea vulnerable to lnc83 mediated inhibition of *Atp2b2* transcript. In our hands, cell remodeling is noted as early as 12 weeks of age because *Actb* transcript levels are no longer stable in 12 week-old B6 cochlea tissue. Published studies indicate that by 60 weeks of age there is a significant decrease in spiral ganglion densities in the cochlea of B6 mice (Shiga et al. 2005). In the next section we will investigate the functional role of lnc83 in mammalian cells directly.

3.4.5 *Lnc83 may function as a transcriptional inhibitor of Atp2b2*

Although mechanistic studies suggest that neither lnc83 nor lnc82 act at the 5kb proximal promoter of *αAtp2b2*, functional studies highlight a potential role for lnc83 in downregulation of *Atp2b2* transcript. When lnc83 was overexpressed in N2A cells, *Atp2b2* transcript was significantly inhibited. The main caveats of this experiment are 1) low *Atp2b2* transcript

expression in N2A cells and 2) Lack of knowledge about the mechanism of *Atp2b2* transcript inhibition. The inhibition caused by the overexpression of the lnc83 construct is somewhat sequence specific as it was compared to N2A cells overexpression the empty pcDNA3.1a vector. Additionally, the lnc82 vector did not significantly inhibit *Atp2b2* transcript (although it was close with a P value= 0.06). Furthermore, experiments in tissue are necessary to determine endogenous effects of lnc83 overexpression and inhibition as well as localization and mechanism of action.

Although more studies are needed to determine the functional roles of lnc82 and lnc83 their developmental and tissue specific expression profiles make them good markers for transcriptional activity and modulation of *Atp2b2* (Watson et al. 2014). With better characterization of these transcripts and their human homologs, they could be used as biomarkers for diseases and disorders associated with *Atp2b2*.

3.4.6 *Characterization of subtle gene-expression changes and human disease*

The involvement of *Atp2b2* in the auditory phenotype of B6 suggests that protein mutations are not the only genetic anomalies that lead to pathologies. Reports of promoter mutations and intron mutations causing diseases are numerous (For review : Epstein 2009). As whole genome sequencing becomes more prevalent, small genetic and epigenetic anomalies responsible for disease continue to emerge. For this reason, it is important to characterize subtle changes in mouse gene expression because these changes will inform the genetic basis of human disease.

In this chapter, we found that *Atp2b2* transcript is downregulated in the brainstem and cochlea of B6 mice. We also identified lnc83 and experimental data suggests that this lncRNA may play a role in inhibiting the expression of *Atp2b2* transcript in B6 mice. In the next chapter we develop two congenic strains that are bred to determine the role of the *Atp2b2* locus and lnc83 in the hearing loss of B6 mice.

Table 3.3. qPCR Primers used in *Atp2b2* and lncRNA gene expression experiments

Primer Name	**Primer Sequence**
Actb F	5' -CCACCATGTACCCAGGCATT- 3'
Actb R	5' -ACAGTGAGGCCAGGATGGAG- 3'
Actg F	5' -GAAGGAGATCACAGCCCTAGCA- 3'
Actg R	5' -GACAGTGAGGCCAGAATG- 3'
Hmbs F	5' -CAGGCCACCATCCAGGTC- 3'
Hmbs R	5' -GAATGTTCCGGGCAGTGATT- 3'
Total *Atp2b2* F	5' -ACTCCTGGGTCAGCATTCC- 3'
Total *Atp2b2* R	5' -TAGTAGCACGAGGCGGTCA- 3'
α*Atp2b2* F	5' -CGGAGTGTGGACTGACAGCA- 3'
α*Atp2b2* R	5' -GGTTACATCAGAGGCGCCAG- 3'
β*Atp2b2* F	5' -GCTGGCGATTGCCTTAGC- 3'
β*Atp2b2* R	5' -GAGGAGTGTCCCCAGGAGTG- 3'
lnc82 F	5' -CAGGCAATGGTAGTTACCCTGTA- 3'
lnc82 R	5' -GAAAGCCACTCAGGGAAGTG- 3'
lnc83 F	5' -CTCATGCTCCTGCTGTGAAG- 3'
lnc83 R	5' -GGTTCACCAACTCCCTGAAG- 3'

The table outlines the primers used to quantify transcript expression in Chapter 3.

Table 3.4. SNPs in the proximal promoter of *Atp2b2*

SNP#	TSS	RS number	B6	BALB/cByJ	DBA/2J	CB	Predicted binding
1	-5227	(RM)	G	G	A	A	Gata2 (CB) AP2 (B6)
2	-4809	rs30659916	C	C	T	T	None
3	-3944	rs30608672	G	G	C	C	TLX, HOXC8, VAX1 (CB)
4	-2188	rs29921976	T	T	A	A	TBPF, MAF1 (B6)
5	-1957	rs29969841	G	G	A	A	BSX, DLX (CB) MAF1 (B6)
6	-1593	rs29975662	T	T	C	C	MAF1(B6)
7	-1588	rs30956043	C	C	T	T	MAF1 (B6)
8	-1192	rs30561839	G	G	A	A	None
9	-111	(RM)	G	G	T	T	SRF, STAT1, MYB (CB) AP4 (B6)

The table outlines the SNPs in the proximal promoter region of the B6 *αAtp2b2* transcript. The original ancestral strains of *dfw*^{2j} (BALB/cByJ) and *dfw*^{i5} (DBA/2J) mutants are included for reference. In *Atp2b2*, BALB/cByJ is B6 like and DBA/2J is CB like. The transcription factors with altered binding predictions due to B6 promoter SNPs are indicated. Additionally, two new SNPs were identified when sequencing this region, these SNPs are identified with the initials RM.

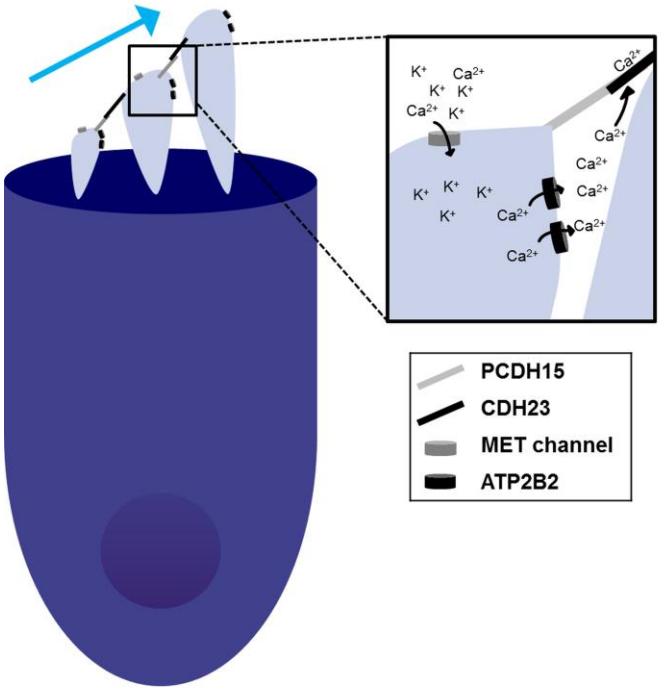

Figure 3.1. Ca^{2+} in the endolymph binds to *Cdh23* and maintains structural integrity

The hypothesized interaction of *Atp2b2* and *Cdh23* in an isolated hair cell. The ATP2B2 pump is located in the stereocilia of the hair cells and helps maintain the Ca^{2+} concentration in the endolymph (Wood et al. 2004). The structural integrity of the tip-link protein CDH23 is dependent on Ca^{2+} concentration. The misreglation of *Atp2b2* transcript in B6 mice could exacerbate the dysfunction of *Cdh23* in B6 mice leading to worsened auditory sensitivity.

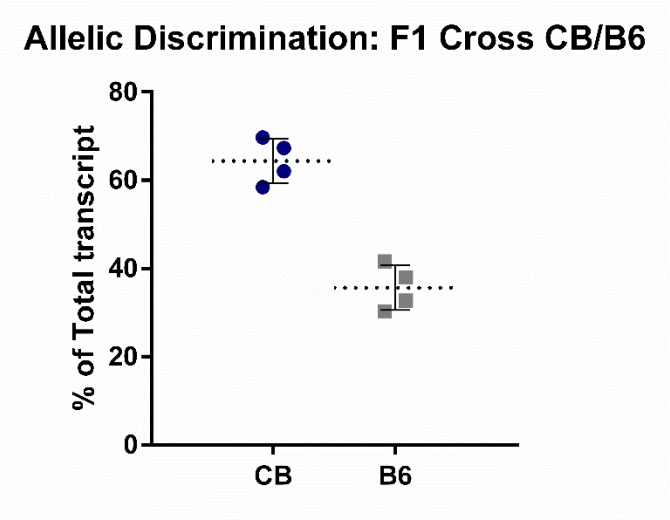

Figure 3.2. Transcript in hybrid mice is predominately from the CB allele

Data from 20 week-old F1 Cross of CB and B6 mice. *Atp2b2* transcript is shown as percent of total. cDNA transcribed from the CB allele is double the cDNA transcribed from the B6 allele. A single technical replicate was performed (n=4) to verify previous experiments in 5 week-old mice (data not shown). Although preliminary, results were significant utilizing a two-tailed unpaired t-test ***p=0.0002. Error bars indicate average of data and standard deviation.

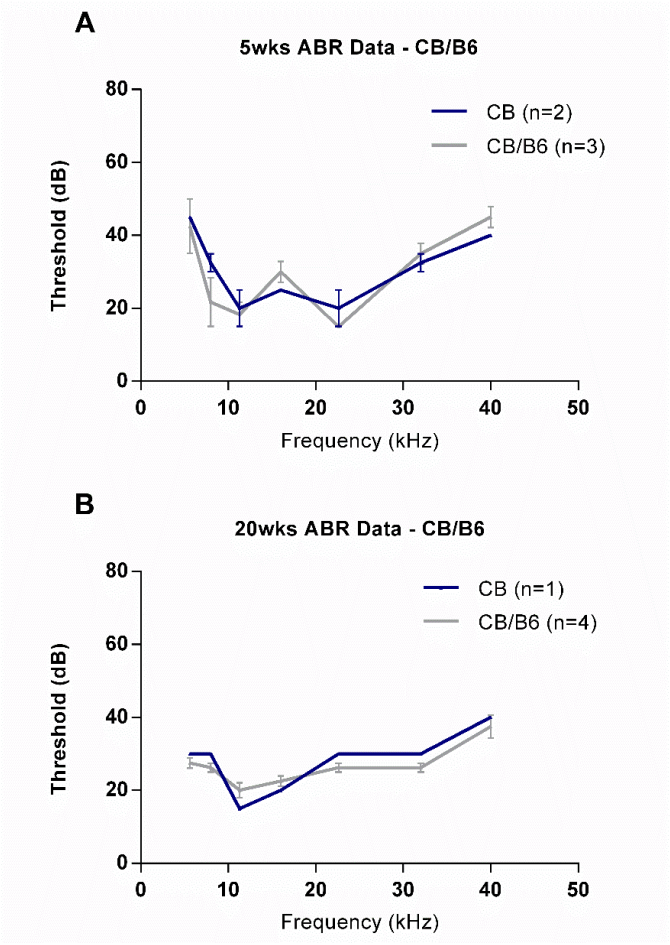

Figure 3.3. CB/B6 mice have hearing similar to CB mice

Hearing of F1 cross of CB/B6 is normal at 5 weeks and 20 weeks of age. Hearing loss in B6 is noted as young as 12 weeks of age. Published studies have shown B6 hearing loss beginning between 14 and 24 weeks of age (Henry 2002; Kane et al. 2012). Published studies show that CB/B6 hybrids have normal hearing out to 24 months (Frisina et al. 2011).This suggests that CB alleles rescue AHL in B6 and indicates that allelic traits contributing to hearing loss are recessive. Error bars indicate average of data and SEM.

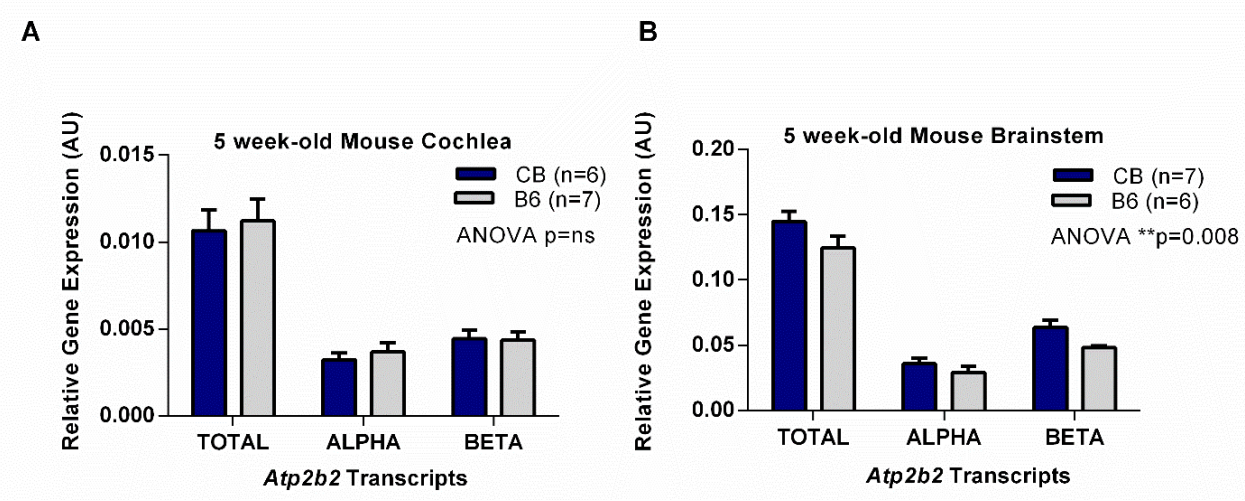

Figure 3.4. *Atp2b2* transcripts are downregulated in brainstem of 5 week-old B6 mice

Atp2b2 transcripts were analyzed in the brainstem and cochlea of CB and B6 inbred strains. Primers recognize *αAtp2b2*, *βAtp2b2* and total recognizes α, β and unknown 5'UTR transcripts expressed in these tissues. Data was analyzed with a 2-way ANOVA to detect the effect of genotype and gene on *Atp2b2* transcript expression. A. At 5 weeks of age there is no genotype effect on *Atp2b2* transcript in the cochlea. B. There is a genotype effect on *Atp2b2* transcript in the brainstem at 5 weeks of age. A Bonferroni post-hoc did not reveal any specific transcripts of the brainstem that are significantly affected. **p=0.008. Error bars indicate average of data and SEM.

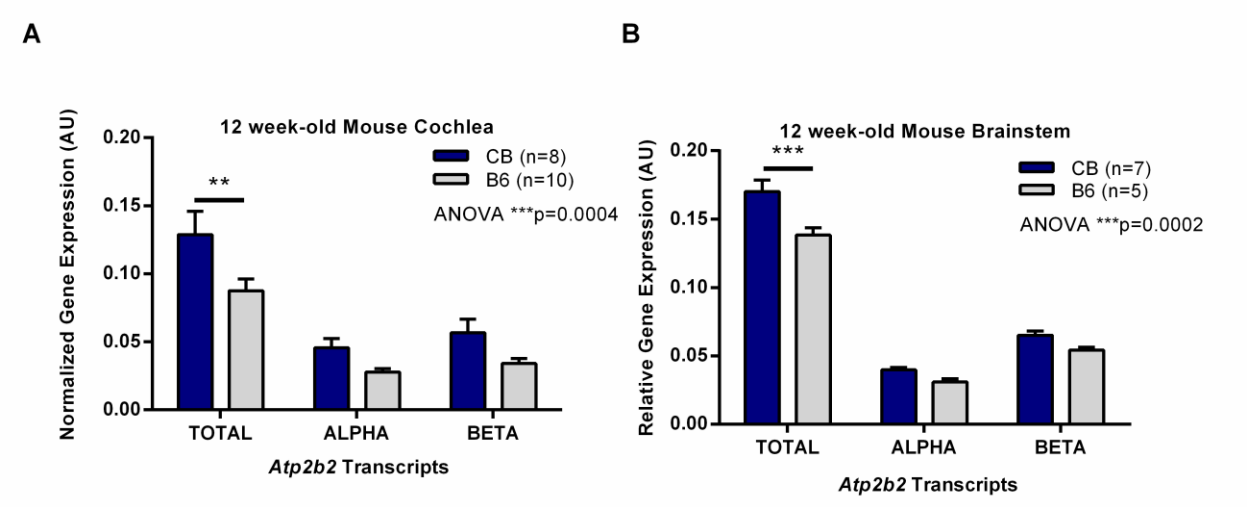

Figure 3.5. *Atp2b2* transcripts are downregulated in 12 week-old B6 mice

Atp2b2 transcripts were analyzed in the brainstem and cochlea of CB and B6 inbred strains. Primers recognize *αAtp2b2*, *βAtp2b2* and total recognizes α, β and unknown 5'UTR transcripts expressed in these tissues. A. At 12 weeks of age there is a significant genotype effect on *Atp2b2* transcript expression in the cochlea, ***p=0.0004 in a two-way ANOVA. A Bonferroni post-test shows total transcript is significantly affected, **p≤ 0.01 B. There is also a genotype effect on *Atp2b2* transcript expression in the brainstem at 5 weeks of age, ***p=0.0002. A Bonferroni post-test indicates that total transcript is significantly affected ***p≤0.001. Error bars indicate average of data and SEM.

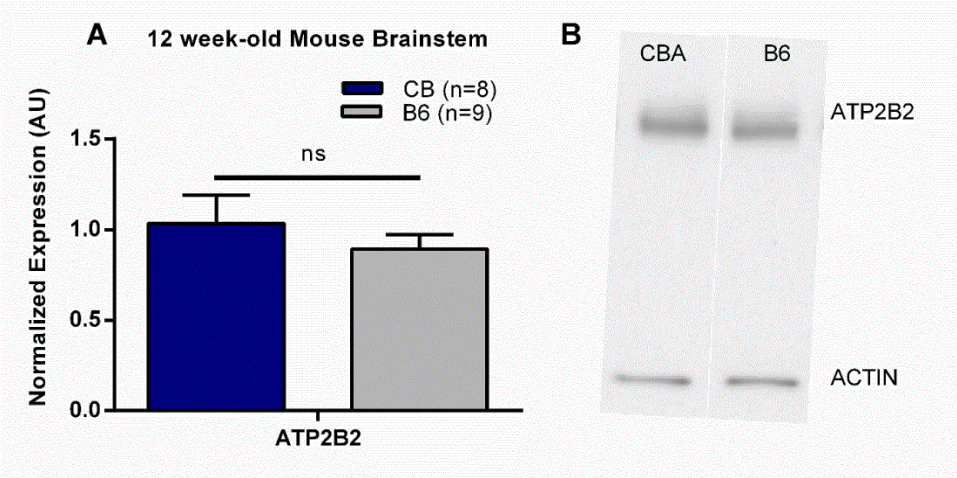

Figure 3.6. ATP2B2 is not significantly different in CB and B6

A. Brainstem ATP2B2 was quantified from CB and B6 inbred strains. Although the trend shows decreased expression of ATP2B2 protein in B6 brainstem it is not significant. This is likely due to the small change in expression and the error in the assay. B. A representative western blot is shown. Error bars indicate average of data and SEM.

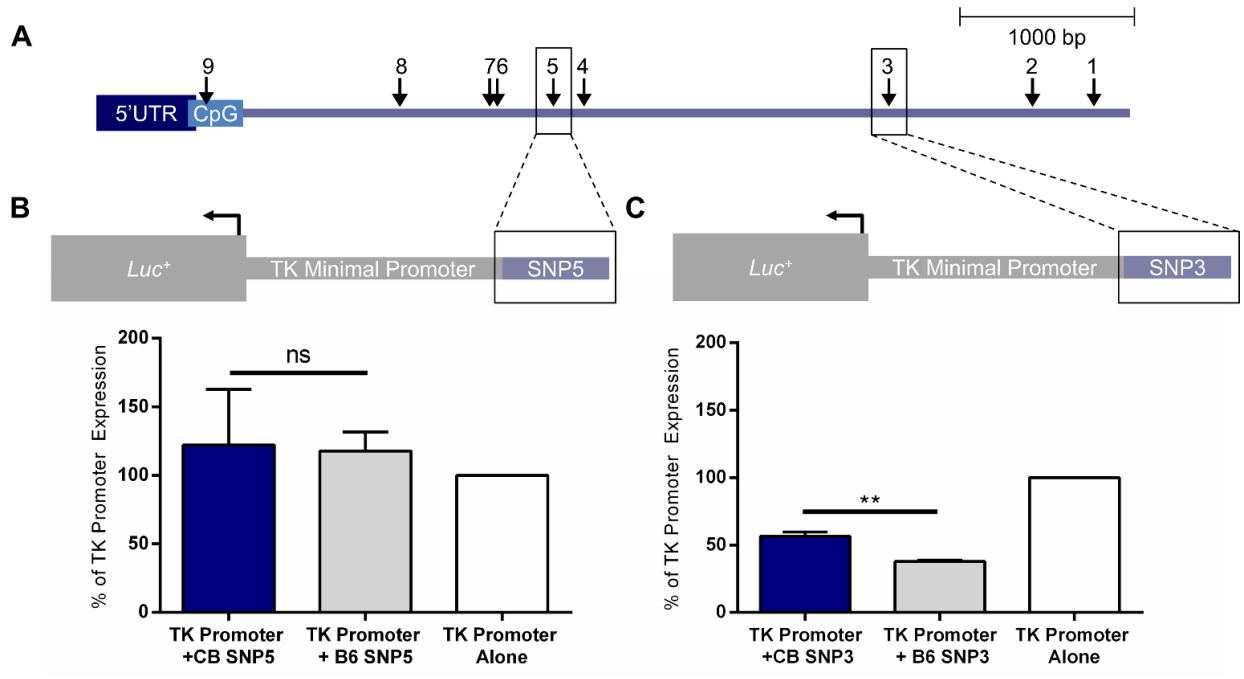

Figure 3.7. SNP3 may decrease activity of the *αAtp2b2* promoter

SNP3 and SNP5 were inserted in front of the TK minimal promoter. The luciferase activity of the constructs containing either the CB or B6 SNP were normalized to baseline TK promoter expression. Two-tailed unpaired t-tests were used to compare the normalized values of the CB SNPs with the B6 SNPs. A. There is no difference in promoter activity with the addition of the CB or B6 SNP5. B. The addition of CB and B6 SNP3 to the TK promoter caused decreased activity. The B6 SNP3 promoter activity was significantly different than the CB SNP3 construct **P≤ 0.001. Error bars indicate average of data and SEM.

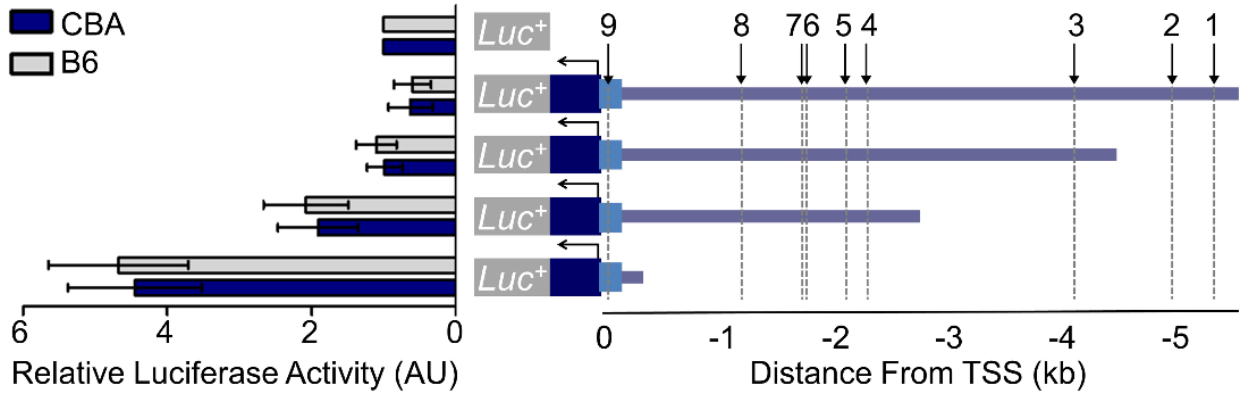

Figure 3.8. CB and B6 *αAtp2b2* promoter activity is the same in OC-1 cells

Luciferase activity of promoter constructs is normalized to empty luciferase vector (pGL3). *αAtp2b2* promoter constructs reveal no difference in luciferase expression between promoters cloned from CB and B6 mouse strains. P=ns utilizing a two-way ANOVA comparing all promoter truncations for a genotype effect. Error bars indicate average of data and SEM.

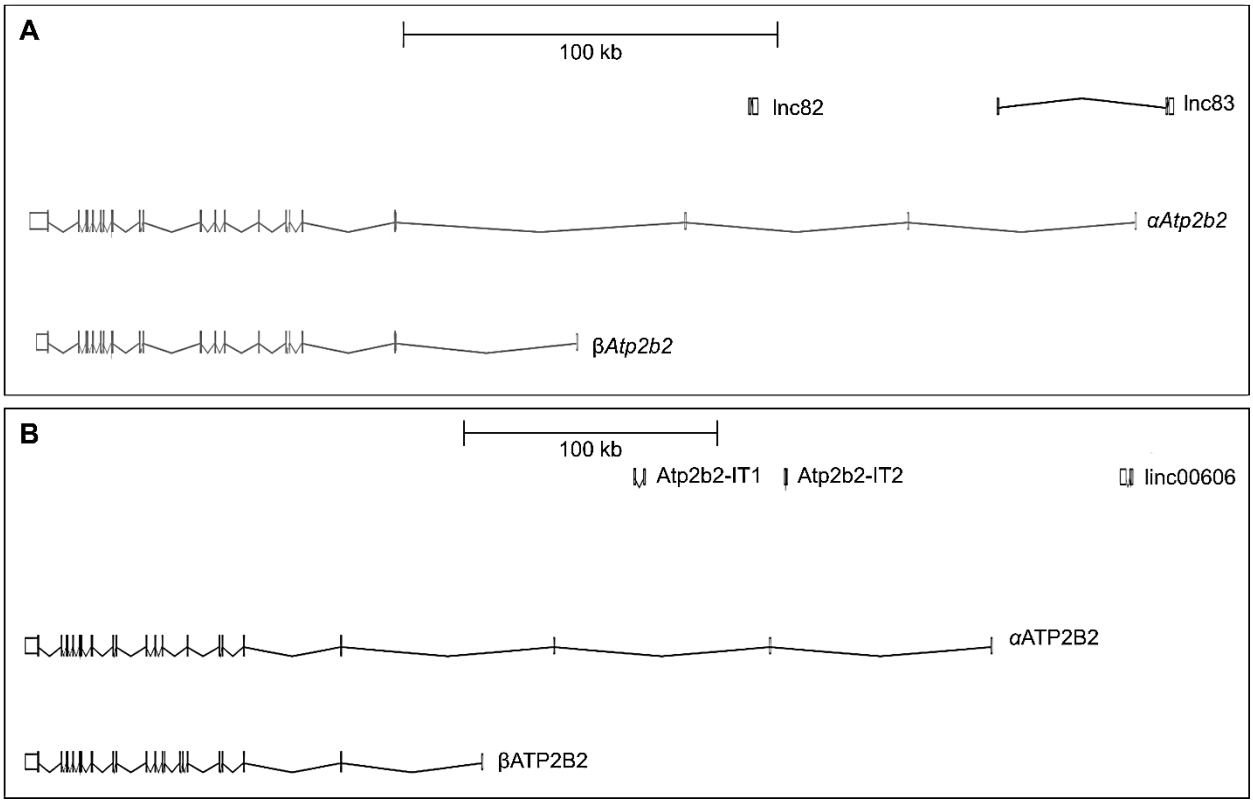

Figure 3.9. Predicted lncRNAs in mouse and human

Cartoon adapted from Ensemble version 82. Shown is the reverse strand of mouse Chr 6:113,742,662 - 114,052, 431 (GRCm38.p4) and the reverse strand of human Chr 3:10,322,505 - 10,809,076 (GRCh38.P3) (Cunningham et al. 2015). A. The two *Atp2b2* transcripts found in mouse brain (α and β) are included for reference. Two lncRNAs are identified in the 5'UTR of *Atp2b2*. The exons of lnc83 are located in the intronic regions surrounding the Iα exon of *αAtp2b2*. The exons of lnc82 are located between the IIα and IIIα exons of the 5'UTR. B. LncRNAs exist in the same region in human *ATP2B2*. Although there is no sequence conservation between mice and humans the presence of lncRNAs in both species indicates mechanistic conservation.

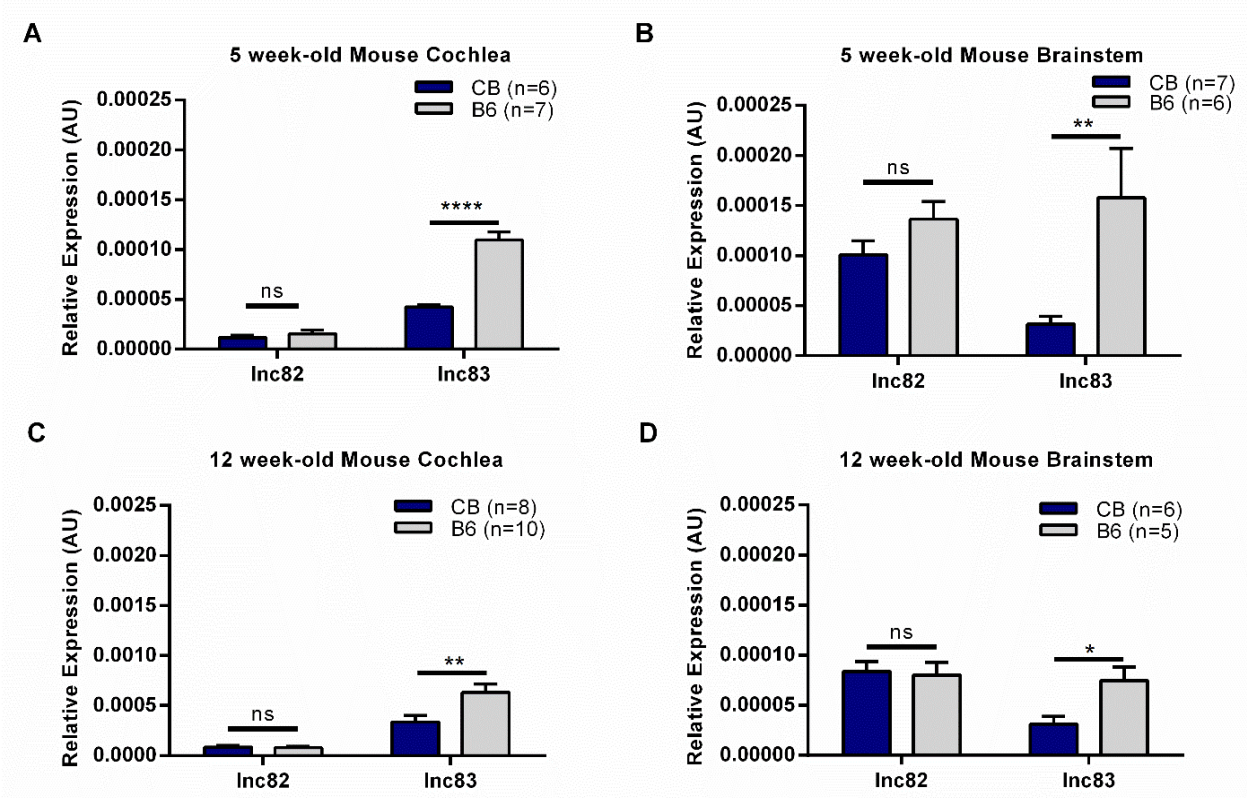

Figure 3.10. Lnc83 is upregulated in B6 brainstem and cochlea

Lnc82 and lnc83 have tissue specific and genotype specific expression profiles. Lnc82 is expressed higher in the brainstem and lnc83 is expressed higher in the cochlea. A, B, C, D - All tissues were compared using the Holm-Sidak method of multiple t-tests. For all tissues at all ages there is no significant difference in expression of lnc82 in B6 mice compared to CB mice. For all tissue types at all ages, lnc83 transcript was significantly upregulated in B6 mice. This implicates a functional role for lnc83 in in the B6 mouse brain. *P≤0.05, **p≤0.01, ***p≤0.001, ****p≤0001. Error bars indicate average of data and SEM.

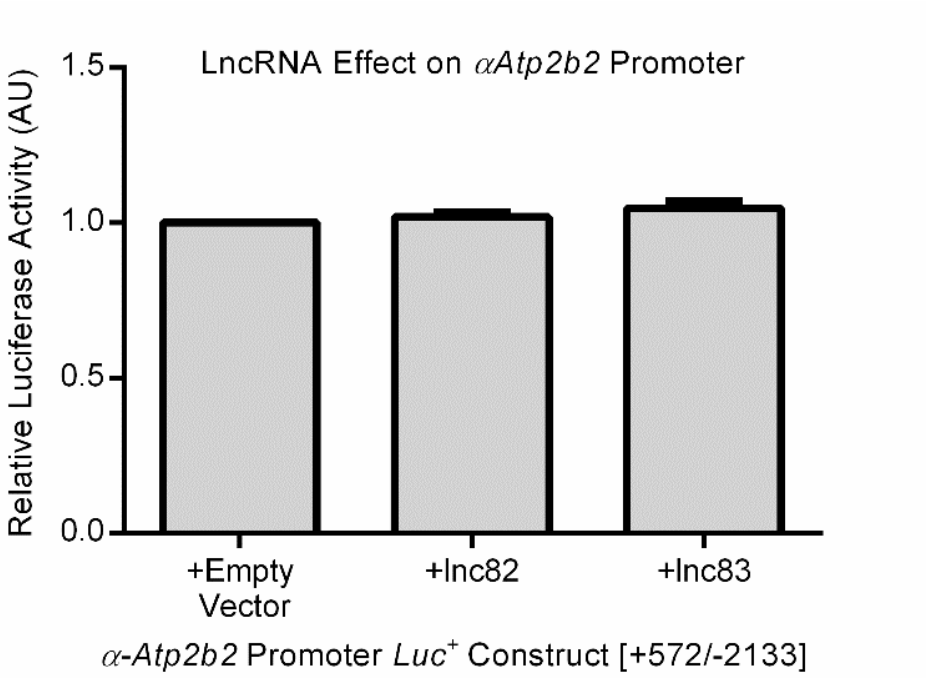

Figure 3.11. Lnc82 and lnc83 do not affect *αAtp2b2* promoter activity

When lnc82 and lnc83 constructs were co-expressed with promoter vector, they did not have an effect on luciferase activity. This suggests that the lncRNAs do not act at the promoter. p=ns utilizing a one sample t-test comparing values to a theoretical value of 1. Error bars indicate average of data and SEM.

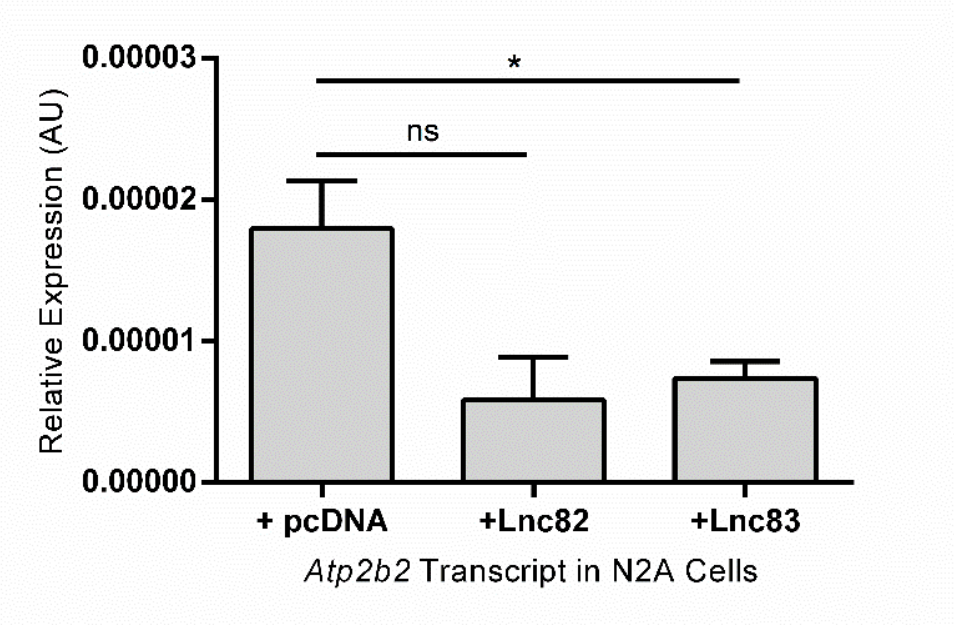

Figure 3.12. Lnc83 inhibits *Atp2b2* transcript expression in N2A cells

To investigate the function of lnc82 and lnc83, they were overexpressed in N2A cells. Compared to control vector, pcDNA3.1a, using a two tailed unpaired t-test. Overexpression of lnc83 significantly inhibits expression of *Atp2b2* transcript in N2A cells, *$p \leq 0.05$. Lnc82 did not have a significant effect on *Atp2b2* transcript expression compared to pcDNA3.1a ($p=0.06$). Error bars indicate average of data and SEM.

Chapter 4. CHARACTERIZATION OF *ATP2B2* IN CONGENIC MICE

Summary

The downregulation of *Atp2b2* transcript in B6 mice is likely caused by genomic elements surrounding the *Atp2b2* gene. Because of *Atp2b2*'s digenic interaction with *Cdh23*, downregulation of *Atp2b2* in B6 likely contributes to AHL in this strain. LncRNA, lnc83, is the proposed mechanism for inhibition of *Atp2b2* transcript in B6 mice. To study the contribution of the *Atp2b2* region in AHL and misregulation of *Atp2b2* and lnc83 transcripts in B6 mice, two congenic strains were bred: (1) B6 haplotype at *Atp2b2* in a CB background, CB.B6^{Atp2b2}, and 2) CB haplotype at *Atp2b2* in a B6 background, B6.CB^{Atp2b2}. We found that CB.B6^{Atp2b2} mice have elevated thresholds at 5.6 kHz at 6 months of age. We also found that the B6.CB^{Atp2b2} mice have intermediate thresholds at high frequencies at 6 months of age. Both CB.B6^{Atp2b2} and B6.CB^{Atp2b2} mice have normal levels of *Atp2b2* transcript but lnc83 transcript is upregulated in CB.B6^{Atp2b2} mice. Although we were unable to show downregulation of *Atp2b2* transcript in the 12 week-old CB.B6^{Atp2b2} mouse brainstem, we were able to show upregulation of lnc83 and elevated hearing thresholds. From this data we conclude that the B6^{Atp2b2} locus is necessary but not sufficient to cause the B6 AHL phenotype.

4.1 INTRODUCTION

In the last chapter, the extent of *Atp2b2* downregulation in B6 mouse brainstem and cochlea was investigated. We found that in 12 week-old mouse, *Atp2b2* transcript levels are decreased. Additionally, lnc83 is implicated as the mechanism for downregulation of *Atp2b2* in B6. In this chapter we attempt to rescue the *Atp2b2* phenotype of B6 by producing a congenic mouse with a CB haplotype at *Atp2b2*. In addition, we will study the effects of B6 *Atp2b2* on the good hearing CB strain by creating a congenic strain with a B6 haplotype at *Atp2b2* in a CB background.

4.1.1 *Investigations of ahl in B6 mice and the involvement of Cdh23*

B6 mice are used for a wide range of research studies and remain a predominant model of AHL. Studies have shown that the progression of hearing loss in these mice starts as early as 3 months of age and quickly progresses. The progression of hearing loss in these mice is equivalent to human hearing loss because it affects the high-frequencies first. Subsequently, low frequencies are affected and eventually the mouse has measurable hearing loss at all frequencies (Henry 2002; Kane et al. 2012). Studies show that by 1 year of age B6 mice are almost completely deaf (Frisina et al. 2011). Anatomical studies have shown that structural changes occur in the cochlea starting at the base and extending to the apex. These changes are numerous and include loss or damage of hair cells, spiral ganglion neurons and the spiral ligament (Henry 2002).

Quantitative trait locus analysis identifies Chr 10 as a contributor to AHL (Noben-Trauth et al. 1997). The region was narrowed by utilizing crosses with *dfw* mice, eventually revealing *Cdh23* as the contributing gene. A SNP in the intronic region of *Cdh23* caused in-frame skipping of exon 7. This polymorphism may lead to altered adhesion or stability of CDH23 and was identified in a number of other inbred strains with known AHL phenotypes such as: BALB/cByJ and DBA/2J

(Noben-Trauth et al. 2003). To date, the mutation in *Cdh23* is still widely accepted as the causal region for AHL in B6 mice. Given the severity of the hearing loss it is interesting that it is caused by a SNP in the intronic region of the gene. This observation illustrates the importance of studying subtle changes in genomic structure as they can have huge implications for disease. The next section will investigate the emerging role of *Cdh23* in AHL.

4.1.2 *Cdh23 congenic mice*

Unlike transgenic mice, congenic strains are made by selective breeding. This technique utilizes chromosomal recombinations to create breakpoints around genes of interest without the use of cloning. The benefit of breeding a congenic strain is that the target gene locus maintains its native chromosomal structure. This makes congenic mice ideal for molecular genetic studies. To better understand the role of *Cdh23* in AHL of B6 mice, The Jackson Laboratory (JAX) created two congenic strains: (1) CB background with B6 at *Cdh23* (CB.B6$^{Cdh23\text{-}ahl}$) and (2) B6 background with CB at *Cdh23* (B6.CB^{Cdh23}). The congenic interval is 50 megabases (Mb) for B6.CB^{Cdh23} [53.46 Mb (rs3696307) to 105.44 Mb (rs13480749)] and 35 Mb for CB.B6$^{Cdh23\text{-}ahl}$ [38.69 Mb (rs13480581) to 74.61 Mb (rs13480654)]. To better understand the genetic makeup of these congenes, a cartoon karyotype of the inbred strains and the congenic mice is included in this thesis (Fig. 4.1 A,B) (Kane et al. 2012).

These mice were created to isolate the *Cdh23*^{ahl} mutation and test its contribution to the AHL phenotype of B6 mice. It was anticipated that the CB.B6$^{Cdh23\text{-}ahl}$ strain would have AHL similar to the B6 inbred strain and that the B6.CB^{Cdh23} would exhibit a rescue phenotype of B6 AHL. When the phenotype of these two congenes was investigated, it was found that this is not the case. Hearing was examined at 8, 16 and 32 kHz at 3, 6, 9, 12, 15, and 18 months of age. At all ages, both congenes had hearing similar to the CB inbred strain at 16 and 32 kHz. Only at 8 kHz did

both congenic mice have an intermediate phenotype that started at around 15 months of age. At 15 and 18 months of age the B6.CB^{Cdh23} mouse had higher thresholds than the CB.B6$^{Cdh23\text{-}ahl}$ mouse (ns). This is surprising because the B6.CB^{Cdh23} mouse was expected to have rescued hearing loss but it was the only mouse that differed from the CB inbred strain with age. Anatomical measurement of hair cell loss in the two congenic strains agrees with the hearing thresholds: B6.CB^{Cdh23} had the most pronounced hair cell loss when compared to the CB inbred strain or CB.B6$^{Cdh23\text{-}ahl}$. These data suggest that another gene in the background of B6 is interacting with the *Cdh23* mutation leading to the full AHL phenotype. In the results section we will discuss the development of two new congenic strains of mice that investigate *Atp2b2'*s role in the B6 AHL phenotype.

4.2 METHODS

4.2.1 *Animals*

The congenic strains: 1) B6 haplotype at *Atp2b2* in a CB background, CBACa.B6-*Atp2b2*$^{C57BL/6J}$ (CB.B6^{Atp2b2}) AND 2) CB haplotype at *Atp2b2* in a B6 background, B6.CBACa-*Atp2b2*$^{CBA/CaJ}$ (B6.CB^{Atp2b2}) and inbred strains B6 and CB were used in age ranges from 5 weeks to 24 weeks (6 months) of age. All animals were male. The congenic strains were backcrossed into CB (JAX Stock No: 000654) or B6 (JAX stock No: 000664), respectively, for eight generations before intercrossing to fix the strains. Three genomic markers were used for selection of *Atp2b2* spanning two meagabases (rs13478978 G/A, rs30564623 G/A and rs13478985 T/C). The congenic interval was identified for both strains: CB.B6^{Atp2b2} (59.53 Mb) and B6.CB^{Atp2b2} (50.34 Mb). *Cdh23* was also monitored during backcrossing and *Cdh23*^{ahl} was crossed out of the CB.B6^{Atp2b2} strain between generation 3 and 4. Tissue was collected from 12 week-old CB.B6^{Atp2b2} and B6.CB^{Atp2b2} brainstem and cochlea. Animals are kept in a 12-h light/dark cycle with minimal environmental exposure to noise. All procedures in this study are approved by the University of Washington Institutional Animal Care and Use Committee.

4.2.2 *Auditory testing*

Auditory sensitivity was measured using ABR. Frequencies tested varied by testing age and included 5.6 kHz, 8 kHz, 16 kHz, 32 kHz and 40 kHz. Prior to auditory screening, mice are anesthetized using a mix of ketamine (130mg/kg) and xylazine (10mg/kg). Once animals are anesthetized they are placed in a sound proof box with a heat lamp/heating pad and secured with a bite bar. The system was calibrated at the beginning of each test session to confirm the output of the speaker was in the normal range. Responses were measured by two electrodes placed

subcutaneously at the forebrain and brainstem. A reference electrode was placed at the hind limb and electrocardiogram recordings were used to monitor anesthesia.

A series of 300 to 500 tones per frequency and intensity were administered. Tones were 5ms long with a 0.5ms rise fall $\cos^2$ function. Brain waves were recorded for 25ms with a 40ms spacing between repetitions. ABRs are amplified 1000x filtered and digitized by a pre-amplifier (P55; Grass Telefactor West Warwick, RI). Post-amp gain ranged from 30-35 (dB) for all animals (Mo.# 3362 K-H Corp). Threshold was determined visually as the lowest intensity that evoked a reproducible and recognizable brain wave in at least two out of three trials.

4.2.3 *qPCR*

Rough dissections of 12 week-old brainstem from CB.B6^{Atp2b2} and B6.CB^{Atp2b2} were performed on the bench top and immediately transferred to a microtube filled with RNA*later*. Cochlea microdissections were performed using a compound light microscope (Zeiss) in RNA*later*. The vestibular portion of the cochleae was removed and vasculature, neuronal tissue and bone were trimmed. Once cleaned, the cochleae were perfused with RNA*later* and stored in microtubes containing more of the solution. Both tissues were stored at 4^{o}C for at least a week to allow the RNA*later* solution to properly perfuse the tissues. Tissues were then stored at -80^{o} C for later use.

RNA was isolated using the RNeasy Plus Universal Mini Kit according to manufacturer's protocol (Qiagen No: 73404). Homogenization for brainstem was accomplished using a Polytron PT 1200 rotor-starter homogenizer. RNA extraction efficiency was measured using a Nanodrop spectrophotometer (ThermoScientific); 260/280 ratios of 2.00 or higher and 260/230 ratios greater than 1.00 were acceptable. If ratios were significantly lower than this tissues were not used. Borderline tissues were used for expression assays and any tissues exhibiting anomalous expression profiles were submitted to a grub's outlier test.

Total RNA (up to 2µg) was reverse transcribed into complimentary DNA (cDNA) using SMARTscribe reverse transcriptase (Clontech) and random hexamer primers (Applied Biosystems). These samples were used for qPCR analysis using BioRad Sybr green master mix. Reactions were performed on a CFX96 from BioRad with CFX96 manager software. Total-*Atp2b2*, *αAtp2b2*, *βAtp2b2*, lnc82 and lnc83 cycle thresholds were normalized to two housekeeping genes (*Actb* and *Actg* for brainstem, *Hmbs* and *Actg* for cochlea). Primer sequences are the same as those previously used in Chapter 3 above. For full analysis techniques see: (Silverstein and Tempel 2006). Data is the average of at least three runs where replicates within a run had a relative standard deviation (std. dev.) of less than 0.03 (std. dev./CT > 0.03 were excluded).

4.3 RESULTS

4.3.1 *Development of Atp2b2 congenic lines*

In the last chapter, two discreet measures were used to show downregulation of *Atp2b2* transcript in B6 cochlea and brainstem. We have also shown that lnc83 is upregulated in B6 cochlea and brainstem. Preliminary assays suggest that lnc83 may downregulate *Atp2b2*. Given the known digenic interaction of *Atp2b2* and *Cdh23*, we decided to develop two congenic strains to investigate the interaction of these two genes in the B6 mouse. The two congenic lines are: (1) B6 haplotype at *Atp2b2* in a CB background, CB.B6^{Atp2b2} and (2) CB haplotype at *Atp2b2* in a B6 background, B6.CB^{Atp2b2}. To better understand the genetic makeup of these congenes, a cartoon karyotype was drawn to visualize the chromosomal composition (Fig. 4.1 C, D). The congenic interval was identified for CB.B6^{Atp2b2} and B6.CB^{Atp2b2}. For both strains the congenic interval is approximately 50 Mb which contains large areas ambiguity. The predicted congenic region (Chr 6: 139,039,752 - 88,697,545) contains over 400 genes (Fig. 4.2). It is expected that the B6.CB^{Atp2b2} will have a rescue phenotype, exhibiting normal levels of *Atp2b2* transcript and lnc83. It is also possible that hearing thresholds could be improved in this mouse. We expect the CB.B6^{Atp2b2} mouse to have downregulated *Atp2b2* and upregulated lnc83 similar to B6. This mouse may also have worsened thresholds when compared to the CB inbred strains.

4.3.2 *Hearing in young mice*

To understand the contribution of *Atp2b2* to hearing sensitivity in B6 mice it is important to also investigate an age at which there is no AHL phenotype. A review of the literature indicates that hearing onset in mice is around P-12 (Mikaelian et al. 1965) but that *Atp2b2* expression and hearing is not stable until sometime between 3 and 4 weeks of age (Chen et al. 2012; Watson et al.

2014). Our own studies indicate that by 12 weeks of age there are detectable changes in the B6 auditory system so we chose a time point close to maturation of hearing, 5 weeks of age. We tested hearing at four frequencies 8, 16, 32 and 40 kHz in the following strains CB, B6, CB.B6^{Atp2b2} and B6.CB^{Atp2b2}. As was expected, at this young age there was no difference in hearing thresholds in any of the strains. During data analysis it was noted that there seems to be slightly elevated thresholds in the B6 inbred mice already at this young age (ns) (Fig. 4.3).

4.3.3 *ABRs at the onset of hearing loss*

As B6 ages, it is known that there are changes to the structure and function of the cochlea. Many studies suggest that the onset of hearing loss in B6 mice is somewhere between 3 and 6 months of age. Using subtler measures, we have been able to detect changes in gene expression of *Actb* in the cochlea at as young as 12 weeks of age. This is also the time point at which *Atp2p2* is downregulated in B6 mouse cochlea and brainstem tissue. For our study, 12 weeks of age was investigated by ABR because it seems to be a critical time point in the progression of AHL in B6 mice. Utilizing a two-way ANOVA we were able to identify a genotype effect on thresholds at 12 weeks of age. A Bonferroni post-test identified that B6. and B6.CB^{Atp2b2} mice have significantly elevated thresholds (compared to CB) at 40 kHz (Fig. 4.4).

4.3.4 *Middle aged ABRs*

Numerous studies exhibit heightened thresholds in B6 mice at 24 weeks of age (Henry 2002; Frisina et al. 2011; Kane et al. 2012). For this reason we chose to investigate the thresholds of the congenic mice at this time point. Due to the well characterized hearing loss at the low frequencies we added 5.6 kHz. At 6 months of age a two-way ANOVA predicts a prominent genotype effect on auditory threshold. Interestingly, the phenotype of the B6.CB^{Atp2b2} congene seems to depart

from the phenotype of the B6 inbred strain at this age. At both 32 kHz and 40 kHz in a Bonferroni post-test, B6.CB^{Atp2b2} has an intermediate phenotype between CB and B6 inbred strains (Fig. 4.5). Additionally, an interaction between genotype and frequency was found. This indicates that some frequencies are differentially affected by strain and were not accounted for in the Bonferroni post-test. Therefore, 5.6 kHz was investigated separately. The thresholds at this frequency were compared using a one-way ANOVA. This test identified that mice with a B6 haplotype at *Atp2b2* (CB.B6^{Atp2b2} and B6) had heightened thresholds at 5.6 kHz compared to mice with a CB haplotype at *Atp2b2* (B6.CB^{Atp2b2} and CB) (Fig. 4.6). This implicates a role for *Atp2b2* in protection against mutations in *Cdh23* at high frequencies and as a primary cause of heightened thresholds at the low frequencies.

4.3.5 *Atp2b2 and lncRNA expression in congenic mice*

Auditory data supports the hypothesis that *Atp2b2* plays a role in AHL of B6 mice. To further investigate this involvement, *Atp2b2* transcript was measured in the brainstem of B6.CB^{Atp2b2} and CB.B6^{Atp2b2} mice at 12 weeks of age. This is a critical time point in AHL progression. We expected to see a rescue of *Atp2b2* transcript downregulation in B6.CB^{Atp2b2} mice and expected to see decreased expression of *Atp2b2* transcript in CB.B6^{Atp2b2} mice. Data was collected and compared to CB and B6 inbred strain data from Chapter 3. Utilizing a two-way ANOVA it was found that there is a genotype difference of *Atp2b2* expression (Fig. 4.7). A Bonferroni post-hoc test indicated that CB, B6.CB^{Atp2b2} and CB.B6^{Atp2b2} have the same levels of *Atp2b2* transcript expression. This suggests that we were able to rescue the downregulation of *Atp2b2* in B6 mice. However, we were not able to show a decrease in *Atp2b2* transcript expression in the CB.B6^{Atp2b2} mice suggesting that there is potentially a compensatory mechanism in CB mice.

We also looked at the expression of lnc82 and lnc83 in the brainstem of the congenes. Given our hypothesis that lnc83 is inhibiting expression of *Atp2b2* in B6 mice we expected that the B6.CB^{Atp2b2} mouse would have normal expression of lnc83. Given the normal expression of *Atp2b2* in the CB.B6^{Atp2b2} mouse we predicted normal expression of lnc83. A two-way ANOVA was used to compare lnc82 and lnc83 expression across all four inbred strains; this includes inbred data from chapter 3. Lnc83 was upregulated in B6 inbred mice and in CB.B6^{Atp2b2} mice which have a B6 haplotype at *Atp2b2*. Lnc82 expression was not significantly different in the congenes, however, a post-hoc test showed that lnc82 levels in the B6.CB^{Atp2b2} mouse were reduced in 12 week-old brainstem. The significance of this finding is unknown (Fig. 4.8).

4.4 DISCUSSION

In this chapter, we have investigated the role of the *Atp2b2* locus in AHL of B6 mice by creating two congenic mouse strains: CB.B6^{Atp2b2} and B6.*CB*^{Atp2b2}. Through testing of auditory sensitivity in aging and study of gene expression we have compelling evidence that *Atp2b2* is contributing to AHL in B6 mice. In this section we will discuss the novel contribution of these findings to previous research, discuss study limitations and describe future experiments. Previous research has mapped the *ahl* locus to mouse Chr 10 specifically to *Cdh23* (Noben-Trauth et al. 2003). Although it is clear that this gene plays a role in hearing loss of mice as well as humans, in the case of B6 mice, *Cdh23* alone is not sufficient to explain the phenotype (Kane et al. 2012). Given the misregulation of the *Atp2b2* locus in B6 inbred mice and the known digenic interaction between *Atp2b2* and *Cdh23* it is likely that *Atp2b2* is a contributor to the B6 AHL phenotype.

4.4.1 *The Atp2b2 gene from CB mice rescues hearing loss in B6 mice*

ABRs of B6.CB^{Atp2b2} suggest that the CB *Atp2b2* locus is capable of rescuing part of the AHL phenotype in B6 mice at 6 months of age, however, there is still high frequency loss. Studies of congenic mice indicate that *Cdh23*^{ahl} alone is incapable of causing an AHL phenotype in CB mice (Kane et al. 2012). Taken together, this data suggests that there may be yet another gene in the B6 background contributing to a multi-genic AHL phenotype. Several studies have proposed other causal genes that could be involved (Park et al. 2011; Wang et al. 2012). A protein of particular interest, programmed cell death 5 (PCDC5), has increased expression in B6 and is correlated with caspase 3 induced apoptosis in hair cells and spiral ganglion neurons in B6 mice (Wang et al. 2012).

Interestingly, both mouse strains with a B6 haplotype at *Atp2b2* (B6 and CB.B6^{Atp2b2}) exhibited moderate hearing loss at low frequency at 6 months of age. This was a surprising finding and was supported by the fact that B6.CB^{Atp2b2} mice did not exhibit low frequency loss. In fact, these mice had hearing identical to CB at 6 months of age. Other studies have indicated that *Atp2b2* may be involved in low frequency hearing loss (Watson and Tempel 2013). Further studies are needed to investigate the hearing thresholds of these congenes at later time points to tease apart the contribution of *Atp2b2* to B6 AHL.

4.4.2 *Lnc83 overexpression and downregulation of the Atp2b2 transcript*

Expression data of the *Atp2b2* transcript in 12 week-old mouse brainstem shows that we were able to rescue B6 downregulation of *Atp2b2* in the B6.CB^{Atp2b2} mouse. However, we were unable to show decreased expression of the *Atp2b2* transcript in the CB.B6^{Atp2b2} mouse. Further studies need to be done in the cochlea of these mice to determine if there is downregulation in other tissue types. Although overall *Atp2b2* expression was not affected in the CB.B6^{Atp2b2} mice, lnc83 expression was increased in these mice. We have suggested that lnc83 overexpression inhibits expression of *Atp2b2* transcript, but from the data in this thesis, it is clear the model is not perfect. Isolated overexpression of both lnc82 (ns) and lnc83 has shown inhibition of *Atp2b2* transcript in N2A cells, but it is highly possible that the relationship is more complex than that. Further studies of the localization of lnc83 and its mechanism of action are needed to understand its fundamental action in regulation of *Atp2b2* and other genes.

Although CB.B6^{Atp2b2} does not have an overall decrease in *Atp2b2* expression, it does have upregulated lnc83. It is possible that lnc83 could affect the regulation of the *αAtp2b2* or *βAtp2b2* transcripts in an immeasurable way. For example, we know that *αAtp2b2* and *βAtp2b2* have unique promoters and it is known that alternate gene promoters can dictate splicing patterns (Wong et al.

2010; Banday et al. 2011). It is therefore postulated that lnc83 affects the splicing of *Atp2b2* leading to altered function or localization of ATP2B2. This model is supported by studies of Zeb2 and ErbAα2 mRNA, in these transcripts, splicing is modulated by lncRNAs (Munroe and Lazar 1991; Beltran et al. 2008) . Further studies investigating the function of lnc83 and *Atp2b2* transcript localization/function in B6 mice are needed to discern the validity of this hypothesis.

4.4.3 *Intronic regions play a role in disease*

In this chapter we have investigated another example of the digenic interaction of *Atp2b2* and *Cdh23*. This is a novel finding in B6 mice and is exciting for the field because it implicates lncRNA in modulation of auditory transduction. Additionally, ATP2B2 protein appears to be unaffected implicating more subtle changes in transcript usage and localization in the B6 phenotype. This study highlights the importance of investigating both exons AND introns of potential disease causing genes.

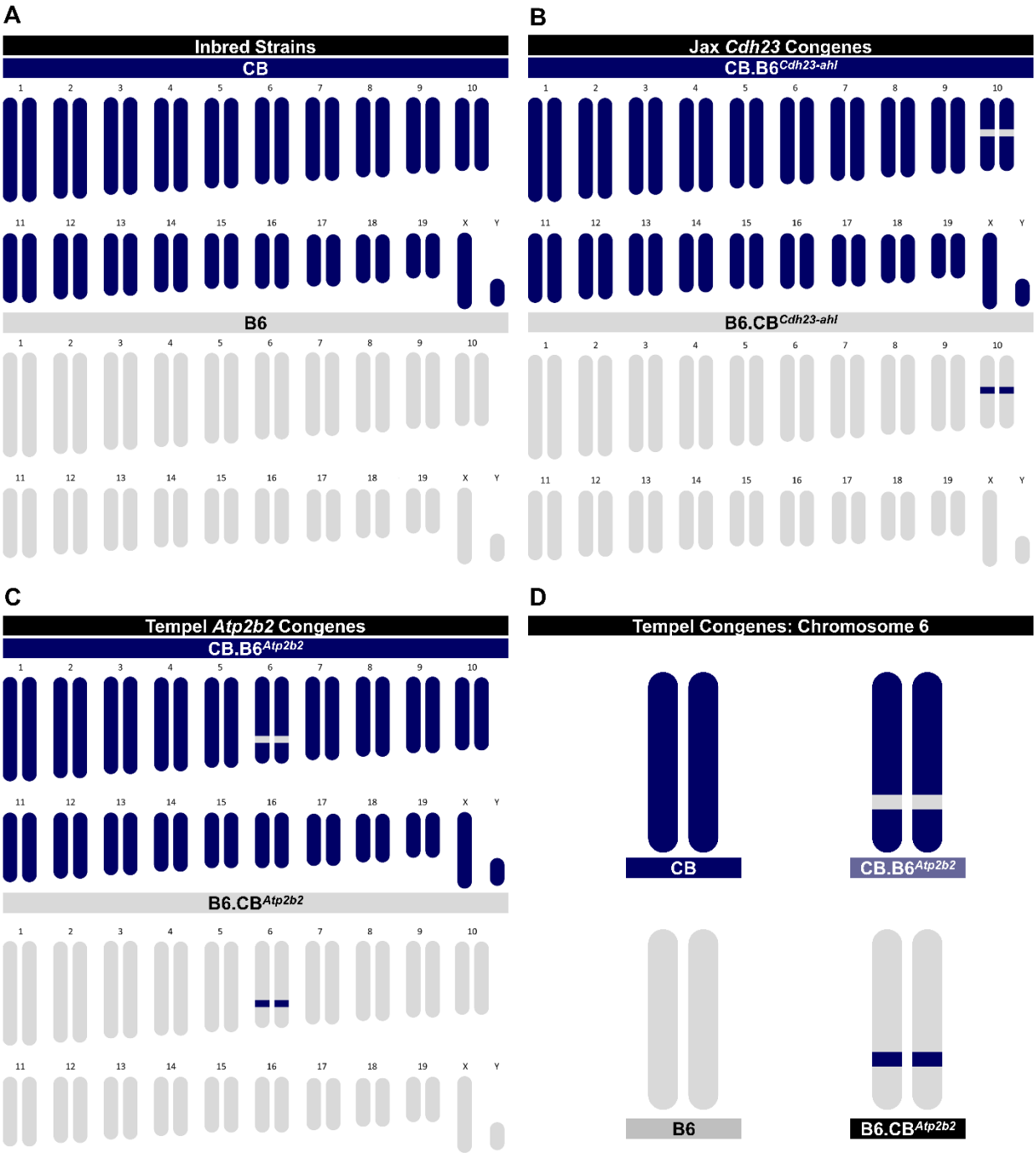

Figure 4.1. Karyotype for inbred and congenic strains

CB.B6^{Atp2b2}- Expected to have downregulation of *Atp2b2* and potentially worse hearing than CB inbred strains. B6.CB^{Atp2b2}-Expected to have normal expression of *Atp2b2* and potentially better hearing than B6 inbred strains.

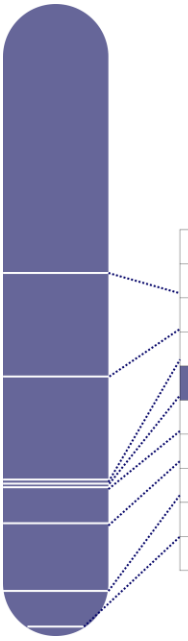

Orientation	RS Number	Location	CB	B6	B6.CB^{Atp2b2}	CB.B6^{Atp2b2}
Downstream	rs242029300	6:63772203	C	T	?	C (?)
Downstream	rs6260853	6:88697545	G	A	A	A
Downstream	rs13478978	6:112800820	G	A	G	A
Atp2b2	rs30564623	6:113723408	G	A	G	A
Upstream	rs13478985	6:114760449	T	C	T	C
Upstream	rs30172783	6:123305972	A	G	A	A
Upstream	rs48506166	6:139039752	G	A	A	G
Upstream	rs30214084	6:147824176	G	A	A	G
Approximate Congenic Interval					50.34 Mb	59.53Mb

Figure 4.2. Congenic intervals at Chr 6

The gene orientation, rs-number and location of the SNPs used to identify the congenic interval are shown. The identity of the SNPs in the inbred strains are included for reference. B6.CB^{Atp2b2}- The broadest congenic interval is estimated as 50.34Mb which contains 24Mb of ambiguity downstream of *Atp2b2* and 16Mb of ambiguity upstream of *Atp2b2*. CB.B6^{Atp2b2}- Low sequencing resolution at rs242029300 leaves some ambiguity however it appears to be a cytosine (C) which indicates that this region of the chromosome is from the CB inbred strain. Given this, the congenic interval is predicted to be 59.53 Mb which contains 25Mb of ambiguity downstream of *Atp2b2* and 9Mb of ambiguity upstream of *Atp2b2*.

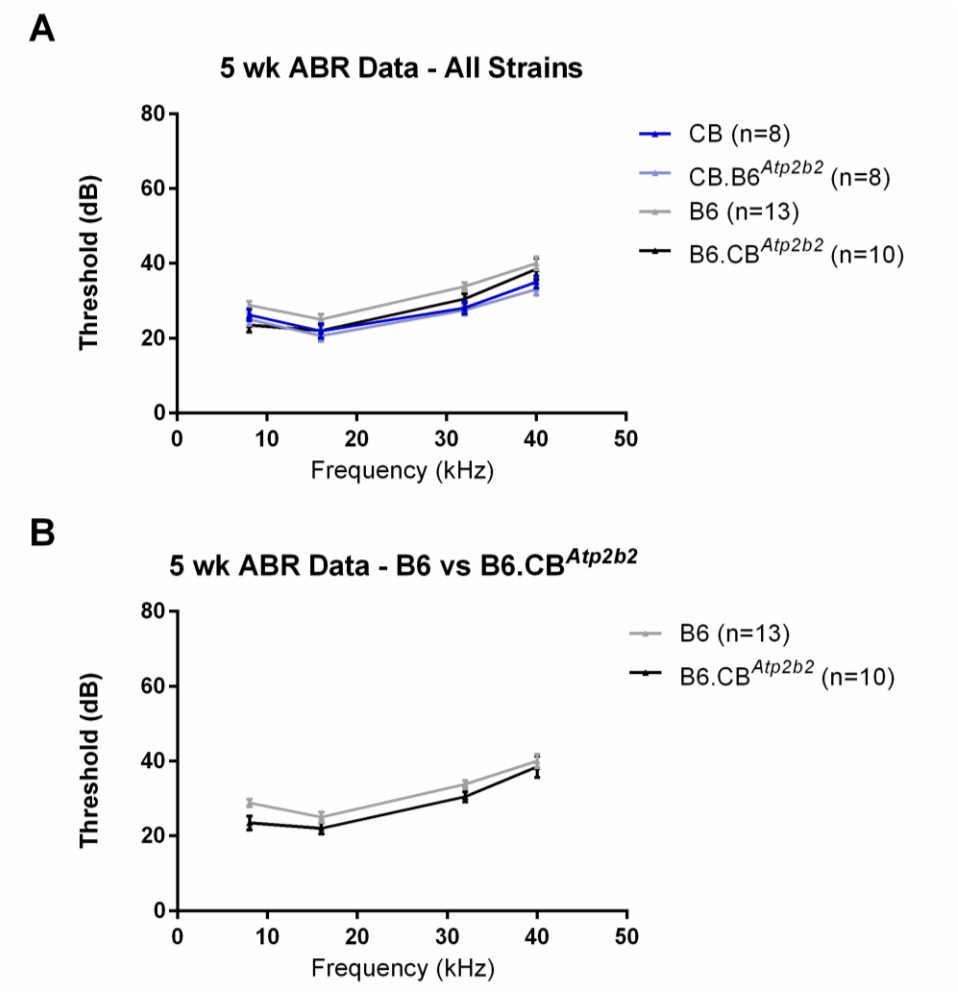

Figure 4.3. 5 week-old congenic and inbred mouse ABRs

At five weeks of age all strains have the same hearing. A two-way ANOVA indicates no effect of genotype across all four strains and no interaction with frequency. Error bars indicate average of data and Standard Error of the Mean (SEM).

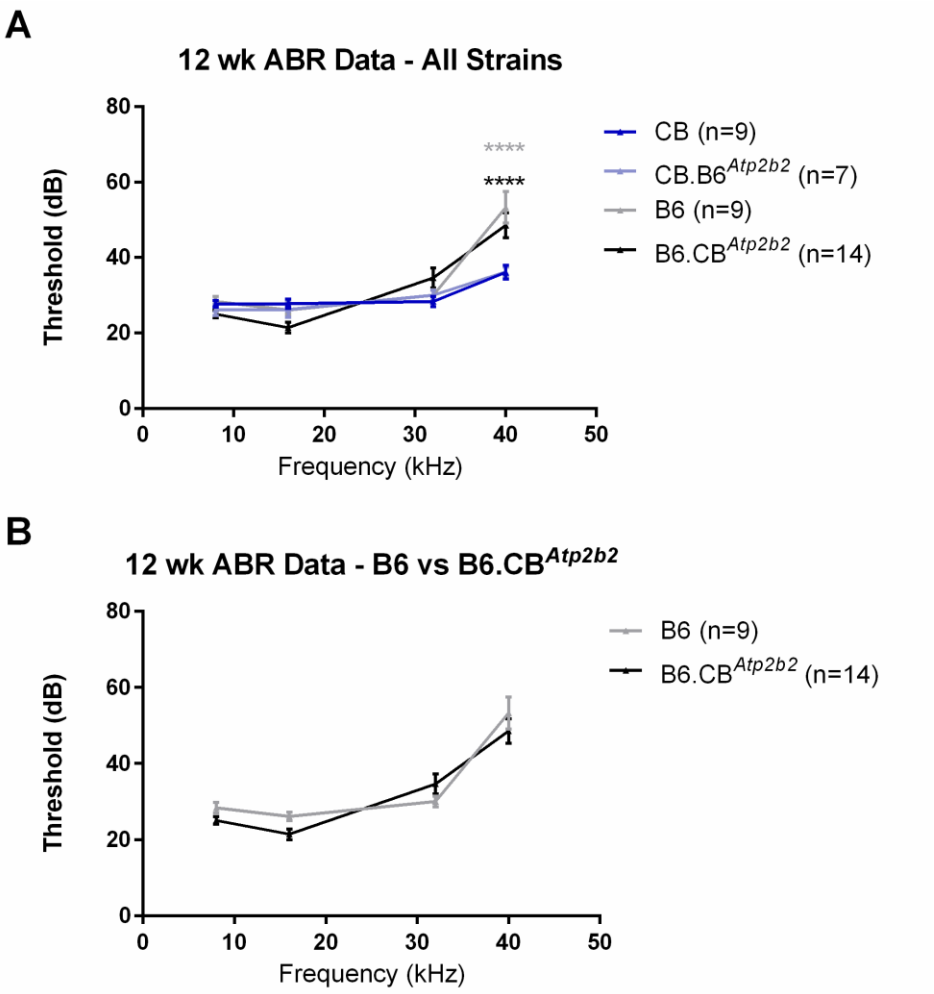

Figure 4.4. 12 week-old congenic and inbred mouse ABRs

At twelve weeks of age there is a genotype effect on hearing thresholds indicated by a two-way ANOVA, *$p \leq 0.05$. The interaction between genotype and frequency at this time point is also significant ****$P \leq 0.0001$. A. All strains are compared to CB. In a Bonferroni post-test both B6 and B6.CB^{Atp2b2} mice were statistically different from CB at 40 kHz (B6 – gray asterisks, B6.CB^{Atp2b2} – Black asterisks). There were no other significant changes. B. B6 mice are compared to B6.CB^{Atp2b2} mice, there are no differences at 12 weeks of age using a two-way ANOVA. Error bars indicate average of data and SEM.

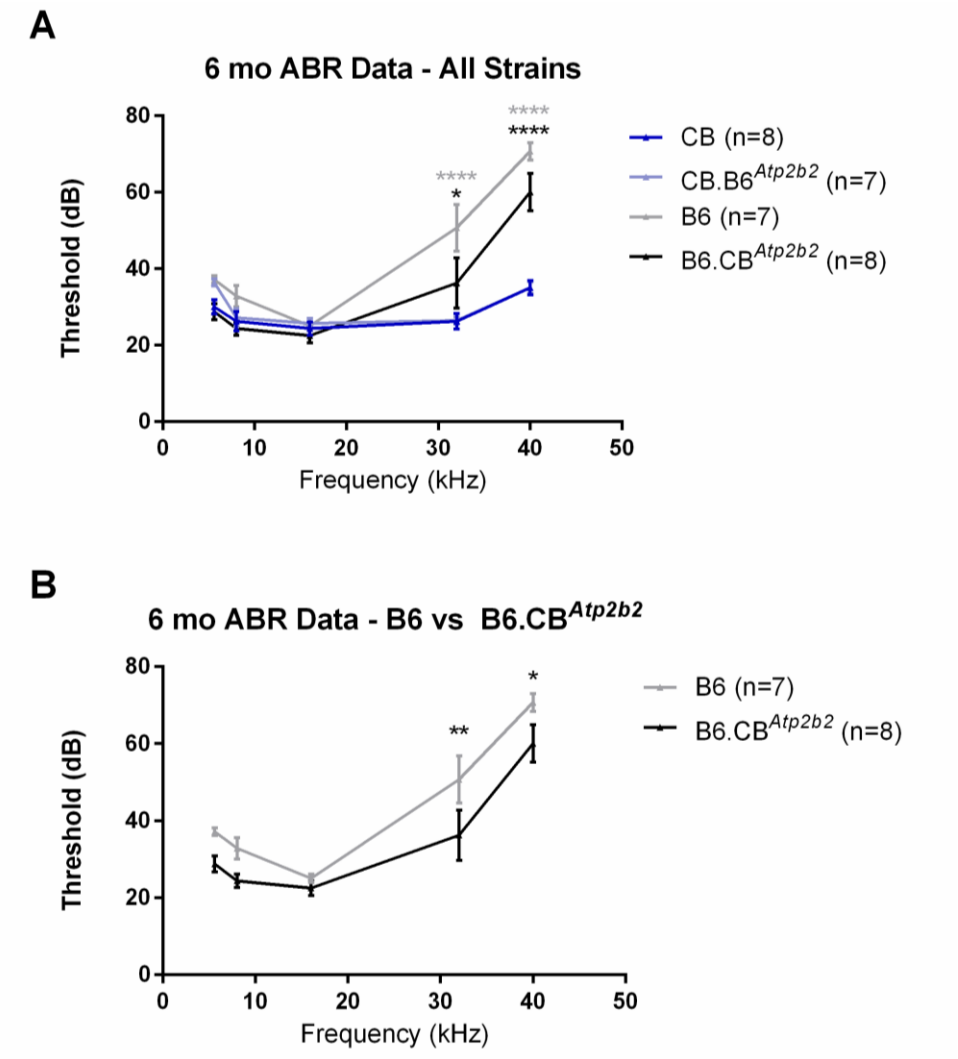

Figure 4.5. 6 month-old congenic and inbred mouse ABRs

At 6 months of age there is a genotype effect on hearing thresholds indicated by a two-way ANIVA, ****p≤0.0001. The interaction between genotype and frequency at this time point is also significant, ****P≤0.0001. A. All strains are compared to CB. In a Bonferroni post-hoc test both B6 and B6.CB^{Atp2b2} were statistically different from CB at 40 kHz and 32 kHz (B6 – gray asterisks, B6.CB^{Atp2b2} – Black asterisks). B. B6 mice are compared to B6.CB^{Atp2b2} mice. At 6 months of age the strains begin to diverge, in a Bonferroni post-hoc test B6 and B6.CB^{Atp2b2} are statistically different at 32 kHz and 40 kHz. Asterisks indicate the following p-values: *P≤ 0.05, **P ≤ 0.01, ***P ≤ 0.001, ****P<0.0001). Error bars indicate average of data and SEM.

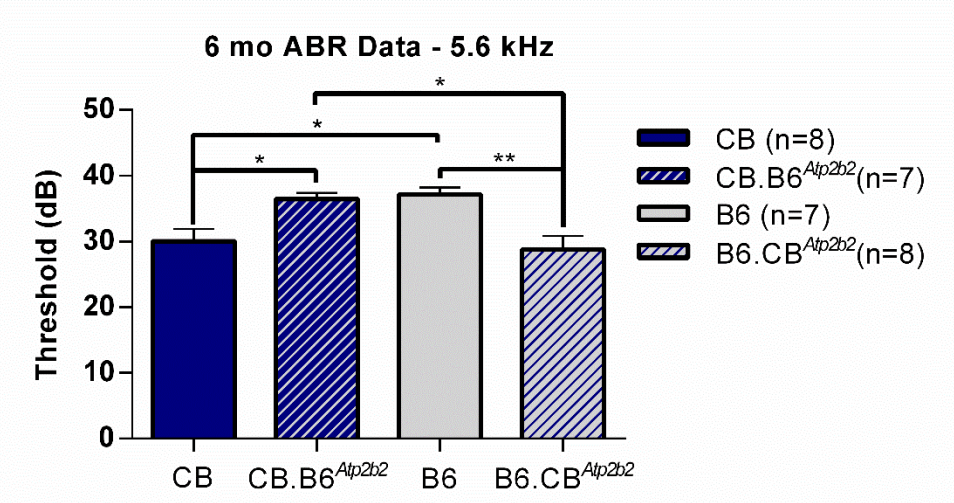

Figure 4.6. 6 month-old congenic and inbred mouse ABRs at 5.6 kHz

Given the interaction between genotype and frequency at 6 months of age, the data was manually analyzed to identify frequencies that may have anomalous dependencies. Using a one-way ANOVA on all four strains at only 5.6 kHz, a genotype effect was identified **$p \leq 0.01$. In a Holm-sidak's post-test it was found that the strains containing B6 like *Atp2b2* (CB.B6^{Atp2b2} and B6) have elevated thresholds at 5.6 kHz. Asterisks indicate the following p-values: *P< 0.05*P < 0.01**, P < 0.001***, P<0.0001****). Error bars indicate average of data and SEM.

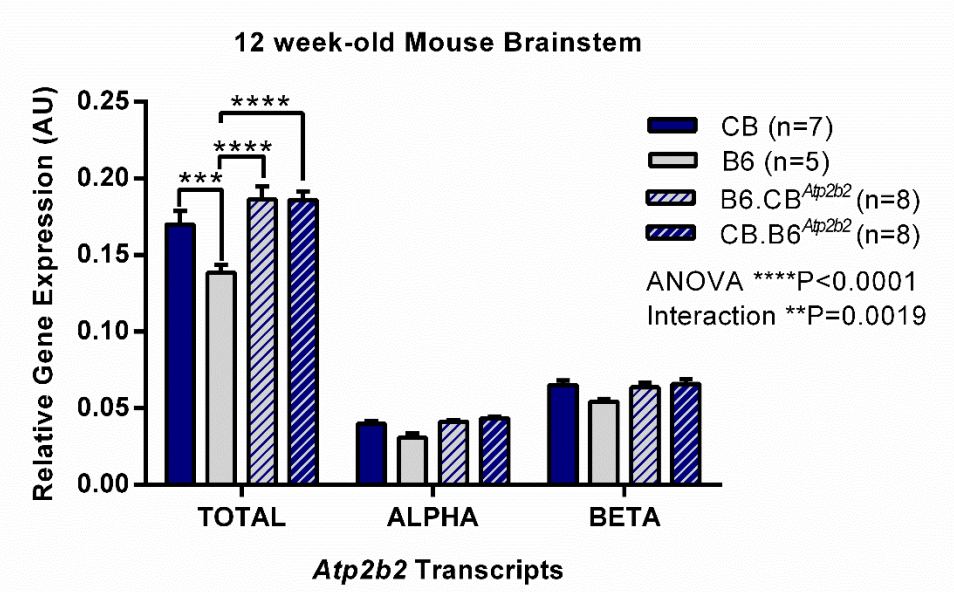

Figure 4.7. *Atp2b2* transcript expression in 12 week-old mouse brainstem

Atp2b2 transcripts were analyzed in the brainstem of CB, B6, CB.B6^{Atp2b2}, and B6.CB^{Atp2b2} inbred strains. CB and B6 Inbred strain data is from figure 3.5. Primers recognize *αAtp2b2*, *βAtp2b2* and total recognizes α, β and unknown 5'UTR transcripts expressed in these tissues. At 12 weeks of age there is a significant genotype effect on *Atp2b2* transcript expression in the cochlea as predicted by a two-way ANOVA. A Bonferroni post-hoc test shows total transcript is significantly affected and the B6 inbred strain has significantly less transcript than the other 3 mouse strains tested. Asterisks indicate the following p-values: **P $\leq$ 0.01, *** P $\leq$ 0.001, ****P$\leq$0.0001. Error bars indicate average of data and SEM.

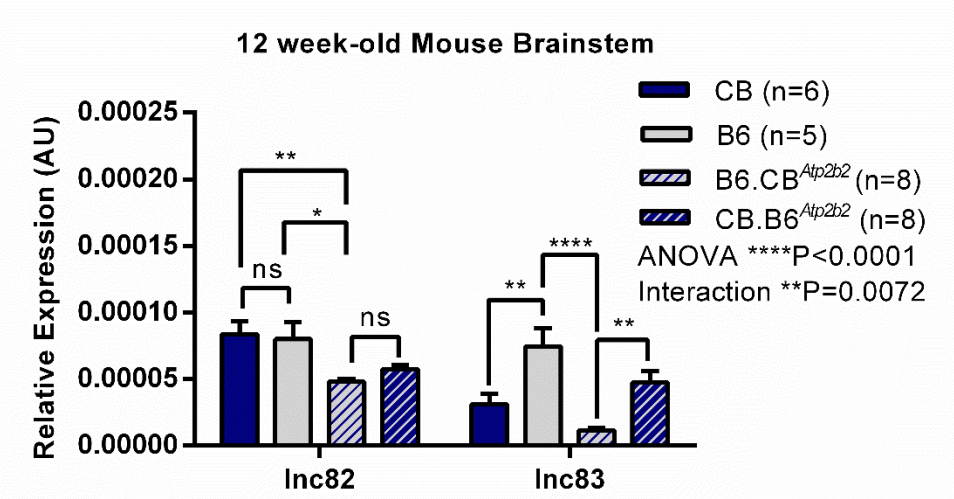

Figure 4.8. LncRNA expression in 12 week-old mouse brainstem

LncRNA transcripts were analyzed in the brainstem of CB, B6, CB.B6^{Atp2b2}, and B6.CB^{Atp2b2} inbred strains. CB and B6 Inbred strain data is from figure 3.10. Primers recognize lnc82 and lnc83. At twelve weeks of age there is a significant genotype effect on lncRNA expression in the brainstem as predicted by a two-way ANOVA. A Bonferroni post-hoc test shows lnc83 us elevated in strains with a B6 haplotype at *Atp2b2* (B6 and CB.B6^{Atp2b2}). Lnc82 is not different when comparing CB vs B6 or CB.B6^{Atp2b2} vs B6.CB^{Atp2b2} but lnc82 is significantly reduced in B6.CB^{Atp2b2} mice. Asterisks indicate the following p-values: *P$\leq$0.05, **P $\leq$ 0.01, *** P $\leq$ 0.001, ****P$\leq$0.0001. Error bars indicate average of data and SEM.

Chapter 5. CONCLUSIONS AND FUTURE STUDIES

This thesis has identified transcriptional elements responsible for regulating *Atp2b2*. Much of which was inferred in part or whole by data from ENCODE and Ensembl. These data sets are extremely powerful tools can inform future research. With fantastic accessibility to this information we were able to use experimentally derived *in silico* data to narrow down our search for the proximal promoter of *Atp2b2*. We were able to compare this promoter to the *ATP2B2* promoter in humans and show similar structural elements including the presence of several lncRNAs. It cannot be stressed enough the wealth of knowledge available to the researcher utilizing and mining these data sets. From ENCODE, SHIELD, tfbind, matInspector, and JAX's MGI database there are many questions about transcriptional regulation that can be answered without even picking up a pipette.

5.1 THE *ATP2B2* PROMOTER AND THE VAST TRANSCRIPTIONAL LANDSCAPE

In this study we characterized the promoter of the α*Atp2b2* transcript. Study of the promoter and in-depth *in silico* analysis of the 5'-region of the *Atp2b2* gene indicates that we are just scratching the surface of transcriptional regulation of this gene. ATP2B2 plays a critical role in Ca^{2+} regulation and is expressed throughout the life of the animal. As is typical with these types of genes it has large intronic regions, a number of splice variants and at least 4 TSS variants. The gene in total is about 300kb in length with over 20 exons. Also, *Atp2b2* is the largest *Atp2b* gene with very specific tissue expression.

Although we have identified an immediate early gene that binds to and activates the *αAtp2b2* promoter, it is expected that further investigation of this region will identify robust and complex transcriptional regulatory mechanisms of *Atp2b2*. Analysis of G-quadraplexes in the intronic

regions and analysis of the β promoter would be the next directions. Additionally, looking at the α promoter in cell lines with robust expression of *Atp2b2* may elucidate further transcriptional modulators of this promoter.

5.2 *Atp2b2* REGULATION IN CB AND B6 INBRED STRAINS

The genetic basis of AHL is extremely complex. Identifying genes in mouse that lead to AHL informs researchers of genes that could be involved in human hearing loss. In this study, we aimed to characterize *Atp2b2* in B6 mice and propose that misregulation of this gene worsens auditory thresholds caused by mutations in the *Cdh23* gene.

Although two assays have identified misregulation in *Atp2b2* transcript in B6, measures of protein expression showed no significant changes. This is likely due to the sensitivity of the western assay and is a caveat that should be addressed. Transcript localization and isoform usage are emerging players in disease. Although total protein is unchanged anomalous isoform expression could be causal. This study characterized two new lncRNAs, lnc82 and lnc83. These genes drive home the importance of acknowledging and studying transcript expression and it is expected that these genes play a functional role in regulation of *Atp2b2*. Future studies are needed to determine the function, localization and mechanism of action of lnc82 and lnc83.

Several experiments that are the "next steps" for characterizing lnc82 and lnc83 follow: To ensure that changes seen in expression of *Atp2b2* are caused by overexpression of the lnc83, silencing RNA (siRNA) should be used to knockdown lnc83 expression. For cytoplasmic knockdown, siRNA can be used to degrade lnc83 via the RNA-Induced Silencing Complex (RISC). For knocking down lnc83 expression in the nucleus, hybrid oligonucleotides created by ISIS pharmaceuticals could be used. These oligonucleotides function as specific knockdowns of RNA in the nucleus in an RNaseH dependent manner (Dias et al., 2002). (For full methods see:

Maamar et al. 2013). Additionally, to determine if the lncRNAs act in a sequence specific manner to regulate *Atp2b2* transcript, a construct with the inverse sequence could be overexpressed in the cells. Lastly, imaging techniques could be used to identify the location of lncRNAs in whole mount dissections of the cochlea.

5.3 DEVELOPMENT OF A NEW *ATP2B2* MODEL IN AUDITORY NEUROSCIENCE

One of our biggest contributions to the field of auditory neuroscience is the development of congenic strains to study the anomalous *Atp2b2* locus in B6 mice. Two strains were bred, one with CB background and B6 at the *Atp2b2* locus and a second 'rescue' mouse with B6 background and CB at the *Atp2b2* locus. Given the subtle changes in B6 *Atp2b2* transcript expression a major difference in the hearing of the congenic mice was not expected. Excitingly, we were able to identify a partial rescue affect in the B6.CB^{Atp2b2} mouse and heightened thresholds in the CB.B6^{Atp2b2} mouse. Till this point, the auditory field has not been able to determine the mechanism of low frequency loss but it appears, at least in this case, that *Atp2b2* locus is a contributor.

Although we were unable to show downregulation of *Atp2b2* in the CB.B6^{Atp2b2} mouse brainstem at 12 weeks of age, these mice have abundant potential for future studies. The localization of *Atp2b2* transcript and ATP2B2 protein should be investigated. The localization of *Atp2b2* transcripts could be predicted using qPCR primers recognizing the splice variants that dictate localization and function. Additionally, the expression of *Atp2b2* transcripts should be measured in the cochlea and the OC of older congenic mice. Lastly, the *Atp2b2* congenes could be bred to their *Cdh23* congenic counterparts from JAX to the digenic interaction between *Cdh23* and *Atp2b2* in B6 mice. These mice will elucidate exciting mechanisms of AHL and inform the molecular basis of the digenic interaction between *Cdh23* and *Atp2b2* in mice and humans.

BIBLIOGRAPHY

Alvarado DM, Veile R, Speck J, et al (2009) Downstream targets of GATA3 in the vestibular sensory organs of the inner ear. Dev Dyn 238:3093–3102. doi: 10.1002/dvdy.22149

Axelsen KB, Palmgren MG (1998) Evolution of substrate specificities in the P-type ATPase superfamily. J Mol Evol 46:84–101.

Banday AR, Azim S, Tabish M (2011) Alternative promoter usage and differential expression of multiple transcripts of mouse Prkar1a gene. Mol Cell Biochem 357:263–274. doi: 10.1007/s11010-011-0897-z

Beltran M, Puig I, Peña C, et al (2008) A natural antisense transcript regulates Zeb2/Sip1 gene expression during Snail1-induced epithelial–mesenchymal transition. Genes Dev 22:756–769. doi: 10.1101/gad.455708

Bermingham NA, Hassan BA, Price SD, et al (1999) Math1: an essential gene for the generation of inner ear hair cells. Science 284:1837–1841.

Bortolozzi M, Brini M, Parkinson N, et al (2010) The novel PMCA2 pump mutation Tommy impairs cytosolic calcium clearance in hair cells and links to deafness in mice. J Biol Chem 285:37693–37703. doi: 10.1074/jbc.M110.170092

Bowl MR, Dawson SJ (2015) The mouse as a model for age-related hearing loss - a mini-review. Gerontology 61:149–157. doi: 10.1159/000368399

Cao X, Mahendran R, Guy GR, Tan YH (1993) Detection and characterization of cellular EGR-1 binding to its recognition site. J Biol Chem 268:16949–16957.

Carafoli E (1991) Calcium pump of the plasma membrane. Physiol Rev 71:129–153.

Carafoli E (1994) Biogenesis: plasma membrane calcium ATPase: 15 years of work on the purified enzyme. FASEB J 8:993–1002.

Carafoli E (2011) The plasma membrane calcium pump in the hearing process: physiology and pathology. Sci China Life Sci 54:686–690. doi: 10.1007/s11427-011-4200-z

Carafoli E (2003) The calcium-signalling saga: tap water and protein crystals. Nat Rev Mol Cell Biol 4:326–332. doi: 10.1038/nrm1073

Cartharius K, Frech K, Grote K, et al (2005) MatInspector and beyond: promoter analysis based on transcription factor binding sites. Bioinforma Oxf Engl 21:2933–2942. doi: 10.1093/bioinformatics/bti473

Charizopoulou N, Lelli A, Schraders M, et al (2011) Gipc3 mutations associated with audiogenic seizures and sensorineural hearing loss in mouse and human. Nat Commun 2:201. doi: 10.1038/ncomms1200

Chen Q, Mahendrasingam S, Tickle JA, et al (2012) The development, distribution and density of the plasma membrane calcium ATPase 2 calcium pump in rat cochlear hair cells. Eur J Neurosci 36:2302–2310. doi: 10.1111/j.1460-9568.2012.08159.x

Chicka MC, Strehler EE (2003) Alternative Splicing of the First Intracellular Loop of Plasma Membrane Ca2+-ATPase Isoform 2 Alters Its Membrane Targeting. J Biol Chem 278:18464–18470. doi: 10.1074/jbc.M301482200

Chittka L, Brockmann A (2005) Perception Space—The Final Frontier. PLoS Biol 3:e137. doi: 10.1371/journal.pbio.0030137

Cieśla M, Boguta M (2008) Regulation of RNA polymerase III transcription by Maf1 protein. Acta Biochim Pol 55:215–225.

Clapham DE (2007) Calcium Signaling. Cell 131:1047–1058. doi: 10.1016/j.cell.2007.11.028

Consortium TEP (2012) An integrated encyclopedia of DNA elements in the human genome. Nature 489:57–74. doi: 10.1038/nature11247

Cunningham F, Amode MR, Barrell D, et al (2015) Ensembl 2015. Nucleic Acids Res 43:D662–D669. doi: 10.1093/nar/gku1010

Daily K, Patel VR, Rigor P, et al (2011) MotifMap: integrative genome-wide maps of regulatory motif sites for model species. BMC Bioinformatics 12:495. doi: 10.1186/1471-2105-12-495

Deckmann K, Rörsch F, Geisslinger G, Grösch S (2012) Identification of DNA–protein complexes using an improved, combined western blotting-electrophoretic mobility shift assay (WEMSA) with a fluorescence imaging system. Mol Biosyst 8:1389. doi: 10.1039/c2mb05500g

Du Y, Carlock L, Kuo TH (1995) The mouse plasma membrane Ca2+ pump isoform 1 promoter: cloning and characterization. Arch Biochem Biophys 316:302–310.

Epstein DJ (2009) Cis-regulatory mutations in human disease. Brief Funct Genomic Proteomic 8:310–316. doi: 10.1093/bfgp/elp021

Fettiplace R, Hackney CM (2006) The sensory and motor roles of auditory hair cells. Nat Rev Neurosci 7:19–29. doi: 10.1038/nrn1828

Ficarella R, Di Leva F, Bortolozzi M, et al (2007) A functional study of plasma-membrane calcium-pump isoform 2 mutants causing digenic deafness. Proc Natl Acad Sci U S A 104:1516–1521. doi: 10.1073/pnas.0609775104

Frisina RD, Singh A, Bak M, et al (2011) F1 (CBA×C57) mice show superior hearing in old age relative to their parental strains: Hybrid vigor or a new animal model for "Golden Ears"? Neurobiol Aging 32:1716–1724. doi: 10.1016/j.neurobiolaging.2009.09.009

Furuta H, Luo L, Hepler K, Ryan AF (1998) Evidence for differential regulation of calcium by outer versus inner hair cells: plasma membrane Ca-ATPase gene expression. Hear Res 123:10–26.

Gates GA, Couropmitree NN, Myers RH (1999) Genetic associations in age-related hearing thresholds. Arch Otolaryngol Head Neck Surg 125:654–659.

Hawkins RD, Bashiardes S, Powder KE, et al (2007) Large Scale Gene Expression Profiles of Regenerating Inner Ear Sensory Epithelia. PLoS ONE. doi: 10.1371/journal.pone.0000525

Henry KR (2002) Sex-and age-related elevation of cochlear nerve envelope response (CNER) and auditory brainstem response (ABR) thresholds in C57BL/6 mice. Hear Res 170:107–115.

Hertzano R (2004) Transcription profiling of inner ears from Pou4f3ddl/ddl identifies Gfi1 as a target of the Pou4f3 deafness gene. Hum Mol Genet 13:2143–2153. doi: 10.1093/hmg/ddh218

Hirawa N, Fujiwara A, Umemura S (2013) ATP2B1 and blood pressure: from associations to pathophysiology. Curr Opin Nephrol Hypertens 22:177–184. doi: 10.1097/MNH.0b013e32835da4ca

Ho PW-L, Pang SY-Y, Li M, et al (2015) PMCA4 (ATP2B4) mutation in familial spastic paraplegia causes delay in intracellular calcium extrusion. Brain Behav 5:n/a–n/a. doi: 10.1002/brb3.321

Horbach T, Gotz C, Kietzmann T, Dimova EY (2015) Protein kinases as switches for the function of upstream stimulatory factors: implications for tissue injury and cancer. Front Pharmacol. doi: 10.3389/fphar.2015.00003

Huarte M, Guttman M, Feldser D, et al (2010) A Large Intergenic Noncoding RNA Induced by p53 Mediates Global Gene Repression in the p53 Response. Cell 142:409–419. doi: 10.1016/j.cell.2010.06.040

Hu SS, Mei L, Chen JY, et al (2014) Expression of Immediate-Early Genes in the Inferior Colliculus and Auditory Cortex in Salicylate-Induced Tinnitus in Rat. Eur J Histochem EJH. doi: 10.4081/ejh.2014.2294

Kane KL, Longo-Guess CM, Gagnon LH, et al (2012) Genetic background effects on age-related hearing loss associated with Cdh23 variants in mice. Hear Res 283:80–88. doi: 10.1016/j.heares.2011.11.007

Kazmierczak P, Sakaguchi H, Tokita J, et al (2007) Cadherin 23 and protocadherin 15 interact to form tip-link filaments in sensory hair cells. Nature 449:87–91. doi: 10.1038/nature06091

Konrad-Martin D, J. Norton S, Mascher KE, Tempel BL (2001) Effects of PMCA2 mutation on DPOAE amplitudes and latencies in deafwaddler mice. Hear Res 151:205–220. doi: 10.1016/S0378-5955(00)00228-8

Kozel PJ, Davis RR, Krieg EF, et al (2002) Deficiency in plasma membrane calcium ATPase isoform 2 increases susceptibility to noise-induced hearing loss in mice. Hear Res 164:231–239.

Lenhard B, Sandelin A, Carninci P (2012) Metazoan promoters: emerging characteristics and insights into transcriptional regulation. Nat Rev Genet. doi: 10.1038/nrg3163

Lomax MI, Gong T-W, Cho Y, et al (2001) Differential Gene Expression Following Noise Trauma in Birds and Mammals. Noise Health 3:19–35.

Maamar H, Cabili MN, Rinn J, Raj A (2013) linc-HOXA1 is a noncoding RNA that represses Hoxa1 transcription in cis. Genes Dev 27:1260–1271. doi: 10.1101/gad.217018.113

McCullough BJ, L. Tempel B (2004) Haplo-insufficiency revealed in deafwaddler mice when tested for hearing loss and ataxia. Hear Res 195:90–102. doi: 10.1016/j.heares.2004.05.003

Mikaelian D, Alford BR, Ruben RJ (1965) Cochlear potentials and 8 nerve action potentials in normal and genetically deaf mice. Ann Otol Rhinol Laryngol 74:146–157.

Minowa O, Ikeda K, Sugitani Y, et al (1999) Altered cochlear fibrocytes in a mouse model of DFN3 nonsyndromic deafness. Science 285:1408–1411.

Mojumder DK, Wensel TG, Frishman LJ (2008) Subcellular compartmentalization of two calcium binding proteins, calretinin and calbindin-28 kDa, in ganglion and amacrine cells of the rat retina. Mol Vis 14:1600.

Munroe SH, Lazar MA (1991) Inhibition of c-erbA mRNA splicing by a naturally occurring antisense RNA. J Biol Chem 266:22083–22086.

Noben-Trauth K, Zheng QY, Johnson KR (2003) Association of cadherin 23 with polygenic inheritance and genetic modification of sensorineural hearing loss. Nat Genet 35:21–23. doi: 10.1038/ng1226

Noben-Trauth K, Zheng QY, Johnson KR, Nishina PM (1997) *mdfw*: A Deafness Susceptibility Locus That Interacts with Deaf Waddler (*dfw*). Genomics 44:266–272.

Olusanya BO, Neumann KJ, Saunders JE (2014) The global burden of disabling hearing impairment: a call to action. Bull World Health Organ 92:367–373. doi: 10.2471/BLT.13.128728

Pan N, Jahan I, Kersigo J, et al (2012) A Novel Atoh1 "Self-Terminating" Mouse Model Reveals the Necessity of Proper Atoh1 Level and Duration for Hair Cell Differentiation and Viability. PLoS ONE 7:e30358. doi: 10.1371/journal.pone.0030358

Park SN, Back SA, Choung YH, et al (2011) Alpha-synuclein deficiency and efferent nerve degeneration in the mouse cochlea: A possible cause of early-onset presbycusis. Neurosci Res 71:303–310. doi: 10.1016/j.neures.2011.07.1835

Penheiter AR, Filoteo AG, Croy CL, Penniston JT (2001) Characterization of the deafwaddler mutant of the rat plasma membrane calcium-ATPase 2. Hear Res 162:19–28. doi: 10.1016/S0378-5955(01)00356-2

Prasad V, Okunade GW, Miller ML, Shull GE (2004) Phenotypes of SERCA and PMCA knockout mice. Biochem Biophys Res Commun 322:1192–1203. doi: 10.1016/j.bbrc.2004.07.156

Rivolta MN (2002) Transcript Profiling of Functionally Related Groups of Genes During Conditional Differentiation of a Mammalian Cochlear Hair Cell Line. Genome Res 12:1091–1099. doi: 10.1101/gr.225602

Rivolta MN, Holley MC (2002) Cell lines in inner ear research. J Neurobiol 53:306–318. doi: 10.1002/neu.10111

Roberts-Thomson SJ (2010) Plasma membrane calcium pumps and their emerging roles in cancer. World J Biol Chem 1:248. doi: 10.4331/wjbc.v1.i8.248

Schippert R, Schaeffel F, Feldkaemper MP (2009) Microarray analysis of retinal gene expression in Egr-1 knockout mice. Mol Vis 15:2720–2739.

Schultz JM, Yang Y, Caride AJ, et al (2005) Modification of human hearing loss by plasma-membrane calcium pump PMCA2. N Engl J Med 352:1557–1564.

Shen J, Scheffer DI, Kwan KY, Corey DP (2015) SHIELD: an integrative gene expression database for inner ear research. Database J Biol Databases Curation. doi: 10.1093/database/bav071

Shiga A, Nakagawa T, Nakayama M, et al (2005) Aging Effects on Vestibulo-Ocular Responses in C57BL/6 Mice: Comparison with Alteration in Auditory Function. Audiol Neurootol 10:97–104. doi: 10.1159/000083365

Silverstein RS, Tempel BL (2006) Atp2b2, encoding plasma membrane Ca2+-ATPase type 2, (PMCA2) exhibits tissue-specific first exon usage in hair cells, neurons, and mammary glands of mice. Neuroscience 141:245–257. doi: 10.1016/j.neuroscience.2006.03.036

Smith ME, Rajadinakaran G (2013) The Transcriptomics to Proteomics of Hair Cell Regeneration: Looking for a Hair Cell in a Haystack. Microarrays Basel Switz. doi: 10.3390/microarrays2030186

Sotomayor M, Weihofen WA, Gaudet R, Corey DP (2010) Structural Determinants of Cadherin-23 Function in Hearing and Deafness. Neuron 66:85–100. doi: 10.1016/j.neuron.2010.03.028

Street VA, McKee-Johnson JW, Fonseca RC, et al (1998) Mutations in a plasma membrane Ca2+-ATPase gene cause deafness in deafwaddler mice. Nat Genet 19:390–394.

Strehler EE (2015) Plasma membrane calcium ATPases: From generic Ca2+ sump pumps to versatile systems for fine-tuning cellular Ca2+. Biochem Biophys Res Commun 460:26–33. doi: 10.1016/j.bbrc.2015.01.121

Tempel BL, Shilling DJ (2007) The plasma membrane calcium ATPase and disease. Subcell Biochem 45:365–383.

Thurman RE, Rynes E, Humbert R, et al (2012) The accessible chromatin landscape of the human genome. Nature 489:75–82. doi: 10.1038/nature11232

Tsunoda T, Takagi T (1999) Estimating transcription factor bindability on DNA. Bioinforma Oxf Engl 15:622–630.

van der Wees J, van Looij MA., de Ruiter MM, et al (2004) Hearing loss following Gata3 haploinsufficiency is caused by cochlear disorder. Neurobiol Dis 16:169–178. doi: 10.1016/j.nbd.2004.02.004

Vandesompele J, De Preter K, Pattyn F, et al (2002) Accurate normalization of real-time quantitative RT-PCR data by geometric averaging of multiple internal control genes. Genome Biol 3:research0034.

Wang KC, Chang HY (2011) Molecular Mechanisms of Long Noncoding RNAs. Mol Cell 43:904–914. doi: 10.1016/j.molcel.2011.08.018

Wang Y, Chu H, Zhou L, et al (2012) Correlation of PDCD5 and apoptosis in hair cells and spiral ganglion neurons of different age of C57BL/6J mice. J Huazhong Univ Sci Technol Med Sci Hua Zhong Ke Ji Xue Xue Bao Yi Xue Ying Wen Ban Huazhong Keji Daxue Xuebao Yixue Yingdewen Ban 32:113–118. doi: 10.1007/s11596-012-0020-z

Watson CJ, Lies SM, Minich RR, Tempel BL (2014) Changes in Cochlear PMCA2 Expression Correlate with the Maturation of Auditory Sensitivity. J Assoc Res Otolaryngol 15:543–554. doi: 10.1007/s10162-014-0454-z

Watson CJ, Tempel BL (2013) A new Atp2b2 deafwaddler allele, dfwi5, interacts strongly with Cdh23 and other auditory modifiers. Hear Res 304:41–48. doi: 10.1016/j.heares.2013.06.003

Wei F, Xu ZC, Qu Z, et al (2000) Role of Egr1 in Hippocampal Synaptic Enhancement Induced by Tetanic Stimulation and Amputation. J Cell Biol 149:1325–1334.

Wingfield A, Panizzon M, Grant MD, et al (2007) A twin-study of genetic contributions to hearing acuity in late middle age. J Gerontol A Biol Sci Med Sci 62:1294–1299.

Wong J, Hyde TM, Cassano HL, et al (2010) Promoter specific alterations of brain-derived neurotrophic factor mRNA in schizophrenia. Neuroscience 169:1071–1084. doi: 10.1016/j.neuroscience.2010.05.037

Wood JD, Muchinsky S, Filoteo A, et al (2004) Low Endolymph Calcium Concentrations in deafwaddler2J Mice Suggest that PMCA2 Contributes to Endolymph Calcium Maintenance. J Assoc Res Otolaryngol. doi: 10.1007/s10162-003-4022-1

Xia A-P, Kikuchi T, Minowa O, et al (2002) Late-onset hearing loss in a mouse model of DFN3 non-syndromic deafness: morphologic and immunohistochemical analyses. Hear Res 166:150–158.

Zheng QY, Yan D, Ouyang XM, et al (2005) Digenic inheritance of deafness caused by mutations in genes encoding cadherin 23 and protocadherin 15 in mice and humans. Hum Mol Genet 14:103–111. doi: 10.1093/hmg/ddi010

VITA

Rebecca R. Minich was born in Kalamazoo, Michigan in 1988. She attended Loy Norrix and the Kalamazooo Area Mathematics and Sciences Center for high school. In 2010, she received a B.S. in Biochemistry with a minor in Environmental Studies from the University of Michigan. That same year Rebecca moved to Seattle to join the Department of Pharmacology at the University of Washington (UW). In her first years as a graduate student she was a trainee of the Auditory Neuroscience Training Grant and an officer of the American Association for Pharmaceutical Scientists. Later, she was a Technology Fellow at the UW technology transfer office as well as a market analyst and team manager for the UW Coulter Translational Research Partnership. Along with her PhD, Rebecca is graduating with a Technology and Entrepreneurship Certificate from the Foster School of Business. Rebecca is a marathon runner, climber and skier. She enjoys sketching, reading and watching movies in her leisure time.